書面繳交結案報告名冊

(PR51013)
選擇條件：89年度；承辦人：林月美；登錄日期：90/05/29～90/05/29；

列印日期：90/05/29
頁　　數：1

繳交日期	收文號	計畫編號	主持人	執行機關	執行期限	成果名稱
90/05/29	0900025627	89-2113-M-032 -005 -	吳慧芬	淡江大學	88/08/01至90/02/28	離子阱串聯質譜儀的正/負化學游離法之應用

合 計 ： 1筆 .

楊秋華 5/29

行政院國家科學委員會補助專題研究計畫成果報告

※※※※※※※※※※※※※※※※※※※※※※※※※※

離子阱串聯質譜儀的正/負化學游離法之應用

※※※※※※※※※※※※※※※※※※※※※※※※※※

計畫類別：☑個別型計畫　□整合型計畫

計畫編號：NSC 89－ 2113 －M － 032 － 005 －

執行期間： 88 年 8 月 1 日至 90 年 2 月 28 日

計畫主持人：吳慧芬

共同主持人：

計畫參與人員：吳慧芬,鍾淼鈞,吳朝欽,林雅萍,何銘益,陳建弘,林佩怡,

本成果報告包括以下應繳交之附件：

□赴國外出差或研習心得報告一份

□赴大陸地區出差或研習心得報告一份

□出席國際學術會議心得報告及發表之論文各一份

□國際合作研究計畫國外研究報告書一份

執行單位：淡江大學化學系

中 華 民 國 90 年 5 月 22 日

Characterization of Phthalic Anhydride and Related Compounds by Negative-ion Chemical Ionization and Collisional Activated Dissociation in an External Source Ion Trap Mass Spectrometer

Hui-Fen Wu*, Chien-Hong Chen, Chao-Ching Wu and Ming-Yi Ho

Department of Chemistry

Tamkang University

Tamsui, Taipei Hsien, 25137, Taiwan, R. O. C.

Abstract

GCQ is the first commercial benchtop ion trap mass spectrometer capable of performing negative ion analysis. A series of halogenated phthalic anhydrides and their derivatives were examined by GCQ, and it was found that since these halogenated compounds possess higher electron affinities, a resonance electron capture process can form negative ions in GCQ easily. Low-energy collisionally activated dissociation can further dissociate precursor ions. From these fragments, the structure of ions can be determined. Therefore, such experiments using GCQ can provide information about negative ions that cannot be detected by a traditional internal ionization ion trap mass spectrometer. In this study, the differentiation of isomers is discussed, and the CAD spectra obtained from methane and oxygen as reagent gases are compared.

Introduction

The subject of negative ions has intrigued traditional mass spectrometry for several decades [1-28], but because the ion trap mass spectrometer (ITMS) which utilizes internal ionization could not perform negative ion analysis, there have been few reports about its use in the past [29-32]. The reason for this dearth of information is that when 70 eV electrons are used, electron capture does not form negative ions efficiently. However, ever since 1996 when the first commercial ion trap mass spectrometer with an external source, Finnigan GCQ, appeared on the market, we have been able to detect negative ions with the conversion dynode (± 15KV). Already GCQ has been reported to possess excellent MS/MS capability in Positive Chemical Ionization (PCI) [33, 34], and the source temperature and reagent gas pressure effect on the PCI and Negative Chemical Ionization (NCI) have been evaluated [34, 35]. In this study, we used the GCQ ion trap to characterize an array of phthalic anhydrides and related compounds with methane and oxygen as reagents using a combination of Negative Chemical Ionization and collisionally activated dissociation (CAD) techniques. The structures of phthalic anhydrides and related compounds are shown in Figure 1. In fact, while none has been done with the ITMS, some structurally related compounds have been characterized by traditional mass spectrometers

in a couple of studies [16, 17] in which, for example, CAD of the molecular anion of phthalic anhydride yielded fragment ions which resulted from the elimination of CO, CO_2 and C_2O_3 [17]. GCQ presents us with certain advantage in the study of NCI and it can provide valuable information about negative ions, which until now could not be detected by a traditional internal ionization ITMS. We will discuss these advantages and, we will also compare the CAD results we obtained by using methane and oxygen as reagent gasses.

Experimental Method

All experiments were carried out in an external source ion trap mass spectrometer (Finnigan MAT GCQ) [33-36]in which NCI was used with methane and oxygen as the reagent gases. The instrument was operated in the mass selective instability mode. The pressures of He buffer gas and NCI reagent gases were 1 mtorr and 4×10^{-4} torr, respectively. The pressure in the ion source region was 100 mtorr measured by a convectron gauge. Ion source temperature was 200°C. Ionization times were set using automatic gain control (AGC). The ion injection time (from source to mass analyzer) was 0.3-25 msec. Collisional experiments were performed by applying a supplementary tickle voltage to the endcaps of the ion trap at $q_z = 0.225$. The collisional activation time was 15 msec. Signal width for selection of the parent ions was from 0.5-1 amu; the collision energy for fragmentation of the parent ions was from 1-3 V. Samples were introduced to the ion source region via a temperature controlled direct insertion probe (DIP) to assist the desorption of the sample. The probe tip was heated to a temperature of 150°C to 300°C at a speed of 80-100°C/min. Spectra were acquired from 50 to 650 amu at a rate of 0.5 s/scan. The identification of all isotope peaks was achieved using "isoform 1.02" software. All compounds were purchased from Aldrich Chemical Company (Milwaukee, WI) except 3,4,5,6-tetrabromophthalimide which was obtained from Alfa Chemical Company (Ward Hill, MA) and 4,5-difluorophthalic anhydride which was purchased from Merck Chemical Company (Darmstadt, Germany).

Results and discussion

Negative Chemical Ionization spectra using methane as reagent gases

NCI spectra typically produce much lower signals than the PCI spectra in the traditional mass analyzer. However, in GCQ, we found that NCI can also produce as intense signals as PCI [33, 34]. GCQ software prints a total ion count at the top of the spectrum as "RIC". In the NCI of GCQ, the negative ionization mode is also very sensitive to the cleanliness of the ion source. Traditionally, methane has been used as the most common reagent gas in many NCI applications [14, 15, 21, 23, 25, 27, 28]. Table 1 lists NCI spectra of all compounds using methane as a reagent gas at the ion source temperature of 200^{0}C. The formation of the NCI products includes the molecular anion, fragment ions, dimeric ions and the ions due to impurities. The intensities of the fragments and dimeric ions are typically quite small compared with the molecular anion or $[M-H]^-$. The largest dimeric ion is $[2M-HCl]^-$ of 4, 5-dichlorophthalimide (73%). To compare the NCI spectra of phthalic anhydride derivatives with that of the phthalimide derivatives, the proton abstraction reactions for phthalimide derivatives were observed typically, because the trace amount of water or oxygen in GCQ lead to the formation of the OH^- ion, which then reacted with the hydrogen atom on the amide. One typical example of this process can be seen in Scheme 1, which shows the probable mechanism for the formation and CAD of $[M-H]^-$ of phthalimide. Since only the OCN^- ions at m/z 42 were produced, this mechanism could be confirmed by CAD results. Regarding phthalic anhydride derivatives, since they do not possess a hydrogen on the oxygen atom, the base peaks are mainly M^- ions except for the 3, 4, 5, 6-tetrabromophthalic anhydride and the 3, 4, 5, 6- tetrabromo-2-sulfobenzoic acid cyclic anhydride, both of which produced $[M-Br]^-$ as the base peaks due to the easily elimination of the Br atom. For bromo-substituent compounds, the base peaks were either $[M-Br]^-$ (3, 4, 5, 6-tetrabromophthalic anhydride) or $[(M-H)-Br]^-$ (3, 4, 5, 6-tetrabromophthalimide). This finding proves that the Br atom is more easily eliminated than Cl atom. In addition, for fluoro-substituent compounds, no F^- ions were ever observed. We only found small neutral losses of HF. When comparing the NCI spectra of the 3, 4, 5, 6-

tetrabromophthalic anhydride with that of 3, 4, 5, 6- tetrabromo-2-sulfobenzoic acid cyclic anhydride, fragment ions such as $[M-CO_2-SO_2]^-$, $[M-Br_2]^-$, $[M-CO_2-SO_2-Br]^-$ or Br_2^- ions were only observed for the latter. Since no fragment ions could be observed in either phthalic anhydride or phthalimide, the halogen-substituent effect would be the main factor for determining the formation of the fragment ions. When comparing the NCI spectra of 4,5-dichlorophthalic anhydride (see Figure 2) with that of 3,6-dichlorophthalic anhydride (see Figure 3), although both spectra were obtained using methane as the reagent gas, several higher chlorinated additional compounds including m/z 324 ($[2M-CO_2-CO-HCl]^-$ ion, 5%), m/z 288 (1%) and m/z 252 ($[M-H+Cl]^-$ ion, 5%) could be observed, and they were observed in the NCI spectra of 3,6-dichlorophthalic anhydride only. The presence of trace amounts of reactive species such as oxygen and water in GCQ can also complicate the NCI spectra in GCQ. For example, the ions at m/z 233, and 198 ($[M+OH]^-$ and $[M+OH-Cl]^-$, Figure 2) could only be observed in 4,5-dichlorophthalic anhydride. That the formation of these ions could only be observed in the methane-spectrum but not in the oxygen-spectrum for NCI of 4,5-dichlorophthalic anhydride suggests the presence of some impurity caused by the anion of phthalic acid formed by hydrolysis rather than an ion formed during the gas phase [35]. The NCI spectra of really pure samples of the two isomers should not show any appreciable differences in GCQ.

Comparison of the CAD results for Negative Chemical Ionization spectra using methane and oxygen as reagent gases.

The CAD technique was applied to the adduct ions, molecular anion, $[M-H]^-$, and fragment ions to investigate the structural information of NCI products. Tables 2 and 3 list CAD findings on the ions formed by NCI using methane and oxygen as reagent gases. Both involved neutral loss spectra of the NCI ions, demonstrating typical fragmentation processes. However, three main differences could be observed. First, NCI spectra with oxygen as the reagent for some halogenated compounds in the GCQ typically produced some oxygenated ions ($[M-X+O]^-$, where X = Cl or Br). The $[M-Cl/Br+O]^-$ ion was formed because the neutral molecule (M) reacted

with some oxygen ions in a nucleophilic reaction [35]. CAD of these ions eliminates CO or CO_2 typically. Second, more fragment ions were produced in the CAD of oxygen-spectra than the CAD of methane-spectra. CAD of M^- of 3,4,5,6-tetrafluorophthalic anhydride using oxygen as reagent gas, for example, produced many more fragment ions than the one using methane as the reagent for the same compound (see Scheme 2). Third, one oxygen atom may quickly attach to the fragment ions during the CAD processes that use oxygen as the reagent. For example, CAD of 3,4,5,6-tetrachlorophthalic anhydride and 3,4,5,6-tetrabromophthalic anhydride produce the base peaks at $[M-Cl+O]^-$ and $[M-Br+O]^-$, respectively.

Differentiation of isomers by GCQ

Isomer differentiation by traditional mass analyzer is difficult [14, 27, 28]. However, it can be easily achieved by GCQ since GCQ possesses excellent tandem mass capability [33, 34]. In fact, isomer differentiation can be done uniquely by GCQ by combining NCI with its MS/MS capability. One example of isomer differentiation is that for the NCI of 4,5-difluorophthalic anhydride from that of 3,6-difluorophthalic anhydride in this study in which both NCI spectra were obtained using methane as the reagent. The NCI spectra for both isomers could be easily differentiated since 3,6-difluorophthalic anhydride produces two characteristic ions at m/z 276 ($[2M-CO_2-CO-HF]^-$ ion, 6%) and m/z 112 ($[M-CO_2-CO]^-$ ion, 8%) while 4,5-difluorophthalic anhydride produces two characteristic ions at m/z 320 ($[2M-CO_2-HF]^-$ ion, 5%) and m/z 201 ($[M+OH]^-$ ion, from the impurity, 6%). CAD of the M^- ions of these two isomers also had different results. CAD of the M^- ions of 3,6-difluorophthalic anhydride produces the ion mainly at m/z 112 through the loss of one CO_2 and CO molecules while CAD of the M^- ions of 4,5-difluorophthalic anhydride only produces one ion at m/z 156 through the elimination of one CO molecule.

Conclusion

In this study, we found an external ionization ion trap mass spectrometer to have excellent NCI capability. Additionally, we found that the use of pure oxygen and methane as NCI reagent

gases in GCQ gave it good sensitivity. These novel experiments provide valuable information regarding past NCI studies that could not be performed by a traditional internal ionization ITMS. We have found combining NCI with CAD in GCQ to be a very useful analytical technique. Moreover, because of its excellent sensitivity in NCI and tandem mass capability, GCQ is also ideal for trace analysis of target compounds in complex mixtures.

Acknowledgments

The support from the National Science Council of the Republic of China (Grant No. NSC 89-2113-M-032-005) and Tamkang University is gratefully acknowledged.

References

[1]J. G. Dillard, *Chem. Rev.*, 1973,73,589.

[2]D. F. Hunt, G. C. Stafford, Jr., F. W. Crow and J. W. Rrssell, Anal. Chem., 1976, 48, 2098.

[3]D. F. Hunt and F. W. Crow, *Anal. Chem.*, 1978, 50, 1781.

[4]J. H. Bowie, *Mass Spectrom. Rev.*, 1984, 3, 161.

[5]H. Budzikiewicz, *Mass Spectrom. Rev.*, 1986, 5, 345.

[6]V. S. Ong and R. A. Hites, *Mass Spectrom., Rev.* 1994, 13, 259.

[7]K. Ueda, S. L. Morgan, A. Fox, J. Gilbart, A. Sonesson, L. Larsson and G. Odham, *Anal. Chem.*, 1989, 61, 265.

[8]K. Mizuishi, M. Takeuchi and T. Hobo, *J. Chromatogr. A*, 1998, 800, 267.

[9]S.-A. Fredriksson, L.-G. Hammarstrom, L. Henriksson and H.-A. Lakso, *J. Mass Spectrom.*, 1995, 30, 1133.

[10]S. A. Tittlemier, M. Simom, W. M. Jarman, J. E. Elliott and R. J. Norstrom, *Environ. Sci. Technol.*, 1999, 33, 26.

[11]Z. Zdrahal, *J. Chromatogr. A*, 1998, 793, 214.

[12]J. R. Moyer and J. L. Elder, *J. Agric. Food Chem.*, 1984, 32, 866.

[13]D. W. Kuehl, M. J. Whitaker and R. C. Dougherty, *Anal. Chem.*, 1980, 52, 935.

[14]M. Oehme, D. Stockl and H. Knoppel, *Anal. Chem.*, 1986, 58, 554.

[15]E. A. Stemmler, R. A. Hites, B. Arbogast, W. L. Budde, M. L. Deinzer, R. C. Dougherty, J. W. Eichelberger, R. L. Foltz, C. Grimm, E. P. Grimsrud, C. Sakashita and L. J. Sears, *Anal. Chem.*, 1988, 60, 781.

[16]T. A. Gillespie, L. Urogdi, A. R. Katritzky and R. A. Yost, *Org. Mass Spectrom.*, 1989, 24, 817.

[17]J. H .Bowie, *J. Am. Chem. Soc.*, 1973, 5795.

[18]H. P. Tannenbaum, J. D. Roberts, R. C. Dougherty , *Anal.Chem.*, 1975, 47, 49.

[19]I. Hahndorf, E. Illenberger, *Int. J. Mass Spectrom Ion Process.*, 1997, 167/168, 87.

[20] A. G. Harrison, Chemical Ionization Mass Spectrometry; CRC Press: Boco Ratan 1983.

[21]L. R. Hilpert, G. D. Byrd and C. R. Vogt, *Anal.Chem.*, 1984, 56, 1842.

[22]J. A. Laramee, B. C. Arbogast and M. L. Deinzer, *Anal. Chem.*, 1986, 58, 2907.

[23]J. M. Trainor and P. Vouros, *Anal.Chem.* , 1987, 59, 601.

[24]G. Drabner and H. Budzikiewicz, *J. Mass Spectrom.*, 1995, 30, 893.

[25]J. R. Hass, M. D. Frlesen, D. J. Harven and C. E. Parker, *Anal. Chem.*, 1978, 50, 1474.

[26]T. Ramdahl and K. Urdal, *Anal. Chem.*, 1982, 54, 2256.

[27]M. V. Buchanan and G. Olerich, *Org. Mass Spectrom.*, 1984, 19, 486.

[28]S. Daishima, Y. Iida, A. Shibate and F. Kanda, *Org. Mass Spectrom.*, 1992, 27, 571.

[29]S. A. McLuckey, G. L. Glish and P. E. Kelley , *Anal. Chem.* ,1987, 59, 1670.

[30]S. Catinella, P. Traldi, X. Jiang, F. A. Londry, R. J. S. Morrison, R. E. March, S. Gregoire, J. – C. Mathurin and J. – C. Tabet, *Rapid Commun. Mass Spectrom.*,1995,9,1302.

[31]B. L. Williamson and C. S. Creaser, *Rapid Commun. Mass Spectrom.*,1997, 11, 1235.

[32]D. W. Berberich and R. A. Yost, *J. Am. Soc. Mass Spectrom*, 1994, 5,757.

[33]H.-F. Wu and Y.-P. Lin, *J. Mass Spectrom.*, 1999, 34,1283.

[34]H.-F. Wu and Y.-P. Lin, *Eur. Mass Spectrom.*, 2000, in press.

[35]H.-F. Wu, *J. Mass Spectrom.*, 2000, in press.

[36]S.-A. Barshick and W. H. Griest, *Anal. Chem.*,1998,70, 3015.

Captions

Figure 1. structures of phthalic anhydride and its structural related compounds.

Figure 2. NCI spectra of 4,5- dichlorophthalic anhydride.

Figure 3. NCI spectra of 3,6- dichlorophthalic anhydride.

Scheme 1. Proposed mechanism for formation and CAD of $(M-H)^-$ of phthalimide.

Scheme 2. Proposed product structure for CAD of M^- of 3,4,5,6-tetrafluorophthalic anhydride using oxygen as reagent gas.

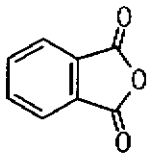

Phthalic anhydride

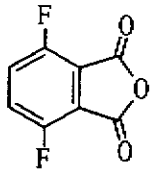

3,6-Difluorophthalic anhydride

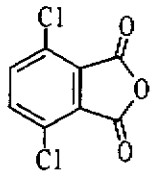

3,6-Dichlorophthalic anhydride

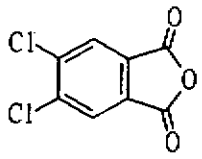

4,5-Dichlorophthalic anhydride

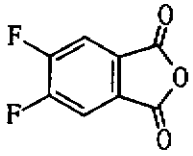

4,5-Difluorophthalic anhydride

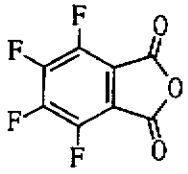

Tetrafluorophthalic anhydride

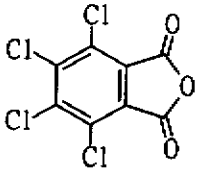

Tetrachlorophthalic anhydride

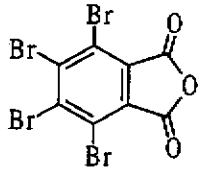

Tetrabromophthalic anhydride

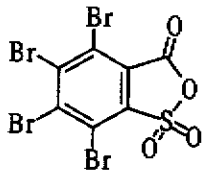

Tetrabromo-2-sulfobenzoic acid cyclic anhydride

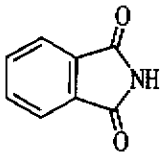

Phthalimide

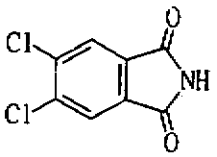

4,5-Dichloro phthalimide

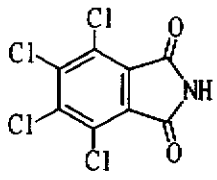

3,4,5,6-Tetrachloro phthalimide

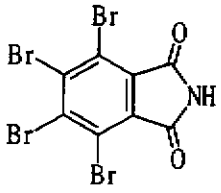

3,4,5,6-Tetrabromo phthalimide

Figure 1.

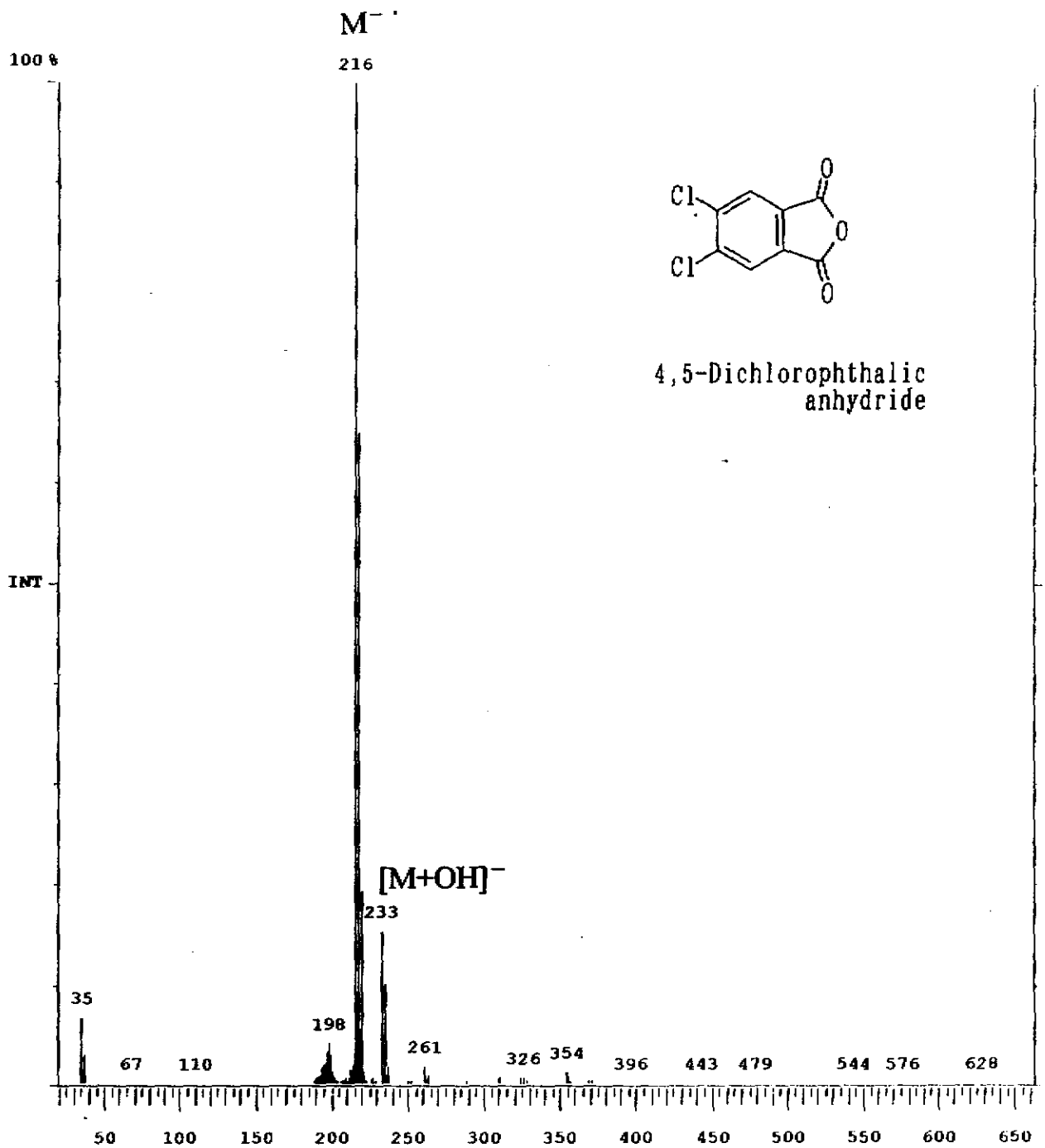
M⁻·
100 %
216
INT
[M+OH]⁻
233
35
198
261
67
110
326
354
396
443
479
544
576
628
50
100
150
200
250
300
350
400
450
500
550
600
650
Cl
Cl
O
O
O
4,5-Dichlorophthalic
anhydride

Figure 2

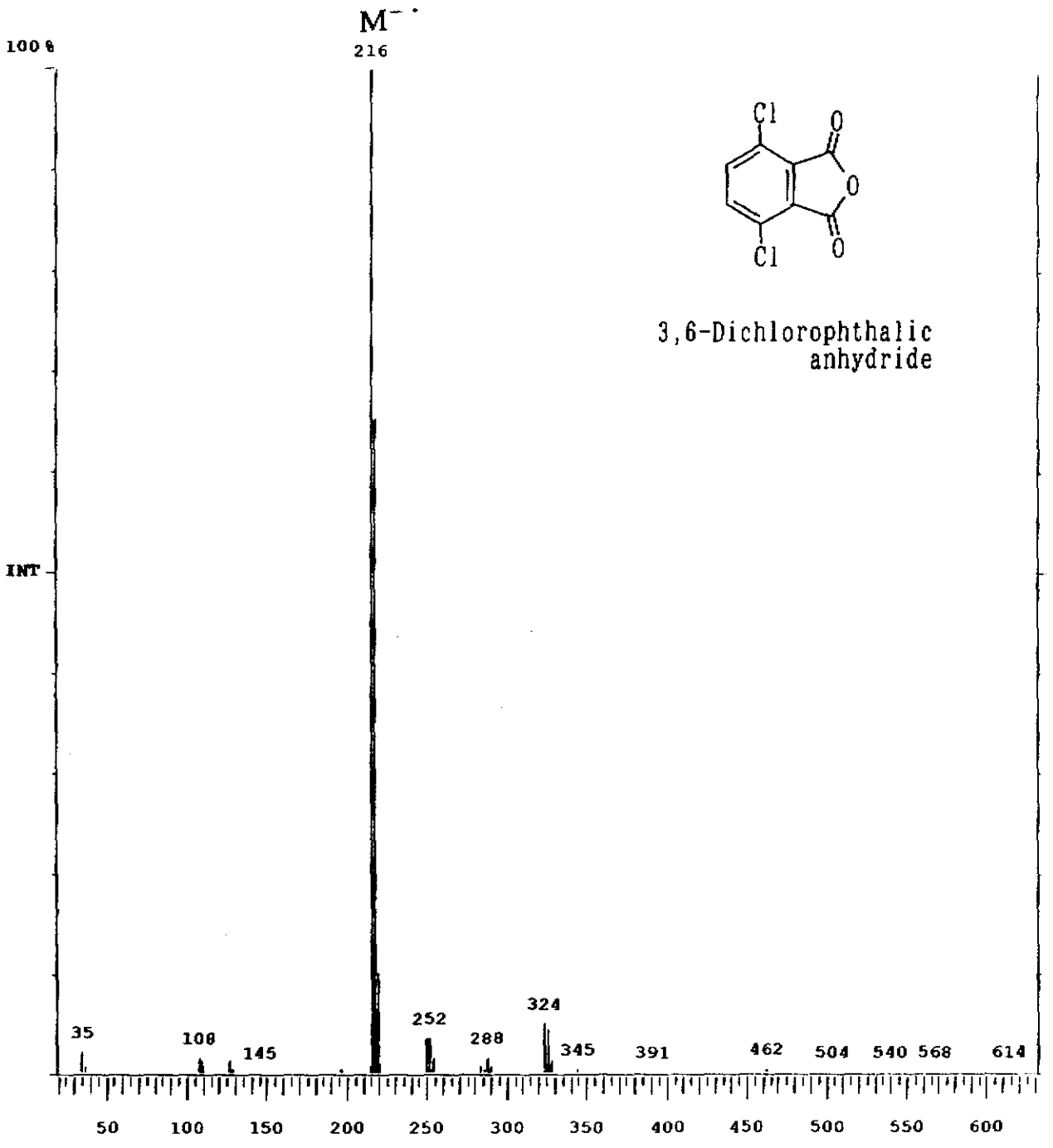
M⁻·
216
100 %
INT
Cl
O
O
O
Cl
O
3,6-Dichlorophthalic
anhydride
35
108
145
252
288
324
345
391
462
504
540
568
614
50
100
150
200
250
300
350
400
450
500
550
600

Figure 3

Phthalic anhydride (148)	$M^{-\cdot}$ 100%
3,6-Difluorophthalic anhydride (184)	$[2M-CO_2-CO-HF]^-$ (276,6%) $M^{-\cdot}$ 100% $[M-CO_2-CO]^-$ (112,8%)
3,6-Dichlorophthalic anhydride (217)	$[2M-CO_2-CO-HCl^{35}]^-$ (326,3%) $[2M-CO_2-CO-HCl^{37}]^-$ (324,3%) 288, 1% $[M-H+Cl^{35}]^-$ (252,3%) $[M-H+Cl^{37}]^-$ (250,3%) $M^{-\cdot}$ 100% Cl^- (37,1%) Cl^- (35,3%)
4,5-Difluorophthalic anhydride (184)	$[2M-CO_2-HF]^-$ (320,5%) $[M+OH]^-$ (201,6%) $M^{-\cdot}$ 100%
4,5-Dichlorophthalic anhydride (217)	$[2M-CO_2-HCl^{35}]^-$ (354, < 1%) $[2M-CO_2-CO-HCl^{35}]^-$ (326, < 1%) $[2M-CO_2-CO-HCl^{37}]^-$ (324, < 1%) $[M+OH]^-$ (233,18%) $M^{-\cdot}$ 100% $[M+OH-Cl^{35}]^-$ (198,4%) $[M+OH-Cl^{37}]^-$ (196,2%) Cl^- (37,3%) Cl^- (35,3%)
Tetrafluorophthalic anhydride (220)	$M^{-\cdot}$ 100%
Tetrachlorophthalic anhydride (286)	$M^{-\cdot}$ 100% Cl^- (37,43%) Cl^- (35,100%)
Tetrabromophthalic anhydride (464)	$M^{-\cdot}$ 20% $[M-Br^{79}]^-$ (385,95%) $[M-Br^{81}]^-$ (383,100%) Br^- (81,83%) Br^- (79,80%)
Tetrabromo-2-sulfobenzoic acid	

	$M^{-\cdot}$ <1%
	$[M-Br^{79}]^-$ (421,93%)
	$[M-Br^{81}]^-$ (419,100%)
	$[M-CO_2-SO_2]^-$ (392,40%)
	$[M-Br^{79}Br^{79}]^-$ (342,6%)
	$[M-Br^{79}Br^{81}]^-$ (340,15%)
	$[M-Br^{81}Br^{81}]^-$ (338,9%)
	$[M-CO_2-SO_2-Br^{79}]^-$ (313,13%)
	$[M-CO_2-SO_2-Br^{81}]^-$ (311,12%)
	$Br^{81}Br^{81-}$ (162,12%)
	$Br^{79}Br^{81-}$ (160,14%)
	$Br^{79}Br^{79-}$ (158,6%)
	Br^- (81,77%)
	Br^- (79,64%)
Phthalimide (147)	$[M-H]^-$ (146,100%)
4,5-Dichlorophthalimide (216)	$[2M-HCl^{35}]^-$ (396,73%)
	$[2M-HCl^{37}]^-$ (394,69%)
	$[2M-HCl^{35}-HCl^{35}]^-$ (360,6%)
	$[2M-HCl^{35}-HCl^{37}]^-$ (358,12%)
	$[M-H]^-$ 100%
	$[M-H-HCl^{35}]^-$ (181,10%)
	$[M-H-HCl^{37}]^-$ (179,38%)
	Cl^- (37,11%)
	Cl^- (35,21%)
3,4,5,6-Tetrachlorophthalimide (285)	$[2M-HCl^{35}]^-$ (534,10%)
	$[2M-HCl^{37}]^-$ (532,10%)
	$[2M-HCl^{35}-HCl^{35}]^-$ (498,1%)
	$[2M-HCl^{35}-HCl^{37}]^-$ (496,2%)
	$M^{-\cdot}$ 100%
	$[M-HCl^{35}]^-$ (249,82%)
	$[M-HCl^{37}]^-$ (247,65%)
	$[M-HCl^{35}-Cl^{35}]^-$ (214,<1%)
3,4,5,6-Tetrabromophthalimide (463)	$[2M-HBr^{79}]^-$ (846,<1%)
	$[2M-HBr^{79}-HBr^{81}]^-$ (764,<1%)
	$M^{-\cdot}$ 12%
	$[M-HBr^{79}]^-$ (383,93%)
	$[M-HBr^{81}]^-$ (381,100%)
	$[M-HBr^{79}-Br^{79}]^-$ (304,3%)
	$[M-HBr^{79}-Br^{81}]^-$ (302,5%)

[M+HBr+Br$^-$]	(300,27%)
Br^-	(81,50%)
Br^-	(79,50%)

Compound	Isolation	Fragment ions
3,6-Difluorophthalic anhydride (184)	$[2M-CO_2-CO-HF]^-$(276)	$-CO_2$ (232,100%)
		$-(CO_2+CO)$ (204,5%)
	$M^{-\cdot}$(184)	$-(CO_2+CO)$ (112,100%)
		96 4%
		76 7%
	$[M-CO_2-CO]^-$(112)	76 100%
4,5-Difluorophthalic anhydride (184)	$[2M-CO_2-HF]^-$(320)	-CO (292,70%)
		$-(CO_2+CO)$ (248,100%)
	$[M+OH]^-$(201)	$-CO_2$ (157,100%)
		$-2CO_2$ (113,55%)
	$M^{-\cdot}$(184)	-CO (156,100%)
		$-(CO_2+CO)$ (112,6%)
4,5-Dichlorophthalic anhydride (217)	$[M+OH]^-$(233)	$-CO_2$ (189,100%)
	$M^{-\cdot}$(217)	$-Cl^{35}+O$ (199,36%)
		$-Cl^{37}+O$ (197,100%)
	$[M+OH-Cl^{35}]^-$(198)	-CO (170,100%)
		$-(CO_2+CO)$ (126,29%)
Tetrafluorophthalic anhydride (220)	$M^{-\cdot}$(220)	-27 (193,7%)
		$-(CO_2+CO)$ (148,100%)
		$C_4F_4^-$ (124,8%)
		$C_4F_2^-$ (86,4%)
Tetrachlorophthalic anhydride (286)	$M^{-\cdot}$(286)	-CO (242,3%)
		$-Cl^{35}Cl^{35}$ (216,23%)
		$-Cl^{35}Cl^{37}$ (214,100%)
		Cl^- (35, 100%)
		Cl^- (37, 13%)
Tetrabromophthalic anhydride (464)	$M^{-\cdot}$(464)	$-Br^{79}$ (385,73%)
		$-Br^{81}$ (383,100%)
Tetrabromo-2-Sulfobenzoic acid cyclic anhydride (500)	556	$-CO_2$ (512,100%)
	$M^{-\cdot}$(500)	$-CO_2$ (456,50%)
		$-Br^{79}+O$ (437,50%)
		$-Br^{81}+O$ (435,100%)
		$-Br^{79}$ (421,24%)
		$-Br^{81}$ (419,23%)

		-($Br^{79}Br^{79}$+O) (358,4%)
		-($Br^{79}Br^{81}$+O) (356,7%)
		-($Br^{81}Br^{81}$+O) (354,4%)
		-(SO_2+CO_2+Br^{79})+O (329,9%)
		-(SO_2+CO_2+Br^{81})+O(327,9%)
		-(SO_2+CO_2+Br^{79}) (313,4%)
		-(SO_2+CO_2+Br^{81}) (311,4%)
	[M-Br^{79}]$^-$(419)	-SO_2 (355,20%)
		-(SO_2+CO_2) (311,100%)
	[M-CO_2-SO_2]$^-$(392)	-Br^{79} (313,80%)
		-Br^{81} (311,100%)
		239 8%
		$Br^{79}Br^{79-}$ (162,17%)
		$Br^{79}Br^{81-}$ (160,50%)
		$Br^{81}Br^{81-}$ (158,22%)
	[M-CO_2-SO_2-Br^{79}]$^-$(313)	$Br^{79}Br^{81-}$ (160,3%)
		Br^- (81,100%)
		Br^- (79,20%)
Phthalimide (147)	[M-H]$^-$(146)	NCO^- (42,100%)
4,5-Dichloro phthalimide (216)	[2M-HCl^{37}]$^-$(394)	-HCl^{35} (358,100%)
	[2M-HCl^{35}-HCl^{37}]$^-$(358)	-CO (330,80%)
		-Cl^{35} (323,100%)
	[M-H]$^-$(215)	-HCl^{35} (179,100%)
	[M-H-HCl^{37}]$^-$(179)	-Cl^{35} (144,100%)
3,4,5,6-Tetrachloro phthalimide (285)	[2M-HCl^{35}]$^-$(534)	-HCl^{35} (498,100%)
		-HCl^{37} (496,90%)
		-(HCl^{35}+CO) (470,80%)
		-(HC^{37}+CO) (468,55%)
	[2M-HCl^{35}-HCl^{37}]$^-$(496)	-CO (468,100%)
	$M^{-\cdot}$ (285)	-HCl^{35} (249,100%)
		-HCl^{37} (247,83%)
		-(HCl^{35}+Cl^{35}) (214,8%)
		-(HCl^{35}+Cl^{37}) (212,6%)
	[M-HCl^{35}]$^-$(249)	-Cl^{35} (214,66%)
		-Cl^{37} (212,100%)
3,4,5,6-Tetrabromo phthalimide (462.7)	$M^{-\cdot}$ (463)	-HBr^{79} (383,100%)
		-HBr^{81} (381,92%)
		-(HBr^{79}+Br^{79}) (304,7%)
		-(HBr^{79}+Br^{81}) (302,22%)

	-(HBr +Br) (300,11%)
$[M\text{-}HBr^{81}]^-$(381)	$-Br^{79}$ (302,100%)
$[M\text{-}HBr^{79}\text{-}Br^{81}]^-$(302)	$-HBr^{79}$ (222,100%)

Table 3. CAD results of ECD by using oxygen as reagent

Compound ions	Isolation	Fragment
4,5-Dichlorophthalic anhydride (217)	$[M\text{-}Cl^{35}+O]^-$(197)	$-CO_2$ (153,100%) $-(CO_2+CO)$ (125,41%)
Tetrafluorophthalic anhydride (220)	$M^{-\cdot}$	$C_5F_3O^-$ (133,73%) $C_4F_4^-$ (124,57%) $C_4F_3^-$ (105,71%) $C_4F_2O^-$ (102,41%) $C_3F_3^-$ (93,22%) $C_4F_2^-$ (86,100%) $C_3F_2^-$ (74,8%)
Tetrachlorophthalic anhydride (286)	$M^{-\cdot}$	$-Cl^{35}+O$ (267,100%) $-Cl^{37}+O$ (265,49%) $-(Cl^{35}+CO_2)+O$ (223,4%) $-(Cl^{37}+CO_2)+O$ (221,1%)
	$[M\text{-}Cl^{35}+O]^-$(267)	$-CO_2$ (221,100%) $-(CO_2+CO)$ (193,28%)
Tetrabromophthalic anhydride (464)	$M^{-\cdot}$	$-Br^{79}+O$ (401,100%) $-Br^{81}+O$ (399,42%) Br^- (81,7%) Br^- (79,6%)
	$[M\text{-}Br^{81}+O]^-$(399)	-45 (354,100%) $-(CO_2+CO)$ (327,35%)

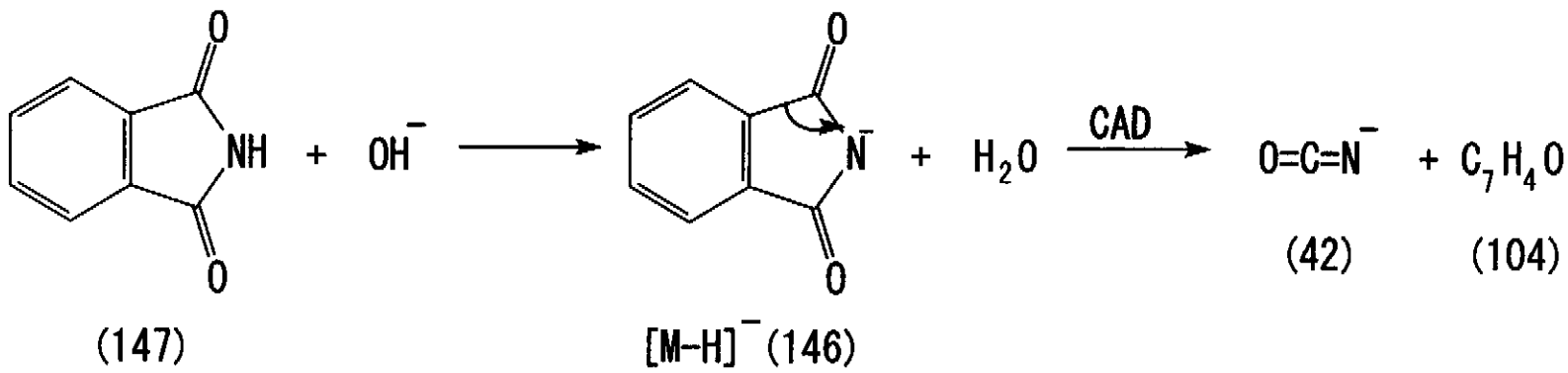

Scheme.1

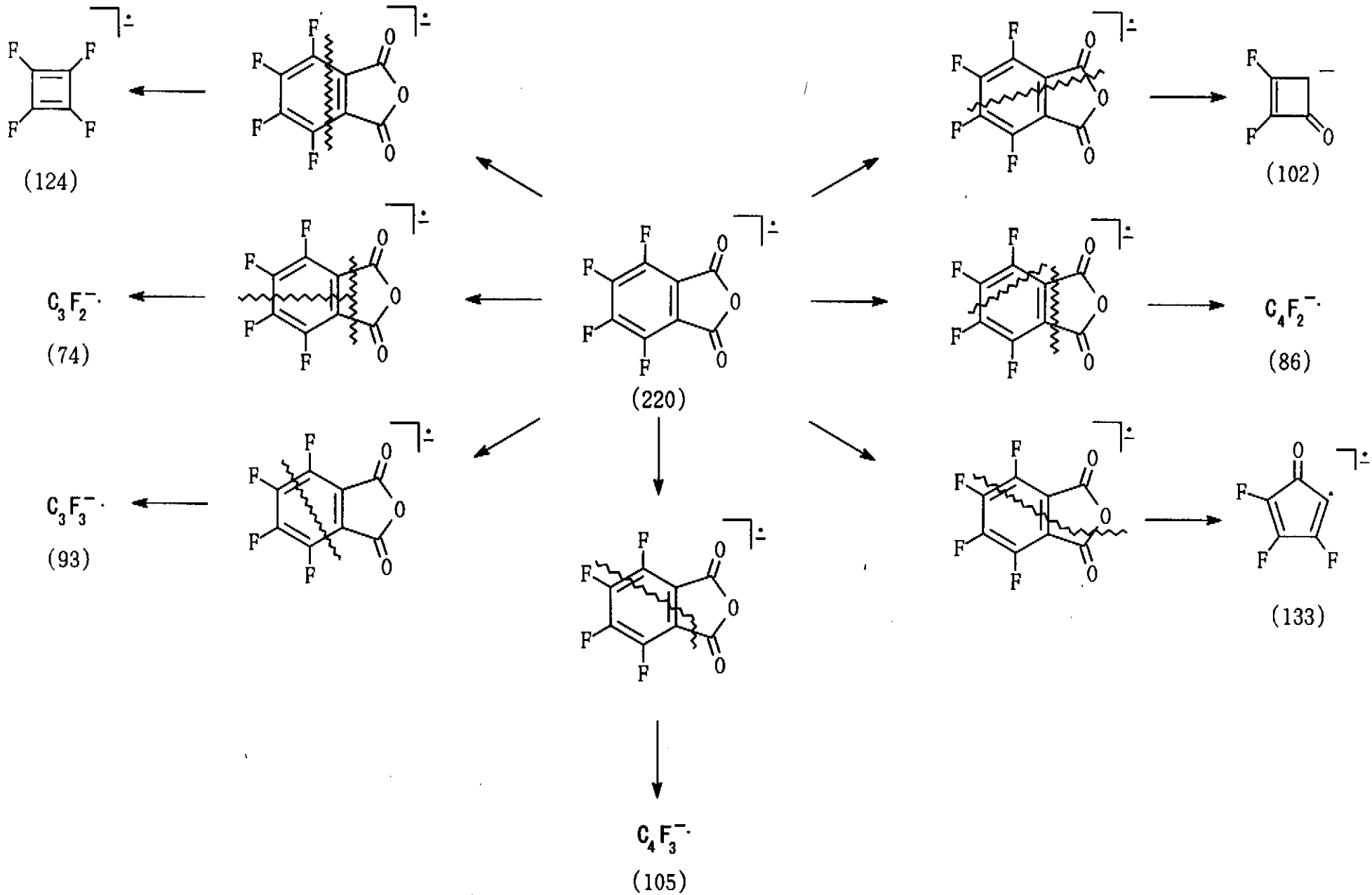

Scheme. 2

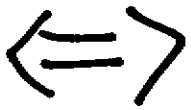

Ion-Molecule Reactions and Collisional Activated Dissociation of Tricyclic Antidepressants in an External Source Ion Trap Mass Spectrometer

Hui-Fen Wu* and Miao-Chun Chung
Department of Chemistry
Tamkang University
Tamsui, Taipei Hsien, 25137, Taiwan, R. O. C.

Abstract:

In this project, we use a series of tricyclic compounds including Iminodubenzyl, Imipramie, Desipramine, Nortriptyline and Amitripyline. Those above-mention compounds are able to treat the disease like melancholia. The instrument, which we used was a Finnigan MAT GCQ ion trap mass spectrometer, equipped with an external EI/CI source. The instrument was operated in the mass-selective instability mode to analysis and detects product ions. We used DME (dimethyl ether) as CI reagent gas and it could produce m/z=45 ($CH_3OCH_2^+$) and m/z=47 ($(CH_3)_2OH^+$) reagent ions in the ion source region. Then reacted with those series of tricyclic compounds and produce product ions including $[M+H]^+$, $[M+13]^+$, $[M+15]^+$, $[M+45]^+$, $[M+47]^+$. By using CAD (Collision Activated Dissociation) technique to make sure the products structure and understand their pathways of dissociation. The GCQ instrument possesses the excellent ability to low abundance ions, so those product ions still are isolated and CAD experiments undertaken successfully. All of these tricyclic compounds can produce $[M+H]^+$, $[M+13]^+$, $[M+15]^+$, $[M+45]^+$, $[M+47]^+$ ions. And all of these reactions can occur in all of the reaction sites by competing with each other. From the results of ion-molecular reactions, we know that the reaction sites including the double bond at carbon-1'in the side chain or the nitrogen atom at the end of side chain influenced the reaction results so huge. For example; from the CAD results, the compounds with secondary amine at the end of side chain will dissociate neutral molecular like CH_3NH_2 or CH_3NCH_2. But if at the end of side chain is tertiary amine, it will drop $(CH_3)_2N$ or $(CH_3)_3N$ or lost entire side chain structure which could be observed and get 195u, 194u, 193u or 191u ions. In this project, we also used theoretical calculation to calculate the heats of formation (ΔHf) and heats of reactions ($\Delta Hrxn$) in order to know the best site of ion-molecular reaction. At last, by using different temperature in order to know the temperature effect of the ion-molecular reaction.

Introduction:

In the drug structure, different kind of functional group and reactive site played the important role of medication and influence it so much. In this research, by using a series of tricyclic compounds, including

Iminodibenzyl, Imipramine, Desipramine, Nortriptyline and Amitripyline which are used to be TCA (tricyclic anti-depressants). Doctor used this series of drugs to treat diseases about melancholia. By using this sieries of important drugs reacted with Dimethyl ether (DME) in order to know the relationship between functional groups and reactivity further. Those five compounds are similar to each other but still have some difference in detail. Various substituents and functional groups on the drug strongly influence their reactivity. Thus, it is important for us to understand the relationship between the drug structure and their reactivity.

As we know, Tandem mass spectrometry is a very sensitive, rapid and powerful tool that can provide us detailed information about structure, functional groups and substituents. This project which have performed by using a Finnigan MAT GCQ ion trap mass spectrometer, equipped with an external EI/CI source. Using DIP (Direct Insertion Probe) system transferred the tricyclic compounds. Dimethyl ether (DME) was used as the CI reagent gas, because it is previously shown to have striking functional group selectivity as a chemical ionization reagent for other organic system. The reactive ions formed are protonated DME, at m/z=47($CH_3O^+HCH_3$) and the methoxymethylene cation ($CH_3O^+=CH_2$), at m/z=45. In an external ion trap mass spectrometer (ITMS), ion/molecular reactions of ($CH_3O^+=CH_2$) with substituted aromatics result in formation of $[M+13]^+$ or $[M+15]^+$ adduct depending on the neutral of the substituents.

In this experiment, these five tricyclic compounds can get a series of protonated ions. They are $[M+13]^+$, $[M+15]^+$, $[M+45]^+$, $[M+47]^+$...and etc. And then combined with CAD (Collision Active Dissociation) technique, to conform the parent ion structure and understand the pathways of dissociation. The Finnigan MAT GCQ instrument possesses the excellent ability to perform on low abundance ions. These product ions could still be isolated and the CAD experiment can be undertaken successfully.

After CAD experiment, use semi-empirical calculation software (Hyper-Chem5.1 ,Hyper-cube .Inc., Gainesville , Florida) to estimate the heats of both the formation (ΔHf) and reaction ($\Delta Hrxn$) of the tricyclic compounds and derive reaction mechanisms in order to determine the possible reactive sites for ion/molecular reaction .By using this theoretical calculation data not only to know the best formation sites

of ions but also to conform the reactive sites and reactive mechanisms which were surmised via CAD results .And use different temperature in order to know the influences of these tricyclic compounds.

Experiment:

In this project, we used a Finnigan MAT GCQ ion trap mass spectrometer, equipped with an external EI/CI source. The instrument was operated in the mass-selective instability mode to analysis and detected product ions. Dimethyl ether was used as CI reagent gas. It could produce m/z=45 and m/z=47 reagent ions in the ion source region. In this experiment, we used DIP (Direct Insertion Probe) system to heat and transferred our compounds into ion source region. The heating range of these series of tricyclic compounds was controlled between 190°C and 240°C, except for Iminodibenzyl, which is controlled at 120°C. We set the temperature climbing rate as 100°C/min, and the pressure of He buffer gas in the instrument was about 1mtorr .The pressure of DME in the ion source region was 8×10^{-5} torr and the ion injection time (from source to mass analyzer) set to 0.3~25msec. The time of scan was 10msec.The temperature of the source region was maintained at 200°C and transferline was 275°C. Signal width for selection of the parent ions was from 0.5~1amu and the collision voltage range of CAD was between 0.5 and 1.2volt. The collision activation time (tickle time) was 15ms. The theoretical calculation software was Hyper-chem Ver 5.1 (Hyper-cube. Inc., Gainseville, Florida) and use AM1 as calculation mode. **The temperature effect of Nortriptyline:** we adjusted the temperature in the ion source region as 100°C, 150°C, 180°C, 200°C, 225°C and transferline was 275°C. We use these series of tricyclic compounds in this project including Iminoebenzyl, Imipramine, Desipramine, Nortiptyline, Amitripyline were purchased from Sigma Chemical Company (St Louis MO) and dimethyl ether was obtained from Aldrich Chemical Company (Milwaukee, WI)

Results and Discussion:

Chemical ionization (CI) has recognized as a soft ionization technique. It should not produce extensive fragment ions, but there are a lot of fragment ions in the spectrum. The reason for that could be the temperature, which in the ion source region is almost to 200°C. The ions might be influenced by high

temperature and further, by using the external ionization, the three lenses guided and accelerated the ions to enter the instrument. At the same time the ions also got high energy and easy to produce fragment ions by collision with other ions. In the ion-molecular reaction, the dimethyl ether ions reacted with those tricyclic compounds and produced a series of ion-molecular product ions including $[M-H]^+$, $[M+H]^+$, $[M+13^+$, $[M+15]^+$, $[M+45]^+$, $[M+47]^+$ and fragment ions. The series of product ions were listed in Table-1. From the Table-1; we knew the relative intensity (%) for each product ion clearly. According to relative intensity, we could understand further the trend of stability of product ions for each tricyclic compound. By using the CAD technique to determine the pathways of dissociation and get the information about neutral losses. Table-2 listed CAD product ions of various parent ions formed by ion-molecular reactions of tricyclic compounds with dimethyl ether ions.

In this experiment, we used Hyper Chem 5.1 software to estimate the heats of formation (ΔHf) and heats of reaction ($\Delta Hrxn$) in order to know the possible reactive sites and determine which site will be attack easily by dimethyl ether ions. At last we know that by changing temperature and pressure influenced the results so much, we use different temperature to make sure the influences of ion-molecular reactions for tricyclic compounds and dimethyl ether ions.

I. Theoretical Calculation:

In this part, we use theoretical calculation to explain the results of this experiment. According to the results of calculation the heats of reaction ($\Delta Hrxn$) and heats of formation (ΔHf), we can understand the most possible pathway of the ion-molecular reactions and the stability of the ion structures. The calculation software which was used is Hyper Chem 5.1 (Hypercube. Inc., Gainesville, Florida), and used semi-empirical AM1 as calculation mode. Form the results of theoretical calculation in Table-3 to Table-6; we knew that these five tricyclic compounds could produce a series of ions including $[M+13]^+$, $[M+15]^+$, $[M+45]^+$, and $[M+47]^+$. Since their heats of reactions are negative, it can divide into two pathways; they are ΔHo (overall) and ΔHs (steps). ΔHo : Represents the heats of reactions from the direct formation of the ions from resultants and, and ΔHs : Represents the heats of reaction from the dissociation of the intermediate ions already formed.

The semi-empirical calculations were used to assist in the determination of protonation sites. The calculation results of $[M+H]^+$ are listed in Table-6. From the Table-6, compare the ΔHs with ΔHo , we can find one thing that in Nortriptyline the values of ΔHs and ΔHo are similar to each other (ΔHs: -25 KJ/mole; ΔHo :-8KJ/mole). So they may have two possible reactive pathways (Step and Overall) when the reactive sites of protonation is proposed base on the amino group (N-protonation) in Nortriptyline. Form Table-6, we can know the major reactive sites of the $[M+H]^+$ ions. When the 5th position in tricyclic structure is nitrogen (N), including Iminodibenzyl, Imipramine and Despramine , then the protonation reactions can occur in both of the double bond and nitrogen atom. But when the 5th position in tricyclic compounds is carbon atom with double bond structure, including Nortriptyline and Amitriptyline, then the protonation reactions can not occur in double bond in tricyclic structure easily except for Amitriptyline. Because the heats of formation and heats of reaction in double bond and Nitrogen atom for Amitriptyline are similar to each other (-13 KJ/mole: -14KJ/mole). The protonation reactions were easily take place in both of these two locations.

The heats of formation and heats of reaction for $[M+13]^+$ ions were estimated in Table-4. Form Table-4, for these series of tricyclic compounds, we know that the values of ΔHo are similar to ΔHs, which indicates that the formation of $[M+45]^+$ intermediate ions is stable. This agrees with the experiment results since the relative intensity of $[M+45]^+$ ions for these series of tricyclic compounds are very strong (Table-1). For Iminodibenzyl, the formation sites of $[M+13]^+$ will be occurred in both of the double bond at carbon-4 and nitrogen-5, because the values of ΔHo at carbon-4 with double bond (-17KJ/mole) and at nitrogen-5 (-17KJ/mole) are very small and similar. For Imipramine and Desipramine, when the reactions occur in the double bond at carbon-4, by catching the hydrogen atom to form double bond and produce $[M+13]^+$ ions or catching the hydrogen atom at carbon-1' in side chain to produce cyclic form. For the Nortriptyline and Amitriptyline in Table-4, the values of ΔHs and ΔHo are all very small in each reactive site, which indicated that the formation of $[M+45]^+$ intermediate ions is stable. On the other words, it will produce a great lot of stable $[M+45]^+$ ions and their relative intensity are also very strong (Nortriptyline: 100%; Amitriptyline: 100%) as shown in Table-1.

Form Table-5, the major reactive sites that can produce $[M+15]^+$ ions in Iminodibenzyl are at carbon-4 on the tricyclic ring. For Imipramine and Desipramine, the major reactive sites are possible at carbon-4 on the tricyclic ring or at nitrogen-3' atoms in side chain. Because the values of ΔHo in different sites are similar to each other. But in both of the Nortriptyline and Amitriptyline, the major reactive sites are at nitrogen-3' atoms in side chain (-31 KJ/mole; -43 KJ/mole) and the minor reactive sites are at carbon-1' atoms in side chain (-12 KJ/mole; -13 KJ/mole). From Table-5, we know that the values of ΔHo are much lower than ΔHs , it's mean that the $[M+15]^+$ ions were directly produced without via formation of $[M+45]^+$ intermediate ions.

II-1. CAD Of the pre-trap fragment ions:

Chemical ionization is a soft ionization method that will not produce extensive fragment ions, but we still could see that there are a lot of fragment ions in our spectrum. According to Brodbelt's studies, in the traditional internal ionization of the ion trap, there were few fragment ions in the CI spectrum by using dimethyl ether (DME) as reagent gas and helium as buffer gas. The ions in the ion trap will collision with the 1 mtorr of He buffer gas, and transfer their internal energy to the buffer gas, and make the ions more stable. So none or very few fragment ions were produced in CI mass spectrum.

After analyzed those fragment ions which should not appear on our ion-molecular reaction spectrum by using CAD technique, we can find out that most of the fragment ions were dissociated from the product ions including $M^{+\cdot}$, $[M+H]^+$ and a little from $[M+13]^+$. We can find that some fragment ions of $[M^+]$, [M+H]+ and $[M+13]^+$ were observed in the CI mass spectrum by using a Finnigan MAT GCQ ion trap mass spectrometer, equipped with an external CI source. Compare it with the Source CID in Triple quadrupole instrument, their results are similar to each other, because the GCQ instrument could perform MS/MS on low abundance, and the product ions could be isolated to do CAD experiment. Thus, the mechanism for the reactions of dimethyl ether with the series of tricyclic compounds could be elucidated in detail.

II-2. CAD of $M^{+\cdot}$ ions:

From the CAD spectra of $M^{+\cdot}$ ions of Iminodibenzyl (figure 6), we knew that the Iminodibenzyl

without including side chain has two different pathways of dissociation; losing CH_3· or C_2H_4 molecular. The m/z=180 (100%) was the major product ions which dissociated from the parent ions ($M^{+\cdot}$) with m/z=195 .The $M^{+\cdot}$ (m/z=195) ions lost one methyl group (CH_3·) in order to form more stable molecular (m/z=180) and it's relative intensity is very strong. From the spectra of ion-molecular reaction products of Iminodibenzyl (Figure 1), the peak of $[M\text{-}CH_3]^+$ was also observed, but it's relative intensity is only about 10%. From figure 2, we got a peak (m/z=235) and it's relative intensity is 100%. Comparing m/z =235 in the ion-molecular reactions spectra with CAD results of $M^{+\cdot}$ ions of Imipramine (Figure 7), we conformed that it was $[M\text{-}(CH_3)_2NH]^+$. And the $M^{+\cdot}$ ions of Imipramine lost a lot of 86u neutral molecular to produce m/z=194 (100%) fragment ions. The $M^{+\cdot}$ (m/z=280) ions of Despramine also lost a lot of 71u neutral molecular and $(CH_3)NH_2$ group to produce fragment ions at m/z=195 and 235. From the Nortriptyline, this compound belongs to secondary amine structure. According to the CAD results of $M^{+\cdot}$ of Nortriptyline , it will lose CH_2NH and then subsequent loss of CH_3· molecular or drop the CH_3· molecular directly. The Amitriptyline with tertiary amine structure lose $[(CH_3)_3]N$ and produce 149u product ions.

II-3. CAD of $[M+H]^+$ ions:

The possible reactive sites of protonation reaction for these series of tricyclic compounds, which reacted with dimethyl ether, could be the double bond (at carbon-4 or carbon-1') or nitrogen atom (at nitrogen-5 or nitrogen-3'). Not only by using the CAD technique to determinate the dissociation pathways of the fragment ions, but also using the theoretical calculation as assist tools. Form the calculation results, which were listed in Table-6, since ΔHo values are much lower than ΔHs, so we can understand that these five tricyclic compounds reacted with $CH_3O^+HCH_3$ (m/z= 47) and directly produce protonation ion $[M+H]^+$, without forming stable intermediate ions $[M+47]^+$ first. For Iminodibenzyl in figure-6, the CAD results of $[M+H]^+$ ions showed that by losing a CH_3· molecular to produce stable m/z= 181 fragment ions. We could suppose that the reaction sites of protonation reaction might be at carbon-4 with double bond which would catch the hydrogen atom and lose CH_3OCH_3 molecular in order to form $[M+H]^+$ protonation ions. By using theoretical calculation results of $[M+H]^+$ of Iminodibenzyl in Table-6 in order to conform our assumption. In Table-6, there are two possible reactive sites, which are at the

carbon-4 with the double bond and nitrogen-5 on the tricyclic ring. The values of ΔHo at carbon-4 with the double bond (-8 KJ/mole) and nitrogen-5 (-10 KJ/mole) on the ring are all very small and similar. It means that those two reactive sites are easy to perform protonation reaction and confirm our assumption.

In the figure 4, the protonation Nortiptyline ion was followed by the elimination of CH_3NH_2 gives the m/z=233 ions. In the CAD spectra of $[M+H]^+$ ions for Nortriptyline, we can also got a peak (m/z=233) which relative intensity is very strong (100%). It tells us that the protonation Nortiptyline ions would lose one CH_3NH_2 molecular in order to form more stable ion-molecular ions which is $[M- CH_3NH_2]^+$ fragment ions. The same situation also could observe in Imipramine and Desipramine.

II-4. CAD of $[M+45]^+$ and $[M+47]^+$ ions:

For these series tricyclic compounds, all of the $[M+47]^+$ ions have low relative intensity (<1% or1%). However, since the GCQ instrument possesses the excellent ability to perform MS/MS on low abundance ions, we can get the CAD results of $[M+47]^+$ ions of Iminodibenzyl and nortriptyline (Table-2). For example; After the CAD experiments of $[M+47]^+$ and $[M+45]^+$ ions of Nortiptyline, the $[M+47]^+$ ions will lose CH_3OH molecular first and then subsequent loss of one molecular of CH_3NH_2 or CH_3NCH_2. The $[M+45]^+$ ions will also lose CH_3OH molecular first and then subsequent loss of one molecular of CH_3NH_2 or CH_3NCH_2 or $CH_3NHCHCH_2$. Containing tertiary amine structure at the end of side chain including Imipramine and Amitriotyline (Table-2) will lose CH_3OH or CH_2O first and then subsequent loss of $(CH_3)_3N$ or $(CH_3)_2NH$ and lose C_2H_4 at last. The Desipramine will lose CH_3OH and then lose $CH_3NHCHCH_2$ or CH_3NHCH_2 or not lose CH_3OH instead of losing $CH_3NHCH_2CH_3$ directly.

The Nortriptyline will lose CH_3OH first and then subsequent loss one molecular of $(CH_3)NH_2$ to produce m/z=245 ions or drop the $CH_3NHCH_2CH_3$ molecular to produce m/z=219 ions. But another possible reactive pathway of Nortriptyline is loss one molecular of CH_3NCH_2 to produce m/z=233 ions. Form the CAD spectra of $[M+45]^+$ ions of Iminodibenzeyl (firure 6), we can see m/z=208 ions obviously which is produced by losing one CH_3OH molecular. And the CAD results of $[M+47]^+$ ions of Iminodibenzyl, by losing CH_3OH and 47u molecular to produce 210u and 195u ions.

Compare these five tricyclic compounds with each other, we can conclude one important thing that

by losing one molecular of CH_3OH, the $[M+47]^+$ ions will produce $[M+15]^+$ ions. And the CAD of $[M+45]^+$ ions of compounds which contain secondary amine structure will lose CH_3OH to produce $[M+13]^+$ ions. Containing tertiary amine structure at the end of side chain including Imipramine and Amitriptyline will form $[M+15]^+$ or $[M+13]^+$ ions and then lose $(CH_3)_3N$ or drop $(CH_3)_2NH$ molecular to produce fragment ions which relative intensity is very strong.

II-5. CAD of $[M+13]^+$ and $[M+15]^+$ ions:

Containing tertiary amine structure at the end of side chain including Imipramine and Amitriptyline, we can understand the pathways of dissociation from the CAD spectra of $[M+13]^+$ ions. By catching a proton from neighboring carbon, the Imipramine will lose one $(CH_3)_3N$ and $(CH_3)_2NCHCH_2$ neutral molecular and then subsequent loss of $CH_3^{\cdot}$ molecular. For Amitripyline, the loss of $(CH_3)_2NHCHCH_2$ can be observed and then continued to lose one molecular of $CH_3^{\cdot}$ or 30u, otherwise we also can see the loss of $(CH_3)_2NHCHCH_2$. Compounds which contained secondary amine at the end of side chain including Desipramine and Nortriptyline, the methylene substitution reactions can occur in this secondary amine at the end of side chain and lose one molecular of CH_3NCH_2. The Iminodibenzyl, which do not contain side chain, will lose $CH_3^{\cdot}$ or C_2H_4 molecular. The $[M+13]^+$ and $[M+15]^+$ ions of these five tricyclic compounds, the $[M+13]^+$ ions could dissociate from $[M+45]^+$ ions, and the $[M+15]^+$ ions could dissociate from $[M+45]^+$ or $[M+47]^+$ ions. For example; for Desipramine and Nortriptyline, the dissociation pathways of forming $[M+13]^+$ ions of Desipramine could see in Scheme 1(A-B) and the dissociation pathways of forming $[M+13]^+$ and $[M+15]^+$ ions of Nortriptyline is list in Scheme 2 (A-E). In those five tricyclic compounds, for Iminodibenzyl which do not contain side chain structure, the $[M+15]^+$ and $[M+13]^+$ ions are a little similar with $[M+H]^+$ and $M^{+\cdot}$, because those above-mention ions are all easy to lose $CH_3^{\cdot}$ molecular. Otherwise, the other four compounds which all contain side chain structure can divide into two groups by determination the order of the amine at the end of side chain; secondary amine and tertiary amine. For the tertiary amine at the end of side chain including Imipramine and Amitripyline, we can find that it is easy for $[M+15]^+$ ions to drop $(CH_3)_3N$ after the CAD experiments. For the secondary amine at the end of the side chain including Desipramine and Nortriptyline, the CAD of

$[M+13]^+$ and $[M+15]^+$ ions of Desipramine are easy to lose 57u molecular. But after the CAD of $[M+15]^+$ and $[M+13]^+$ ions of Nortriptyline, we get the neutral loss of CH_3NHCH_3 and 83u molecular and their relative intensity are all very strong.

III. The temperature effect for formation of the ion-molecular products in the source region:

In this part, we control the ion source temperature at 100°C, 150°C, 180°C, 200°C, 220°C in order to observe the temperature effect on the ion-molecular reactions of Nortriptyline with DME ions was evaluated in the external chemical ionization source of the ion trap. The ion trap mass analyzer was not temperature controlled. The relationship between the relative intensity and different temperature are shown in Table-9. The results show that the temperature effect varied depending on the specific ions. From the results, some ions show a negative trend with temperature. The relative intensity of ion-molecular product ions including $[M+13]^+$, $[M+15]^+$, $[M+45]^+$, $[M+47]^+$ decrease with increasing temperature. But some fragment ions like 193u, 233u, 245u seem not to depend too much on temperature variation, the reason for that may be due to the ions themselves. Those fragment ions including 193u, 233u, 145u, are very easy to dissociate anytime, so they are not much influenced by temperature changing. Form Table-9, the relative intensity of fragment ions including 220u, 203u, 202u decrease with increasing temperature until 200°C, at which temperature, there is a significant increase in their intensity. The reason may be due to the fact that at this temperature, ions may experience more energetic collision and make a great lot of fragment ions. But when the temperature reaches 225°C, for some fragment ions like 220u, 202u, 203u, the thermal degradation phenomenon could be observed. We suppose that in this high temperature, the fragment ions dissociate again and again by more powerful collisions and decrease their intensity.

IV. Conclusion:

In this research, for those series of tricyclic compound, the different functional group or different order of amine at the end of side chains structure will influence the CAD results so much. For example; a

compound with secondary amine at end of side chain will produce $[M+13]^+$ more easily or when the functional group at 5th position on ring is nitrogen, it will trend to produce $[M+45]^+$ and $[M+47]^+$ ions and take advantage of forming cyclic structure. Compare Nortriptyline with the other tricyclic compounds, the reactivity of Nortriptyline is more excellent than the other tricyclic compounds. This is why we choose Norteiptyline as sample to do temperature effect experiment. We use Nortriptyline as sample to react with DME ions at different temperature in order to understand the influences of the reactivity. Beside, by combination of the mechanisms proposed for CAD and the theoretical calculation method, the possible reactive sites for formation of ion-molecular products could be determined. By the way, although the abundance of our ion-molecular products of $[M+13]^+$, $[M+15]^+$, $[M+45]^+$, $[M+47]^+$ were very small, the GCQ ion trap mass spectrometer possesses excellent tandem mass capability and low detection limits for CAD. Form the experiment of temperature effect, we can find that by changing the temperature can influence the formation of adduct ions and fragment ions a lot. When the temperature is rising, the adduct ions were influenced a lot by temperature and trend to dissociate, so the intensity of adduct ions become small. Study of this project can understand the reactivity of the drug structure and relationship between different kind of function group and different reactive site. Those above-mention results can help us to research new drug or develop the derivatives of these series tricyclic compounds. This research can provide all circles the information about some important drug structures and reactive sites.

參考資料：

1. H.Hopkala and G.Misztal . *Pharmazie.*, **1996**,51, 96.
2. D.J.Sequeira and H.W.Strobl, *J.Chromatogr.B.*, **1995**, 673,251.
3. K.Johnsen and K.E.Rasmussen, *J.Pharmecut.Biomed.*, **1998**, 1159-1169.
4. A. Aumatell and R.J. Wells, *J.Chromatogr.B.* **1995**, 669,331.
5. Z.Wang and W.G.Mcgimpsey, *J.Phys.Chem* , **1993**, 38,9668-9672.
6. P.Ghahramani, M.S.Lennard, *J.Chromatogr.B.*, **1996**, 685, 307.

7. S.Ulrich and J.Martens, *J.Chromatogr.Biomed.Sci.Appl.*, **1997,** 696, 217 -234.

8. T.Fujii,Y.Kurihara,H.Arimoto and Y.Mitsutsuka, *Anal.Chem.*, **1994,** 66, 884-1889.

9. M.Schafer , H.Budziewicz and H.Brzezinka ,*Spect.Int.J.*, **1997,** 213-226.

10. A. Rubello,G.Volpe and D. Favretto, *Ripad.Commun.Mass.Spectrom.*, **1996,** 1097-1102.

11. J. S. Brodbelt, J. N. Louris and R. G. Cooks, *Anal. Chem.*, **1987**, 59, 1278-1285.

12. T. Keough, *Anal. Chem.*, **1982**, 54, 2540-2547.

13 J. Brodbelt, C.-C. Liou anf T. Danovan, *Anal. Chem.*, **1991**, 63, 1205-1209.

14. J. X. Shen and J. Brodbelt, *J. Mass Spectrom.*, **1996**, 31, 1389-1398.

15. T. Donovan and J. Brodbelt, *J. Am. Soc. Mass Spectrom.*, **1992**, 3, 47-59.

16. C.-C. Liou, E. S. Eichmann and J. S. Brodbelt, *Org. Mass Spectrom.*, **1992**, 27, 1098-1104.

17. T. Donovan, C.-C. Liou and J. Brodbelt, *J. Am. Soc. Mass Spectrom.*, **1992**, 3, 39-46.

18. T. Donovan and J. Brodbelt, *Biol. Mass Specrtom.*, **1992**, 21, 254-258.

19. E. S. Eichmann and J. S. Brodbelt, *Org. Mass Spectrom.*, **1993**, 28, 665-671.

20. J.J. Isbell and J. S. Brodbelt, *J. Am. Soc. Mass spectrom.*, **1996**, 7, 565-572.

21. E. S. Eichmann and J. S. Brodbelt, *Org. Mass Spectrom.*, **1993**, 28, 737-744.

22. T. D. McCarley and J. Brodbelt, *Anal. Chem.*, **1993**, 65, 2380-2388.

23. A. Colorado and J. Brodbelt, *Anal. Chem.*, **1994**, 66, 2330-2335.

24. T. Donovan and J. Brodbelt, *Org. Mass Spectrom.*, **1992**, 27, 9-16.

25. G. F. Bauerle, Jr, B. J. Hall, N. V. Tran and J. S. Brodbelt, *J. Am. Soc. Mass Spectrom.*, **1995**, 7, 250-260.

26. C.-C. Liou, J. Isbell, H.-F. Wu, J. S. Brodbelt, R. A. Bartsch, J. C. Lee and J. L. Hallman, *J. Mass Spectrom.*, **1995**, 30, 572-580.

27. G. F. Bauerle, Jr and J. S. Brodbelt, *J. Am. Soc. Mass Spectrom.*, **1995**, 6, 627-633.

28. J. S. Brodbelt, *Mass Spectrom. Rev.*, **1997**, 16, 91-110.

29. M. Tang, J. Isbell, B. Hodges and J. Brodbelt, *J. Mass Spectrom.*, **1995**, 30, 977-984.

30. E. J. Alvarez and J. S. Brodbelt, *J. Mass Spectrom.*, **1995**, 30, 625-631.

31. E. J. Alvarez and J. S. Brodbelt, *J. Mass Spectrom.*, **1996**, 31, 901-907.

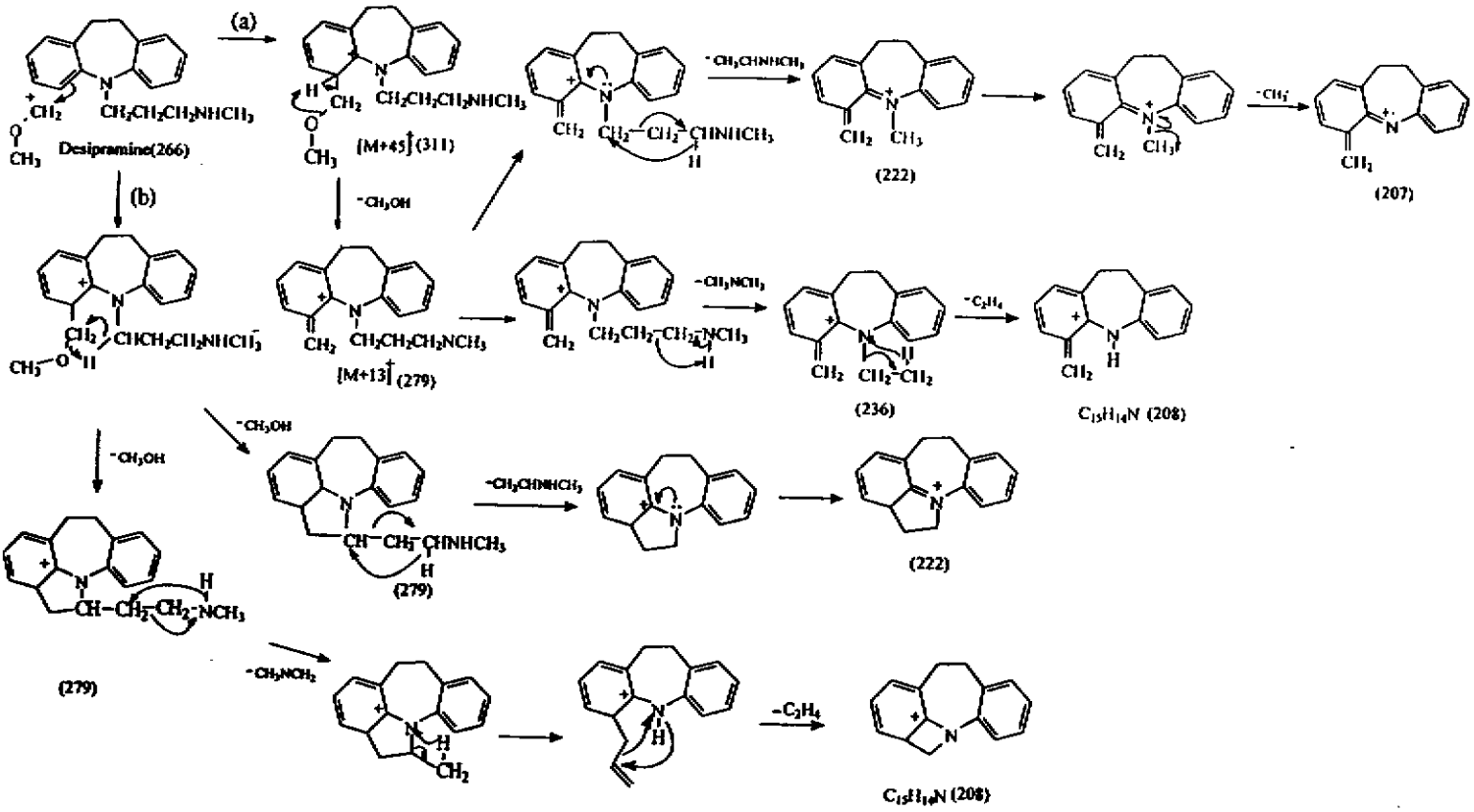

Scheme 1A.

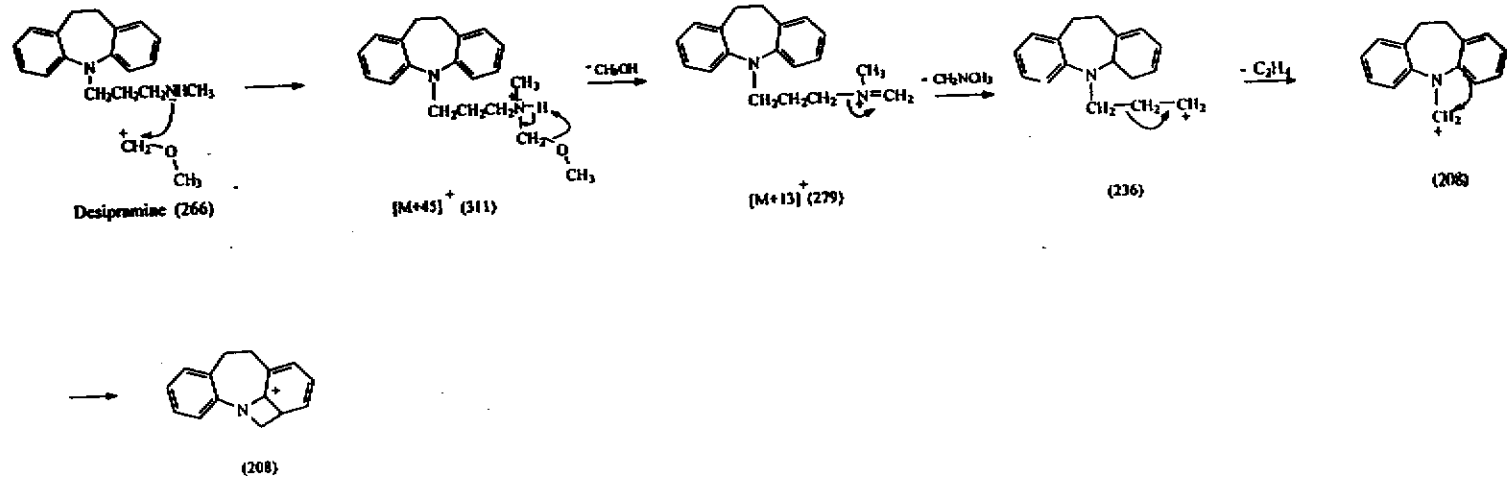

Scheme 1B

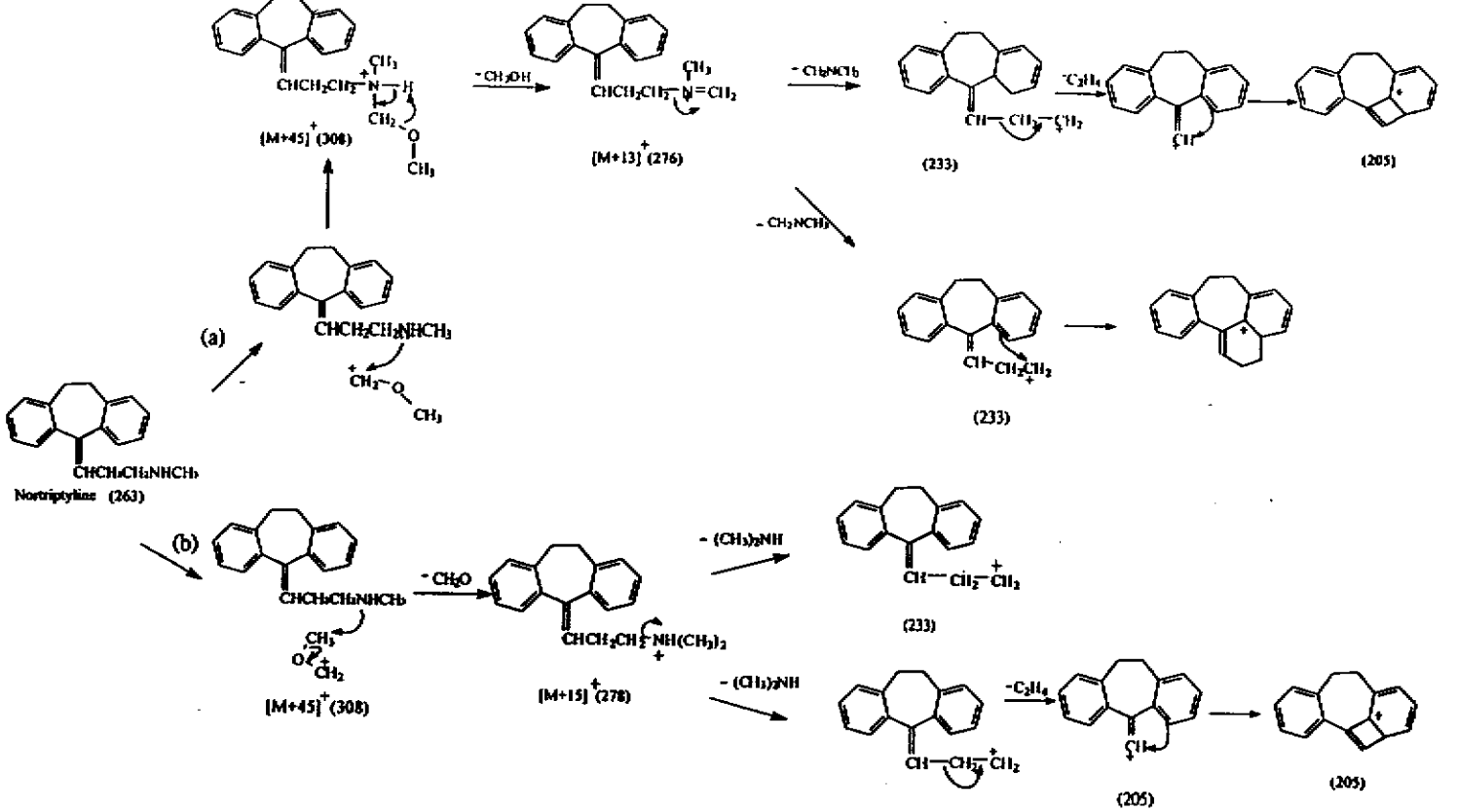

Scheme 2A

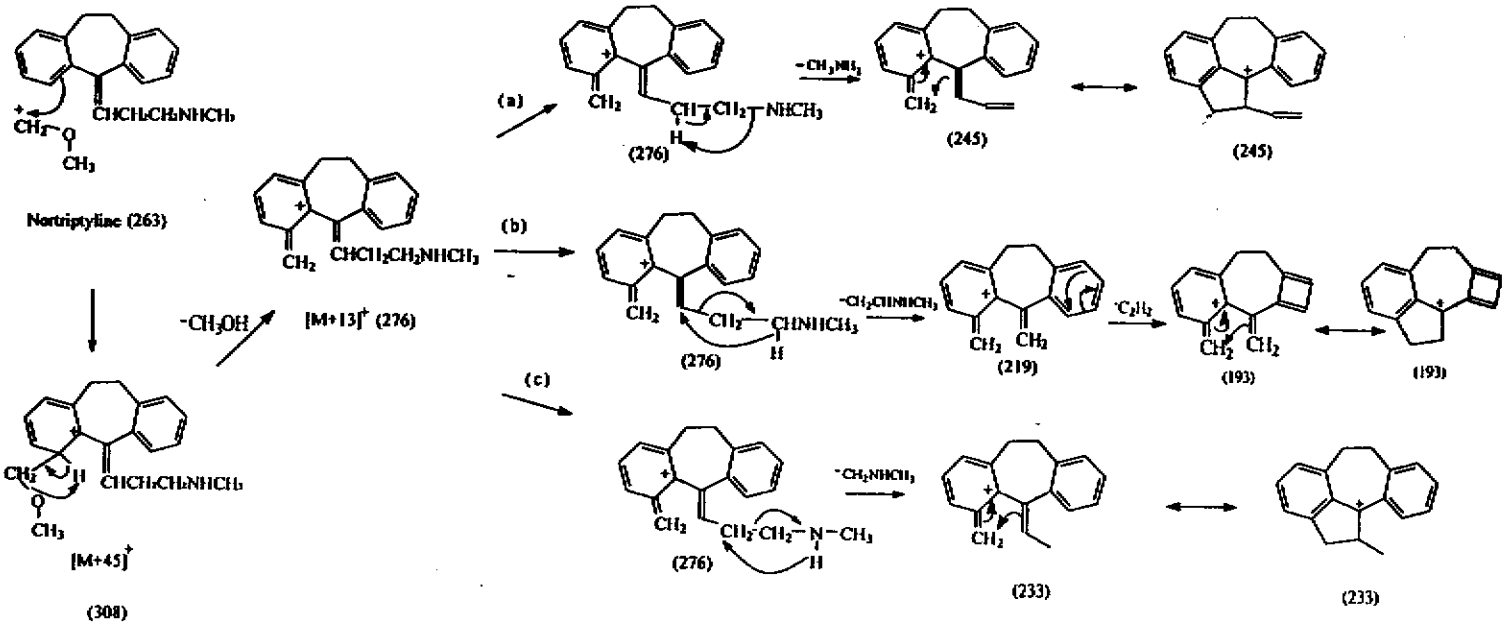

Scheme 2B

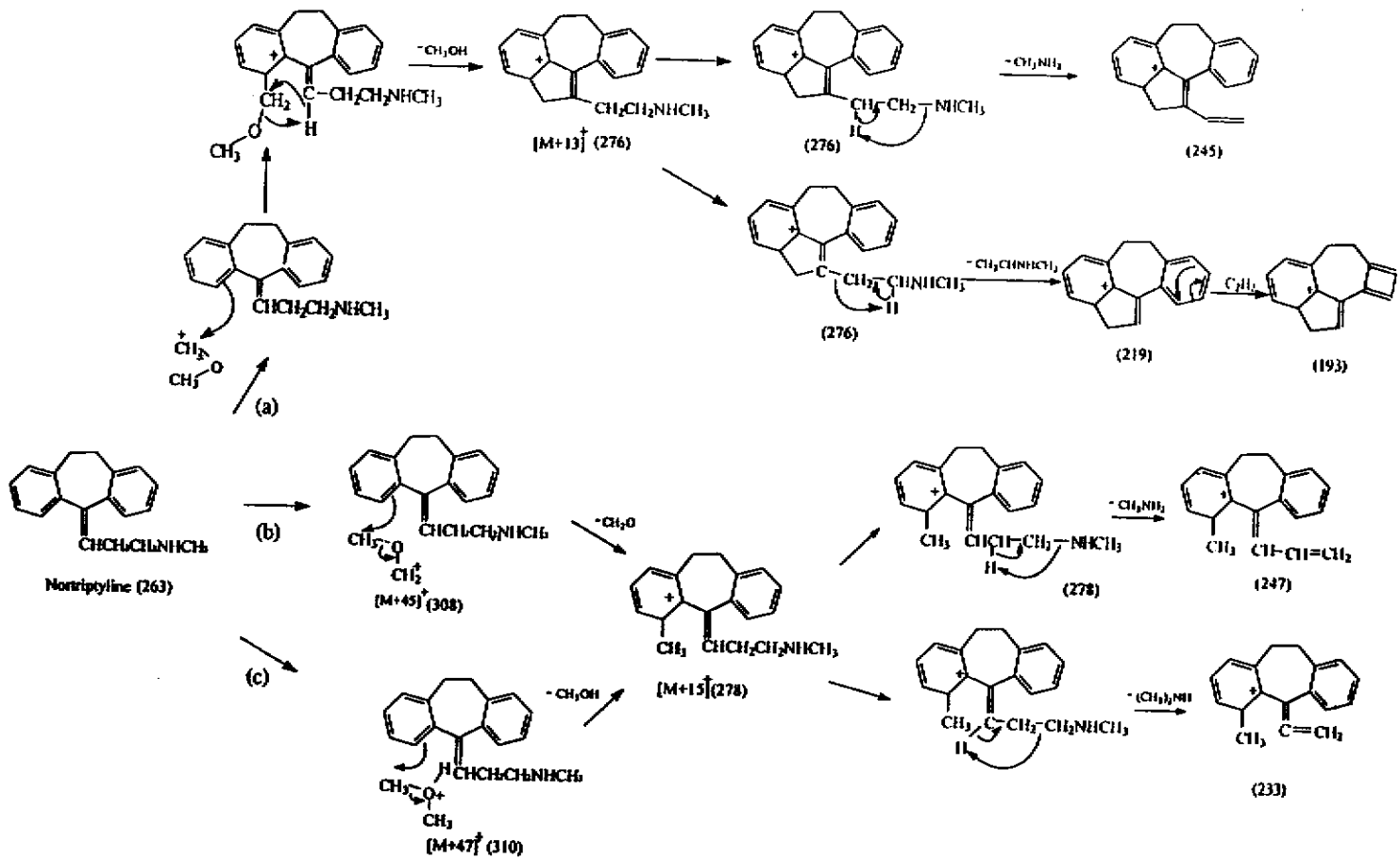

Scheme 2C

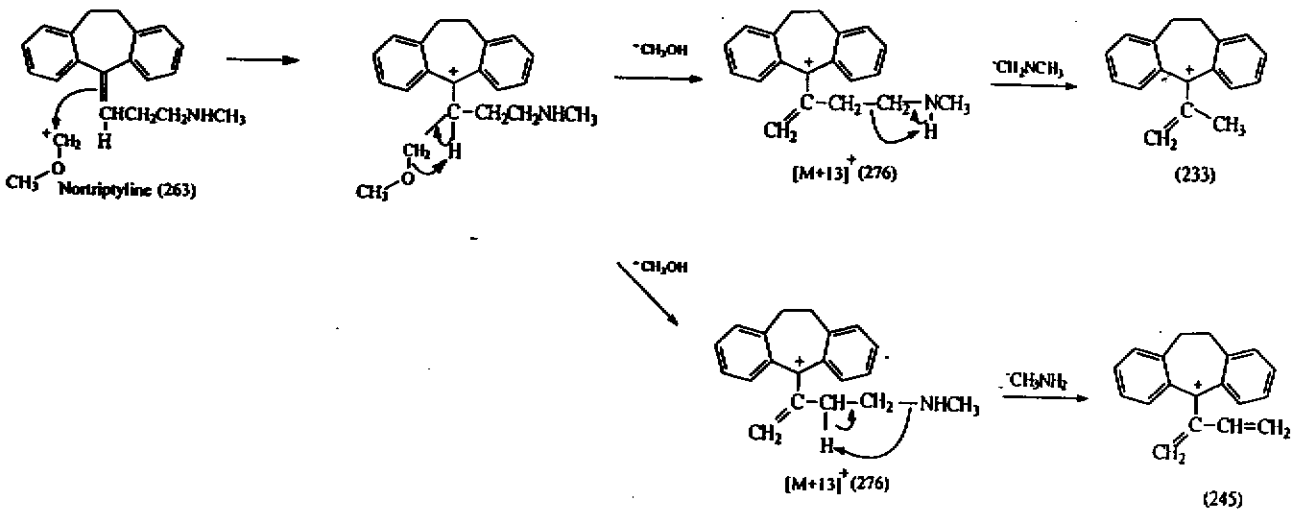

Scheme 2D

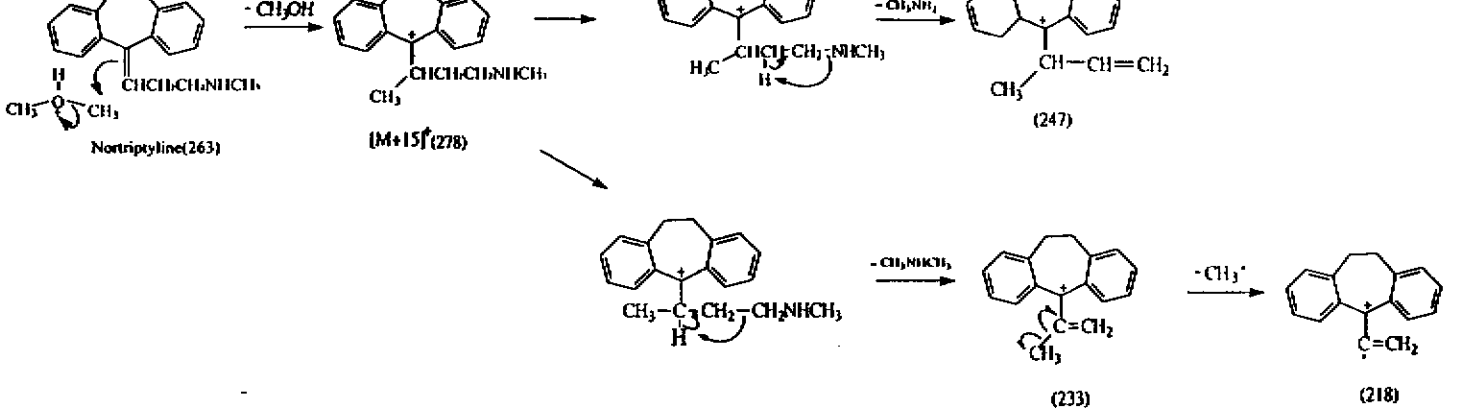

Scheme 2E

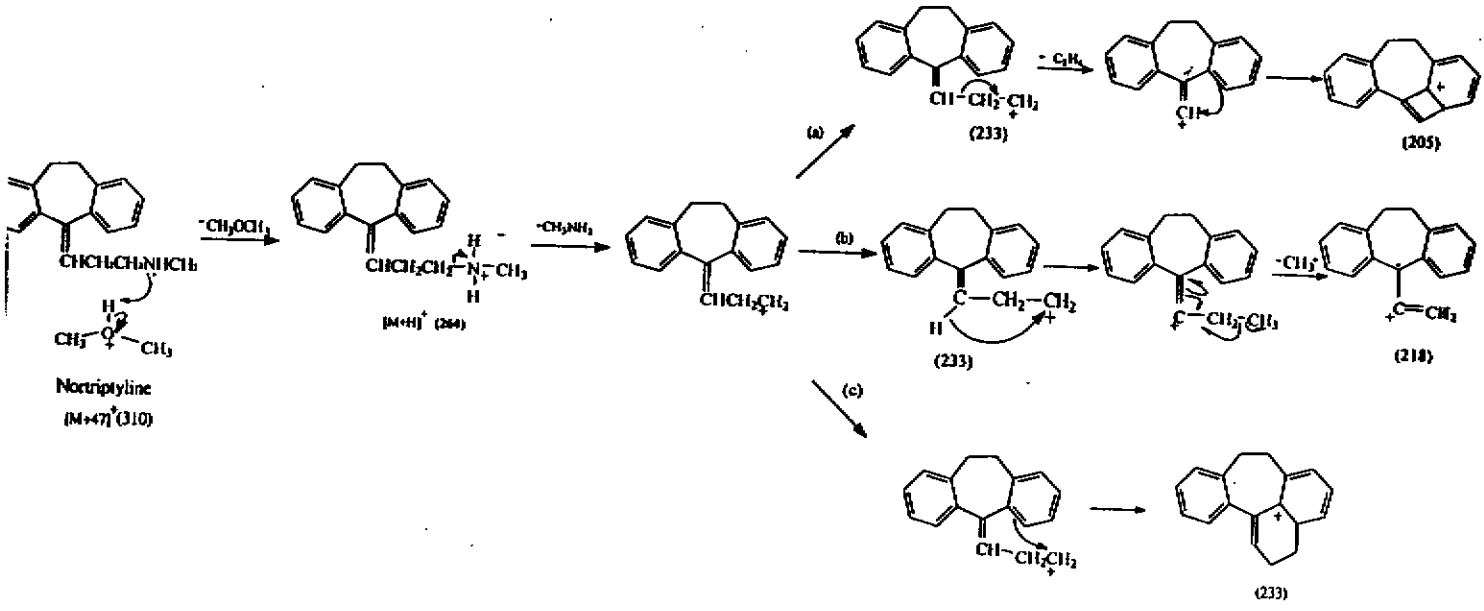

Scheme 3A

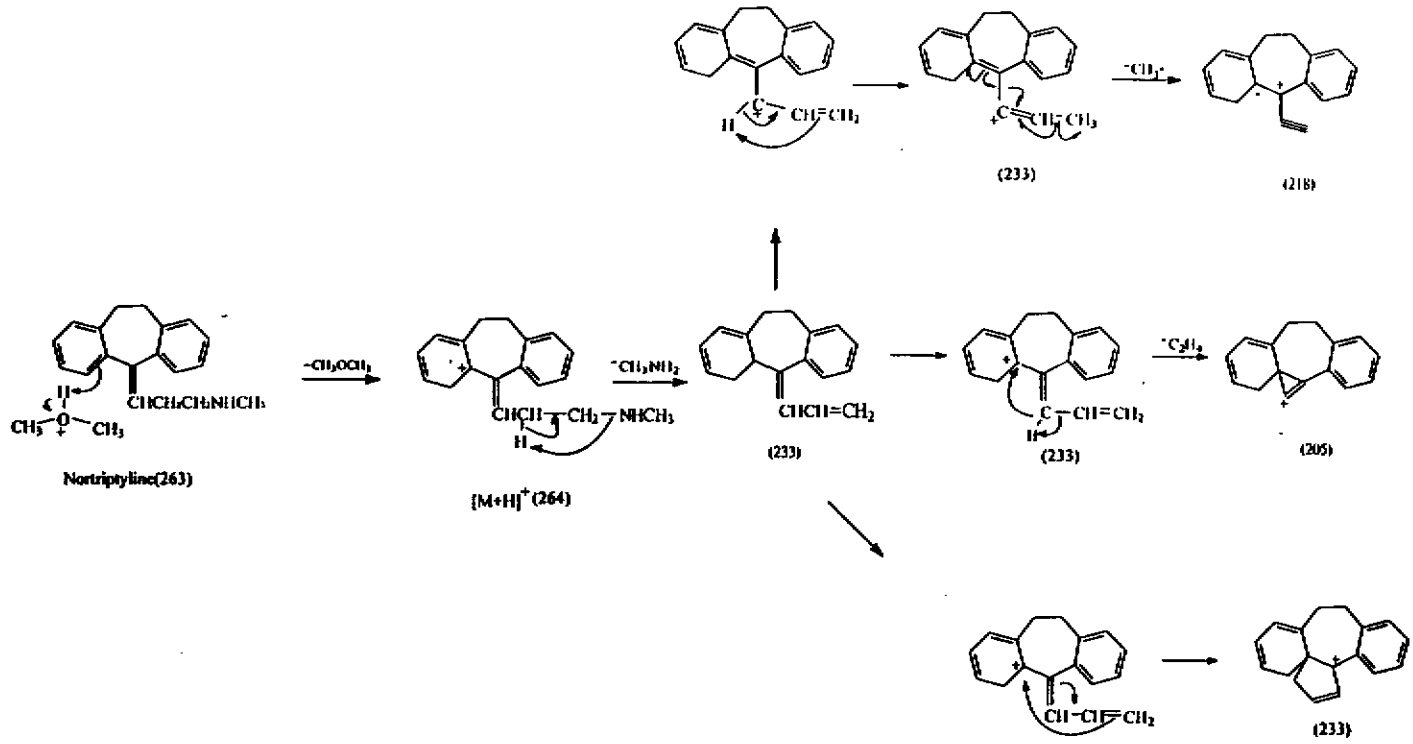

Scheme 3B

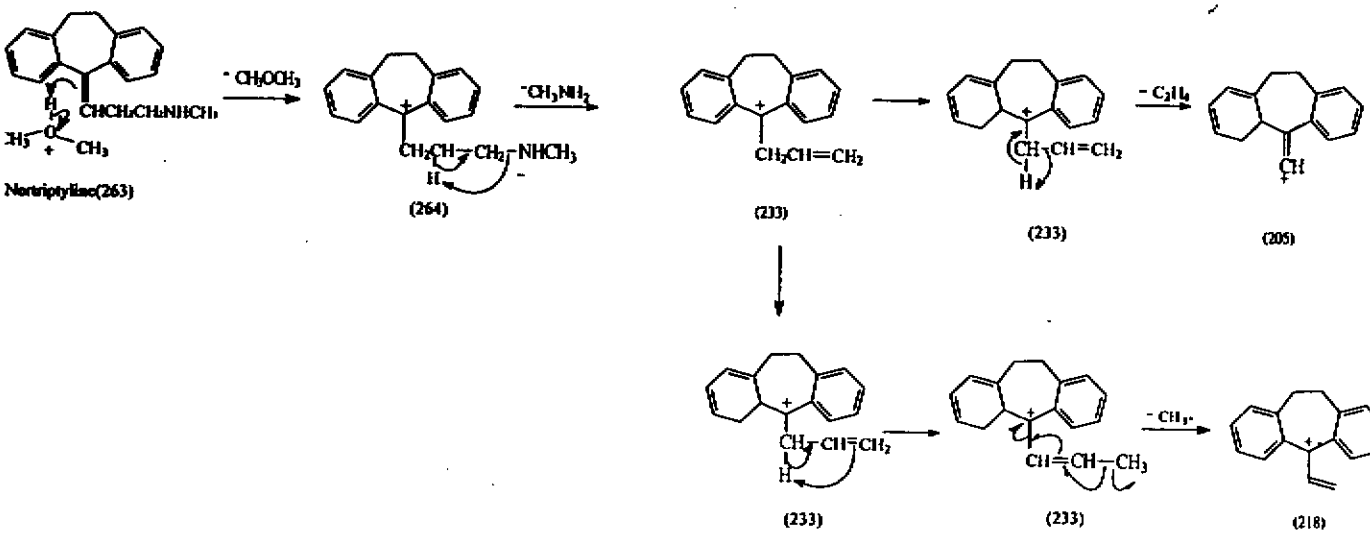

Scheme 3C

Table 1. 三環系抗鬱劑與化學游離試劑(DME)的離子/分子產物結果表

Iminodibenzyl(195)	$[M+47]^+$(242,<1%) $[M+45]^+$(240,4%) $[M+15]^+$(210,1%) $[M+13]^+$(208,27%) $[M+H]^+$(196,32%) $M^{+\cdot}$(195,100%) $[M-H]^+$(194,46%) $[M+H-CH_3\cdot]^+$(181,7%) $[M-CH_3\cdot]^+$(180,21%) $[M-H-CH_3\cdot]^+$(179,3%) $[M-C_2H_4]^+$ (167,5%) $[M-CH_3\cdot-C_2H_4]^+$(152,2%)
Imipramine(280)	$[M+47]^+$(327,<1%) $[M+45]^+$(325,2%) $[M+15]^+$(295,<1%) $[M+13]^+$(293,<1%) $[M+H]^+$(281,14%) $M^{+\cdot}$ (280,66%) $[M+H-(CH_3)_2NH]^+$(236,20%) $[M-(CH_3)_2NH]^{+\cdot}$ (235,100%) 234,82% $[M+H-(CH_3)_3N]^+$(222,6%) $[M-(CH_3)_2NH-CH_3\cdot]^+$(220,16%) $[M+H-(CH_3)_3$ N-$CH_3\cdot]^+$(208,16%) $[M+H-(CH_3)_2N-CH_3\cdot]^{+\cdot}$(207,4%) 195,54% 194,48% $[M+H-(CH_3)_2NH-CH_3\cdot-C_2H_4]^{+\cdot}$ (193,38%) $[M-(CH_3)_2NH-CH_3\cdot-C_2H_4]^+$(192,18%)
Desipramine(266)	$[M+45]^+$(311,<1%) $[M+15]^+$(281,<1%) $[M+13]^+$(279,5%) $[M+H]^+$(267,20%) $M^{+\cdot}$ (266,79%) $[M+H-CH_3NH_2]^+$ (236,16%) $[M-CH_3NH_2]^{+\cdot}$ (235,95%) 234,63% $[M-CH_3NH_2-CH_3\cdot]^+$(220,14%) $[M+H-CH_3NH_2-C_2H_4]^+$ (208,38%)
	$[M-CH_3NH_2-30]^{+\cdot}$ (205,5%) $[M\cdot-CH_3NHCH_2CHCH_2]^+$ (195,100%) 194,47% 193,56% $[M\cdot-CH_3NHCH_2CHCH_2-CH_3\cdot]^+$ (180,10%)
Nortriptyline(263)	$[M+47]^+$(310,<1%) $[M+45]^+$(308,26%) $[M+15]^+$(278,5%) $[M+13]^+$(276,23%) $[M+H]^+$(264,100%) $M^{+\cdot}$(263,10%) $[M+13-CH_3NH_2]^+$(245,2%) $[M+H-CH_3NH_2]^+$(233,9%) $[M-CH_3NCH_2]^{+\cdot}$(220,73%) $[M+13-CH_3NCH_2-C_2H_4]^+or[M+15-CH_3NHCH_3-C_2H_4]^+$(205,4%) 203,59% 202,77% 193,% $[M+H-CH_3NHCH_2CH_2CH_3]^+$(191,40%)
Amitripyline(277)	$[M+45]^+$(322,3%) $[M+15]^+$(292,<1%) $[M+13]^+$(290,<1%) $[M+H]^+$(278,11%) $M^{+\cdot}$ (277,<1%) 245,5% $[M+H-(CH_3)_2NH]^+$(233,9%) $[M+H-(CH_3)_2NH-CH_3\cdot]^+$(218,12%) 217,34% 215,25% $[M+H-(CH_3)_2NH-30]^+$(203,66%) 202,77% $[M+H-(CH_3)_2NH-CH_2CHCH_3]^+$(191,31%)

Table 2. 三環系抗鬱劑與化學游離試劑(DME)之加成離子(adduct ion)的相對強度表

	$[M+H]^+$	$[M+13]^+$	$[M+15]^+$	$[M+45]^+$	$[M+47]^+$
Iminodibenzyl(195)	32%	28%	1%	4%	<1%
Imipramine(280)	14%	<1%	<1%	2%	<1%
Desipramine(266)	20%	5%	<1%	<1%	0%
Nortriptyline(263)	100%	22%	5%	26%	1%
Amitripyline(277)	11%	1%	<1%	3%	0%

Table 3. Iminodibenzyl(195) CAD 的結果

$[M+47]^+$(242)	$-CH_3OH$(210,100%) 195,9%
$[M+45]^+$(240)	$-CH_3OH$(208,100%)
$[M+15]^+$(210)	$-CH_3$(195,100%) 180,27%
$[M+13]^+$(208)	$-CH_3$(193,100%) $-C_2H_4$(180,10%) 167,3%
$[M+H]^+$(196)	$-CH_3$(181,100%) $-C_2H_4$(168,3%)
$M^{+\cdot}$(195)	$-CH_3$(180,100%) $-C_2H_4$(167,3%)
$[M-H]^+$(194)	$-CH_3$(179,3%)
$[M-CH_3]^+$(180) 167	$-C_2H_4$(152,100%) 140,69%
165	$-C_2H_2$(139,26%)

Table 4.Imipramine(280) CAD 的結果

$[M+45]^+$(325)	$-CH_3OH$(293,4%) $-(CH_2O+(CH_3)_3N)$(236,100%) $-(CH_3OH+(CH_3)_2NCHCH_2)$(222,3%) $-(CH_2O+(CH_3)_3N+C_2H_4)$(208,66%) 193,3%
$[M+15]^+$(292)	$-(CH_3)_3N$(236,94%) $-((CH_3)_3N+C_2H_4)$(208,100%) 223,11% 194,8%
$[M+13]^+$(293)	$-(CH_3)_3N$(234,3%) $-(CH_3)_2NCHCH_2$(222,100%) $-((CH_3)_2NCHCH_2+CH_3\cdot)$(207,8%)
$[M+H]^+$(281)	$-(CH_3)_2NH$(236,48%) $-((CH_3)_2NH+C_2H_4)$(208,%) 195,100%
$M^{+\cdot}$(280)	$-(CH_3)_2NH$(235,16%) -86(194,100%)
$[M-HN(CH_3)_2]^{+\cdot}$(235)	$-CH_3$(220,100%) 205,18% 193,6%
234	$-CH_3$(219,100%) 204,19% 193,6%
$[M.-HN(CH_3)_2-$ $N.CH_3]^+$(220)	$-CH_3$(205,100%) 193,4% $-C_2H_4$(192,3%)
195	$-CH_3$(180,100%)

Table 5.Desipramine(266) CAD 的結果

$[M+45]^+$(311)	-CH_3OH(279,100%) -$CH_3NHCH_2CH_3$(252,19%) -(CH_3OH+CH_3NCH_2)(236,18%) -(CH_3OH+$CH_3NHCHCH_2$)(222,19%) 181,12%
$[M+15]^+$(281)	-CH_3NH_2(248,18%) 252,57% -$CH_3NHCHCH_2$(224,100%) -($CH_3NHCHCH_2$+CH_3)(208,54%)
$[M+13]^+$ (279)	-CH_3NCH_2(236, 79%) -$CH_3NHCHCH_2$(222,100%) -(CH_3NCH_2+C_2H_4)(208,6%) -($CH_3NHCHCH_2$+CH_3)(207,15%)
$[M+H]^+$ (267)	-CH_3(252,5%) -(CH_3NH_2)(236,45%) -(CH_3NH_2+C_2H_4)(208,3%) -($CH_3NHCH_2CHCH_2$)(196,100%) 195,22%
M^+ (266)	-CH_3NH_2 (235,92%) 195,100%
$[M-H_2NCH_3]^+$(235)	-CH_3(220,100%) 204,8% 193,8%
234	-CH_3(219,100%) 204,33%
$[M-H_2NCH_3-CH_3]^+$ (220)	-CH_3(205,100%)
$[M+H-H_2NCH_3-C_2H_4]^+$ (208)	-CH_3(193,100%)
$[M-CH_3NHCH_2CHCH_2]^+$ (195)	-CH_3(180,100%)

Table 6. Nortriptyline(263) CAD 的結果

$[M+47]^+$(310)	-CH_3OH (278,100%) -(CH_3OH +CH_3NH_2)(247,23%) -(CH_3OH +CH_3NCH_2)(235,16%) 195,91%
$[M+45]^+$(308)	-CH_3OH(276,73%) -(CH_3OH+CH_3NH_2)(245,24%) -(CH_3OH+CH_3NCH_2)or-(CH_2O+CH_3NHCH_3) (233,25%) -(CH_3OH+$CH_3NHCHCH_2$)(219,9%) 193,100%
$[M+15]^+$(278)	-CH_3NH_2(247,15%) -CH_3NHCH_3(233,100%) -(CH_3NHCH_3+CH_3)(218,6%) -(CH_3NHCH_3+C_2H_4)(205,10%) 191,25%
$[M+13]^+$(276)	-CH_3NH_2(245,57%) -CH_3NCH_2(233,32%) -$CH_3CH_2NHCH_3$(219,5%) -(CH_3NCH_2+C_2H_4)(205,4%) 193,100%
$[M+H]^+$(264)	-CH_3NH_2(233,100%) -(CH_3NH_2+CH_3)(218,3%) -(CH_3NH_2+C_2H_4)(205,3%) 191,13%
M^+(263)	-CH_3(248,12%) -CH_2NH(234,100%) -CH_3NCH_2(220,52%) -(CH_3NCH_2+CH_3)(205,2%)
$[M+13-H_2NCH_3]^+$(245)	-CH_3(230,100%) -C_2H_4(217,57%) 203,13%
$[M+H-CH_3NH_2]^+$ (233,8.8%)	-CH_3(218,100%) -C_2H_4(205,25%) 203,12%

$[M\cdot-CH_3NH_2]^+$(220)	$-CH_3\cdot$(205,100%) $-C_2H_5\cdot$(191,22%) 178,15%

Table 7. Amitripyline(277) CAD 的結果

$[M+45]^+$(322)	$-CH_3OH$(290,33%) $-(CH_3OH+(CH_3)_2NH)$(245,100%) $-(CH_2O+(CH_3)_3N)$ (233,85%) $-(CH_2O+(CH_3)_3N+CH_3\cdot)$(218,12%) $-(CH_3OH+(CH_3)_2NH+C_2H_4)$(217,12%) $-(CH_2O+(CH_3)_3N+C_2H_4)$(205,9%) 191,18%
$[M+15]^+$(292)	264,10% $-(CH_3)_2NH$(247,100%) $-(CH_3)_3N$(233,52%) $-((CH_3)_3N+CH_3\cdot)$(218,7%) $-((CH_3)_3N+C_2H_4)$(205,4%) 191,7%
$[M+13]^+$(290)	$-(CH_3)_2NH$(245,100%) $-((CH_3)_2NH+CH_3\cdot)$(230,14%) $-(CH_3)_2NHCHCH_2$(219,16%) $-((CH_3)_2NH+30)$(215,7%) 207,7%
$[M+H]^+$(278)	$-(CH_3)_2NH$(233,100%) $-((CH_3)_2NH+CH_3)$(218,28%) $-((CH_3)_2NH+C_2H_4)$(205,15%) 191,43%
$M^{+\cdot}$ (277)	$-CH_3OH$(245,10%) $-(CH_3)_3N$(232,24%) $-(CH_3OH+C_2H_4)$(20,5%) 194,100%
$[M+13-(CH_3)_2NH]^+$(245)	$-CH_3\cdot$(230,100%) 215,37% $-C_2H_4$(217,44%) $-(C_2H_4+CH_3\cdot)$(202,11%)
$[M+H-(CH_3)_2NH]^+$(233)	$-CH_3\cdot$(218,100%) $-C_2H_4$(205,28%) $-(CH_2CHCH_3+42)$(191,39%)
$[M+13-(CH_3)_2NH-C_2H_4]^+$ (217)	$-CH_3\cdot$ (202,100%)

Table 8.三環系抗鬱劑藥物離子/分子反應理論計算結果

Table 8-1：Heat of formation:(KJ/mole)

	M	Reactive site	$[M+H]^+$	$[M+13]^+$	$[M+15]^+$	$[M+45]^+$	$[M+47]^+$
Iminodibenzyl	41	4	207	230	204	162	145
		5	205	230	210	173	-
Imipramine	60	4	214	262	211	177	155
		成環	-	219	-	-	-
		3'	207	-	213	175	147
Desipramine	60	4	209	238	213	166	152
		成環	-	214	-	-	-
		3'	199	-	210	165	142
Nortriptyline	52	4	227	234	231	191	175
		成環	-	232	-	-	-
		1'	214	-	215	177	156
		3'	201	228	205	162	165
Amitriptyline	57	4	232	237	236	195	180
		成環	-	236	-	-	-
		1'	218	-	220	185	161
		3'	217	-	198	171	142

Heat of reaction : (KJ/mole)

Table 8-2：Iminodibenzyl 在各反應位置生成$[M+H]^+$離子的生成熱與反應熱

		Site of attack				
		double bond			Nitrogen	
Iminodibenzyl		1	2 '	3	4	5
$[M+H]^+$	ΔH_f	220	205	205	207	205
	ΔH_{rxn}	5	-10	-10	-8	-10

(單位：KJ/mole)

Table 8-3：生成$[M+47]^+$與$[M+45]^+$離子之反應熱

$[M+47]^+$ compound	Site of attack				$[M+45]^+$	Site of attack			
	double bond		Nitrogen			double bond		Nitrogen	
	4	1'	5	3'		4	1	5	3'
iminodibenzyl	-26	-	3	-		-36	-	-25	-
imipramine	-35	-	-	-43		-41	-	-	-43
desipramine	-38	-	-	-48		-52	-	-	-53
nortriptyline	-7	-26	-	-17		-27	-33	-	-48
amitriptyline	-8	-27	-	-45		-23	-44	-	-30

(單位：KJ/mole)

Table 8-4：由$[M+45]^+$離子失去 CH_3OH 生成$[M+13]^+$離子之反應熱

$[M+13]^+$ compound	Site of attack									
	double bond						Nitrogen			
	4		1'		cyclic		5		3'	
	ΔH_r	ΔHs	ΔH_r	ΔHs	ΔH_r	ΔHs	ΔH_r	ΔHs	ΔH_r	ΔH_r
Iminodibenzyl	-17	20	-	-	-	-	-17	9	-	-
Imipramine	-3	38	-	-	-47	-6	-	-	-	-
Desipramine	-28	44	-	-	-52	<1	-	-	-34	18
Nortriptyline	-24	-5	-26	-7	-26	-7	-	-	-30	18
Amitriptyline	-25	-6	-27	-7	-27	-7	-	-	-	-

(單位：KJ/mole)

Table 8-5：由$[M+45]^+$離子失去 CH_2O 生成$[M+15]^+$離子之反應熱

	Site of attack							
	double bond				Nitrogen			
	4		1'		5		3'	
	ΔH_r	ΔHs	ΔH_r	ΔHs	ΔH_r	ΔHs	ΔH_r	ΔHs
Iminodibenzyl	-21	16	-	-	-14	11	-	-
Imipramine	-32	8	-	-	-	-	-35	13
Desipramine	-32	21	-	-	-	-	-35	18
Nortriptyline	-5	14	-21	12	-	-	-31	17
Amitriptyline	-6	14	-21	<1	-	-	-43	9

(單位：KJ/mole)

Table 8-6：生成$[M+H]^+$離子之反應熱

$[M+H]^+$	Site of attack							
compound	double bond				Nitrogen			
	ΔH_r	ΔHs	ΔH_r	ΔHs	ΔH_r	ΔHs	ΔH_r	ΔHs
	4		1'		5		3'	
Iminodibenzyl	-8	18	-	-	-	-	-10	-
Imipramine	-20	15		-	-	-	-27	16
Desipramine	-25	16	-	-	-		-35	13
Nortriptyline	1	8	-12	14	-	-	-25	-8
Amitriptyline	1	8	-13	13	-	-	-14	31

(單位：KJ/mole)

Table 9.化合物 nortriptyline 在不同溫度下的離子/分子產物的相對強度

PEAK\Temperture(℃)	100	150	180	200	225
$[M+47]^+$	3.16	1.68	0.65	0.65	0.31
$[M+45]^+$	78.44	48.36	23.44	25.93	4.46
$[M+15]^+$	10.12	7.09	3.53	4.98	2
$[M+13]^+$	48.6	40.13	22.25	22.53	9.14
$[M+H]^+$	100	100	100	100	100
M^+	21.26	12.74	8.33	9.98	6.67
245^+	11.78	12.08	5.65	2.48	3.18
233^+	13.46	15.1	8.43	8.8	11.04
220^+	25.97	15.56	11.95	73.07	21.37
203^+	17.42	12.35	7.92	59.09	27.99
202^+	13.12	10.48	5.8	77.45	20.04
193^+	20.73	20.1	10.85	18.68	9.07

Table 10.三環系抗鬱劑在化學游離試劑壓力 $4\sim5\times10^{-4}$ 下之離子/分子產物

化合物	$[M+H]^+$	$[M+13]^+$	$[M+15]^+$	$[M+45]^+$	$[M+47]^+$
Iminodibenzyl(195)	57%	100%	1%	71%	1%
Imipramine(280)	40%	15%	48%	100%	2%
Desipramine(266)	83%	100%	30%	74%	1%
Nortriptyline(263)	52%	28%	15%	100%	1%
Amitripyline(277)	41%	6%	17%	100%	1%

Table 11.三環系抗鬱劑在不同壓力(化學游離試劑壓力 $4\sim5\times10^{-4}$)下之 $I_{[M+H]^+}/I_{M^+}$ 的變化

化合物 壓力(torr)	Iminodibenzyl (195)	Imipramine (280)	Desipramine (266)	Nortriptyline (263)	Amitriptyline (277)
8×10^{-5}	0.32	0.21	0.25	10	11
$4\sim5\times10^{-4}$	1.78	2.86	7.55	5.78	10.25

Characterization of Purine and their Derivatives by Positive Chemical Ionization and Collisional Activated Dissociation in Ion Trap Mass Spectrometer with an External Ionization Source

Hui-Fen Wu*, Ya-Ping Lin and Pei-Yi Lin,

Department of Chemistry

Tamkang University

Tamsui, Taipei Hsien, 25137, Taiwan, R. O. C.

摘要:

此研究將針對於以多種不同的化學游離試劑氣體，且在 PICI 的化學游離模式下，分析嘌呤類(purine)化合物以及與此類化合物結構類似的化合物之 chemical ionization mass spectra，故本實驗為分析並比較當試劑氣體分別為 DME, O_2 與 CH_4 時，嘌呤類(purine)化合物以及與此類化合物結構類似的化合物之 PICI (positive ion chemical ionization)之 chemical ionization mass spectra;及比較當游離模式為 PICI 時，分別以 O_2、CH_4 及 DME(Dimethyl ether)為試劑氣體與待測化合物的離子/分子反應結果。並藉由對所生成之產物離子進行碰撞活化解離(CAD)，進一步瞭解產物離子的裂解途徑與反應機構的推導。

比較 O_2、CH_4 及 DME 與嘌呤類化合物的離子/分子反應結果，發現當試劑氣體為 CH_4 與 DME 時明顯的比當試劑氣體為 O_2 時產生較少的碎片離子，且由 CH_4 與 DME 試劑氣體與嘌呤類化合物進行離子/分子反應可得到較多相關於嘌呤類化合物之結構訊息以及官能基的反應性，因此綜合 CH_4 與 DME 的離子/分子反應結果，再加上與 O_2 進行離子/分子反應之嘌呤類化合物中僅 6-Mercaptopurine 與 O_2 進行加成反應，可知-SH 官能基之反應性較其他嘌呤類化合物強。

導論:

至今市售的離子阱質譜儀中僅有此 Finnigan 公司之 GCQ 因有+/-15kV 可變式 dynode，並且因 GCQ 的化學游離方式為外部游離法，因此可減少 background 的污染並提高偵測的靈敏度，故此 GCQ 極適合應用於 PICI 方面的研究。

在嘌呤類化合物中，Adenine 為所有核酸的基本成份之一，存在於核糖核酸和去氧核糖核酸中。6-Mercaptopurine 主要用於癌的化學治療，且為治療腫瘤(尤其兒童性白血病)的化學治療藥劑，並兼有免疫抑制作用，能抑制免疫母細胞和免疫活性細胞的形成，此藥的應用曾是器官移植術的重大發展。此類化合物對人體而言皆是極重要的藥物。而在此之前，本研究所分析之待測物皆未有質譜方面的分析研究。

本研究的主要目的在於以不同的化學游離試劑氣體且在化學游離模式為 PICI 的情況下，分析嘌呤類(purine)化合物以及與此類化合物結構類似的化合物之 chemical ionization mass spectra，相信必能由這些化學游離試劑氣體應用於外部游離的離子阱質譜儀的 PICI 的分析結果，提供學術界、工業界與醫藥界一些使用 Finnigan 公司之 GCQ 應用方面所須之訊息，並希望未來能研發出新而有效的適用於外部游離的離子阱質譜儀的 PICI 的化學游離試劑氣體。此外，4-Aminopyrazolo pyrimidine 與 Adenine 為 isomer，因此本計劃的另一研究主題為 isomer 的區別，將針對此二 isomer 化合物做一番探討。

選擇 DME、O_2 與 CH_4 作為 PICI 的化學游離試劑氣體，是因為在眾多的化學游離試劑中 CH_4 是最常用也是應用最廣泛的化學游離試劑氣體，這是由於 CH_4 的質子親和力相當低，因此 CH_4 所形成的 CH_5^+離子相當容易將質子轉移給待測物而使待測物離子化；而二甲基醚(DME)在傳統的內部游離之離子阱質譜儀，是對官能基極具選擇性之最有效的化學游離試劑氣體。文獻上關於 O_2 在質譜方面的分析應用大都作為負離子的化學游離試劑氣體，應用於 PICI 方面則非常少，因此本文選擇 O_2 作為 PICI 的化學游離試劑氣體，並與不同的試劑氣體如 DME 與 CH_4 比較其優劣。

實驗:

實驗所使用的分析儀器為 Finnigan 公司之 GCQ，游離方式則採取外部化學游離法，並以 mass-selective instability mode 進行正和負離子的反應與偵測。正離子的化學游離試劑氣體為甲烷以及二甲基醚(DME)，化學游離試劑氣體的壓力為 8×10^{-5} torr。以氦氣做為離子阱譜儀的緩衝氣體(buffer gas)，氦氣的壓力為 1 mtorr。外部化學游離法的樣品導入方式是以 DIP (Direct Insert Probe)探針將分析物導入游離源區，再以 100 ℃/min 將分析物加熱，升溫範圍由 150～350℃，游離源區的溫度則維持在 200℃，離子注入質譜儀的時間則是 25msec，而質譜掃瞄之速率為 10msec。離子進行碰撞活化解離(CAD)時之 q_z 值為 0.225，碰撞活化解離時間為 15msec，碰撞活化解離電壓範圍為 0.5～2.0 eV，選擇母離子時的訊號寬度由 0.5 至 1 Da。所有的藥物及化合物皆購自 Aldrich chemical company (Milwaukee)。

結果與討論:

現今，在離子阱質譜儀的分析研究中以 PICI 的游離模式較廣為應用，此次研究以 PICI 的游離模式作分析，而且此次研究針對多種不同的化學游離試劑氣體做分析比較，以找出新的適用於外部游離的離子阱質譜儀 PICI 的試劑氣體。本實驗亦將以 PICI 對藥物化合物進行一系列的 chemical ionization 的串聯質譜分析比較，能對藥物化合物的官能基及結構有更深的了解，使離子阱串聯質譜可更廣泛的應用於其他環境、

藥物和毒物等方面。

1. 在 PICI 模式下，嘌呤類化合物與甲烷(化學游離試劑氣體)之離子/分子反應結果

由文獻得知以甲烷為化學游離試劑氣體會在游離源區形成的 primary ion 有 CH_4^+、CH_3^+、CH_2^+、CH^+、C^+、H_2^+、H^+等試劑離子，以及 secondary ion 有 CH_5^+、$C_2H_5^+$、$C_2H_4^+$、$C_2H_3^+$、$C_2H_2^+$、$C_2H_7^+$、$C_3H_7^+$、$C_3H_5^+$等試劑離子，但是 source 區域的 pressure 大小對這些試劑離子的相對離子強度有很大的影響。此次研究之嘌呤類化合物化合物與甲烷進行離子/分子反應後大都有$[M+41]^+$、$[M+29]^+$、$[M+H]^+$、M^+等離子形成，且 base peak 亦大都為$[M+H]^+$離子，其中 2,6-Dichloropurine 反而較易生成 M^+離子，而不易有 adduct ion 的生成。

Adenine、4-Aminopyrazolo pyrimidine、2-Amino-6-purinethiol 及 6-Chloropurine 等化合物則較易與甲烷所生成的試劑離子進行加成反應與質子轉移反應，而有$[M+41]^+$、$[M+29]^+$、$[M+H]^+$及 M^+等離子形成，而其中 2-Amino-6-purinethiol 及 6-Chloropurine 更有$[M+15]^+$離子的生成，針對 6-Chloropurine 的$[M+15]^+$離子做 CAD 後，經與當試劑氣體為 DME 時之 6-Chloropurine 所產生之$[M+15]^+$離子(即為$[M+CH_3]^+$離子)的 CAD 結果比對後，發現 6-Chloropurine 與 CH_4 所產生之$[M+15]^+$離子的確為$[M+CH_3]^+$離子。而 2-Amino-6-purinethiol 雖然無 DME 之數據結果可比對，但由於其 CAD 結果之 base peak 為掉落 48u，可經推導得知此 48u 為 CH_3SH 分子，可知此$[M+15]^+$離子亦為$[M+CH_3]^+$離子。

2. 在 PICI 的模式下，嘌呤類化合物與 DME 的離子/分子反應結果

此離子阱質譜儀的分析物導入方式為外部游離模式，當汽化的分析物與試劑離子進行離子/分子反應後再以三對電板導入 analyzer 區域，因此雖然化學游離方式為"soft"的游離方式不會產生很多碎片離子，但因通過三對電板時，離子容易因電板的加速得到動能而易發生解離。但由嘌呤類化合物與 DME 的離子/分子反應圖譜以及嘌呤類化合物與甲烷的正/負 chemical ionization mass spectra 皆只發現到極少數的碎片離子且相對離子強度皆不高，而且嘌呤類化合物與 DME 的離子/分子反應圖譜之 base peak 皆為$[M+H]^+$離子，可知嘌呤類化合物的主要結構不易裂解成碎片離子。

由嘌呤類化合物與 DME 的離子/分子反應結果，發現嘌呤類化合物皆會生成$[M+45]^+$離子，且其相對離子強度約為 14-46%，以及 4-32%的$[M+13]^+$離子與$[M+15]^+$離子，其中$[M+15]^+$離子的相對離子強度又比$[M+13]^+$離子高，尤其是 6-chloropurine 幾乎不生成$[M+13]^+$離子，可知嘌呤類化合物與 DME 反應生成$[M+13]^+$離子的主要反應位置為 6 號碳上的官能基，且由 Brodbelt 等人所發表的文獻得知會與 m/z 45 的試劑離子反應而生成$[M+13]^+$離子的官能基為-NH、$-NH_2$、-SH、-OH 及 phenyl ring 等等。而生成$[M+15]^+$離子的主要反應位置則可由 CAD 結果做推導，由 CAD 結果發現進行$[M+15]^+$離子加成反應的主要反應位置不是 6 號碳上的官能基，而應該是 purine 環上的 C 或是 N 上，這是因為嘌呤類化合物的$[M+15]^+$離子 CAD 後可發現皆會掉落大量的 6 號碳上的官能基，可知$[M+15]^+$離子的甲基加成並非在 6 號碳上的官能基，再加上皆會掉落 41u (CH_2CNH)中性分子，可推知甲基加成的主要反應位置不是 6 號碳上的官能基，而應該是在 purine 環上。

3. 在 PICI 的模式下，嘌呤類化合物與 O_2 的離子/分子反應結果

由嘌呤類化合物與 O_2 的 chemical ionization mass spectra 發現，O_2 極易與嘌呤類化合物進行 charge detachment reaction，因此 mass spectra 的 base peak 幾乎皆為 M^+離子，而其中僅 6-Mercaptopurine 與 O_2 進行加成反應生成$[M+O]^-$，但相對離子強度僅 1%，由其 CAD 結果可知進行加成反應的反應位置為 6 號碳上的-SH 官能基。

4. 比較當游離模式為 PICI 時，分別以 O_2、CH_4 及 DME 為試劑氣體與嘌呤類化合物的離子/分子反應結果

當試劑氣體為 CH_4 與 DME 時的離子/分子反應結果產生較少的碎片離子，且經由試劑氣體與嘌呤類化合物進行離子/分子反應所產生的的加成離子，而可得到更多相關於嘌呤類化合物之結構訊息以及官能基的反應性。例如，當試劑氣體為 DME 時，若嘌呤類化合物的 6 號碳上之官能基為-NH_2 或是-SH 時，則較易與 $CH_2O^+CH_3$(m/z 45)之試劑離子進行乙基化反應而生成$[M+13]^+$離子，而當 6 號碳上之官能基為-Cl 時則不會進行乙基化反應，除此之外，還可觀察到 6-Mercaptopurine 與 6-Chloropurine 等含 S 與含 Cl 之嘌呤化合物比含 N 之 Adenine 與 4-Aminopyrazolo pyrimidine 更容易生成$[M+15]^+$離子，而當試劑氣體為 CH_4 時，僅 2-Amino-6-purinethiol 的含 S 之嘌呤化合物有$[M+15]^+$離子的生成，且由 CAD 結果可知進行甲基化的主要反應位置為-SH。綜合 CH_4 與 DME 的離子/分子反應結果，可推知-SH 官能基對甲基化與乙基化反應之反應性較其他嘌呤類化合物強。而相較於 CH_4 與 DME，當試劑氣體為 O_2 時會有較多的碎片離子產生，且 O_2 主要與嘌呤類化合物進行 charge detachment reaction，再加上與 O_2 進行離子/分子反應之嘌呤類化合物中僅 6-Mercaptopurine 與 O_2 進行加成反應而生成$[M+O]^+$離子，可獲得的結構訊息以及官能基的反應性則較 CH_4 與 DME 少。由嘌呤類化合物與 O_2 的 chemical ionization mass spectra 發現 base peak 皆為 M^+離子，而以 CH_4

與 DME 為試劑氣體的 mass spectra 之 base peak 則大都為$[M+H]^+$離子，僅除了電負度較大的 2,6-Dichloropurine 之 base peak 為 M^+離子。

Adenine (MW:135.13)及 4-Aminopyrazolo pyrimidine (MW:135.13)此二化合物為同分異構物(isomer)，而當以質譜儀在化學游離模式下進行分析鑑定此二化合物時，由於所生成的 M^+ 及$[M+H]^+$離子的 m/z 值相同，因此較難以區別此二化合物，而由本實驗室之實驗結果亦發現到不論是當試劑氣體為 CH_4 或是 DME，皆可觀察到 Adenine 及 4-Aminopyrazolo pyrimidine 此二 isomer 的離子/分子反應產物及其 relative intensity 幾乎完全相同，可知要區別 isomer 的確有其困難度，因此本實驗室進一步將這些離子/分子反應時所產生的加成離子進行碰撞活化解離（CAD）技術，期望經由 CAD 時所產生之碎片離子的特異性及其解離途徑來區別此二 isomer。由 DME 與 Adenine 及 4-Aminopyrazolo pyrimidine 進行離子/分子反應所產生的$[M+45]^+$及$[M+15]^+$離子之 CAD 結果發現，Adenine 的$[M+45]^+$離子 CAD 後所生成的$[M+15]^+$及$[M+13]^+$離子之相對離子強度幾乎相同，而 4-Aminopyrazolo pyrimidine 的$[M+45]^+$離子 CAD 後所生成的$[M+15]^+$離子則僅只有$[M+13]^+$離子之相對離子強度的一半。且 Adenine 的$[M+15]^+$離子 CAD 後之 base peak 為$[M+15-NH_3]^+$碎片離子，而 4-Aminopyrazolo pyrimidine 的$[M+15]^+$離子 CAD 後之 base peak 則為$[M+15-28]^+$碎片離子。

3.水合現象

由 PICI mass spectra 發現嘌呤類化合物很容易發生水合現象，而 H_2O 的來源有可能是在 Trap 中殘留的水分子或是當以 DIP 導入化合物樣品時隨之進入 Trap 中的水分子，由嘌呤類化合物與 DME、CH_4 及 O_2 的離子/分子反應產物之 CAD 結果則可觀察到水合現象，尤其是含 Cl 的化合物，由 6-Chloropurine 與 CH_4 進行離子/分子反應所生成的產物（如$[M+29]^+$、$[M+15]^+$、$[M+H]^+$、及 M^+離子）之 CAD 結果發現均有掉落 HCl or Cl 再加 H_2O 的碎片離子，其中$[M+15-HCl+H_2O]^+$(m/z 151)離子的相對離子強度更高達 19%。且在 Adenine 與 DME 進行離子/分子反應所生成的$[M+H]^+$離子之 CAD 結果中甚至可觀察到加成兩個 H_2O 的水合現象，$[M+H-NH_3+H_2O]^+$(m/z 137)，$[M+H-NH_3+2H_2O]^+$(m/z 150)，而相對離子強度分別為 6%及 3%。

4.$[M+41]^+$及$[M+29]^+$離子之 CAD 結果

由實驗結果觀察到結構上具有 Cl 離子之嘌呤類化合物皆不易形成$[M+41]^+$及$[M+29]^+$離子，而 Adenine、4-Aminopyrazolo pyrimidine 及 2-Amino-6-purinethiol 皆會形成$[M+41]^+$及$[M+29]^+$離子，因此以下將針對可形成$[M+41]^+$及$[M+29]^+$離子之嘌呤類化合物做一番探討與比較。由甲烷所生成之 $C_3H_5^+$及 $C_2H_5^+$試劑離子對於 Adenine、4-Aminopyrazolo pyrimidine 及 2-Amino-6-purinethiol 此三化合物而言皆為極佳的 proton donor，尤其是 $C_2H_5^+$離子，由此三化合物之$[M+29]^+$離子的 CAD 圖譜觀察到其 base peak 皆為化合物與 $C_2H_5^+$離子進行 proton transfer 反應後所形成的$[M+H]^+$離子，且此三張 CAD 圖譜幾乎完全一致，皆有掉落 NH_3、28 及 28+NH_3 等中性分子所形成之碎片離子，且 relative intensity 也大致相同。而由此三化合物之$[M+41]^+$離子的 CAD 圖譜可觀察到此三化合物與 $C_3H_5^+$離子的鍵結以 4-Aminopyrazolo pyrimidine 最弱，且此三化合物與 $C_3H_5^+$離子亦會進行大量的 proton transfer 反應，但是效果卻不若與 $C_2H_5^+$離子來的好。Adenine 及 4-Aminopyrazolo pyrimidine 此二 isomer 與 $C_3H_5^+$試劑離子的反應截然不同，4-Aminopyrazolo pyrimidine 與 $C_3H_5^+$離子的鍵結較弱，而 Adenine 與 $C_3H_5^+$離子的鍵結則較強，且在與 $C_3H_5^+$離子進行 proton transfer 反應後會繼續解離出數個氮氫化合物而形成碎片離子，而 4-Aminopyrazolo pyrimidine 則無。

4.$[M+H]^+$、$[M+2]^+$及$[M+3]^+$離子之 CAD 結果

由表一之離子/分子反應結果發現帶有一個 Cl 離子的 6-chloropurine 僅有$[M+H]^+$離子的生成，Adenine 及 4-Aminopyrazolo pyrimidine 此二 isomer 則有$[M+H]^+$及$[M+2]^+$離子的生成，而帶有一個 SH 及 NH_2 官能基的 2-Amino-6-purinethiol 則有$[M+H]^+$、$[M+2]^+$及$[M+3]^+$離子的生成。

結論:

此次研究的研究目的在於以多種不同的化學游離試劑氣體，且分別在 PICI 的化學游離模式下，分析嘌呤類(purine)化合物以及與此類化合物結構類似的化合物之 chemical ionization mass spectra。發現 PICI 能提供相關於化合物的結構訊息以及官能基的反應性，且在 PICI 的模式下產生的碎片離子較少。由 PICI 實驗結果，可知 DME 的確對嘌呤類化合物具有良好的選擇性，皆會對 purine 主結構的碳原子或是氮原子進行甲基化反應，以及對 6 號碳上的-NH_2 或 -SH 官能基進行乙基化反應，而且由 PICI spectra 還發現到含 S 的嘌呤類化合物之反應性極佳，尤其是對 alkyl group 的反應性。此外，發現嘌呤類化合物極易發生水合反應，尤其是當嘌呤類化合物的 6 號官能基掉落後，由 CH_4 與 DME 與嘌呤類化合物的離子/分子反應圖譜中即可 2 看到水合現象，且水分子與嘌呤類化合物的鍵結很強。

參考文獻:
1. M. P. F scher, L. Serrano-Andr 睿 and B. O. Roos, *J. Am. Soc. Mass Spectrom.*, **1997**,119,6168-6176.
2. A. Holm 悌, A. Broo, B.Albinsson and B. Nord 悌, *J. Am. Soc. Mass Spectrom.*, **1997**,119,12240-12250.
3. Y. J. Abul-Hajj, K. Tabakovic and I. Tabakovic, *J. Am. Soc. Mass Spectrom.*, **1995**,117,6144-6145.
4. J. M. Butler, P. Jiang-Baucom,M. Huang, P. Belgrader and J. Girard, *Anal. Chem.*, **1996**, 68, 3283-3287.
5. P. Singhal and W. G. Kuhr, *Anal. Chem.*, **1997**, 69, 4828-4832.
6. P. Singhal and W. G. Kuhr, *Anal. Chem.*, **1997**, 69, 3552-3557.
7. K. Komeda, S. Iwamoto, S. Kominami and T. Ohnishi, *Photochem. Photobiol.*, **1997**, 65, 115-118.
8. S. Hortelano and L. Bosca, *Mol. Pharmacol.*, **1997**, 51, 414-421.
9. F. L. Mi, Y. C. Tseng, C. T. Chen and S. S. Shyu, *J. Microencapsulation.*, **1997**, 14, 211-223.
10. F.-L. Mi, C. –T. Chen, Y. –C. Tseng, C. –Y. Kuan and S. –S. Shyu, *J. Controlled Release.*, **1997**, 44, 19-32.
11. H. –Y. Hwang, T. Gilberts, A. Jardim, S. shih and B. Ullman, *J. Boil. Chem.*, **1996**, 271, 30840-30846.
12. K. G. Davidson, S. M. Acton, H. A. Barr and T. E. Nicholas, *Am. J. Physiol.*, **1997**, 272, L106-L114.
13. R. J. Parry and J.C. Hoyt, *J. Bacteriol.*, **1997**, 179, 1385-1392.

表一、離子/分子反應結果（甲烷正離子）

6-Chloropurine(154.56)

$[M+41]^+$(195,1%)
$[M^{37}+29]^+$(185,4%)
$[M+29]^+$(183,12%)
$[M+H]^+$(155,100%)
M^+(154,9%)

Adenine(135.13)

$[M+41]^+$(176,7%)
$[M+29]^+$(164,46%)
$[M+H]^+$(136,100%)
M^+(135,8%)
$[(M+H)-NH_3]^+$(119,1%)

4-Aminopyrazolo pyrimidine(135.13)

$[M+41]^+$(176,3%)
$[M+29]^+$(164,34%)
$[M+H]^+$(136,100%)
M^+(135,14%)
$[(M+H)-NH_3]^+$(119,1%)

2-Amino-6-purinethiol(167.19)

$[M+41]^+$(208,2%)
$[M+29]^+$(196,9%)
$[M+15]^+$(182,15%)
$[M+2]^+$(169,9%)
$[M+H]^+$(168,100%)
M^+(167,15%)
$[(M+H)-NH_3]^+$(151,4%)

2,6-Dichloropurine(189.01)

$[M+41]^+$(229,<1%)
$[M+29]^+$(217,<1%)
$[M+H]^+$(189,77%)
M^+(188,100%)
$[M-Cl+H_2O]^+$(171,21%)
$[M-Cl]^+$or$[M-Cl+H_2O-HCl+H_2O]$(153,24%)
$[M-Cl+H_2O-HCl]^+$(135,33%)

表二、6-choropurine(154.56)的 CAD 結果：(甲烷正離子)

$[M^{37}+29]^+$ (185)	$-HCl^{37}+H_2O$(165,<1%)
	$-C_2H_4$(157,100%)
	$-HCl^{37}$(147,2%)
	$-(C_2H_4+HCl^{37})+H_2O$(137,2%)
	$-(C_2H_4+HCl^{37})$(119,25%)
$[M+29]^+$ (183)	$-HCl+H_2O$(165,<1%)
	$-C_2H_4$(155,100%)
	-HCl(147,1%)
	$-(C_2H_4+HCl)+H_2O$(137,4%)
	$-(C_2H_4+HCl)$(119,25%)
$[M+15]^+$ (169)	$-HCl+H_2O$(151,19%)
	-HCl(133,100%)
	-(HCl+HCN)(106,12%)
$[M+H]^+$ (155)	$-HCl+H_2O$(137,6%)
	-HCl(119,100%)
	-(HCl+HCN)(92,7%)
$M^{+\cdot}$ (154)	$-Cl+H_2O$(137,6%)
	-Cl(119,100%)
	-(Cl+HCN)(92,9%)

表三、Adenine (135.13)的 CAD 結果　　(甲烷正離子)

$[M+41]^+$ (176)	-NH_3(159,100%)
	-HCN(149,78%)
	-C_2H_4or$CH_2N^{\cdot}$(148,53%)
	-C_3H_4(136,62%)
	-$C_3H_5^{\cdot}$(135,67%)
	-C_3H_6(134,24%)
	-(C_2H_4+HCN)or($CH_2N^{\cdot}$+HCN)(121,12%)
	-(C_2H_4+$NHCH_2$)or($CH_2N^{\cdot}$+$NHCH_2$)(119,9%)
	-($C_3H_5^{\cdot}$+HCN)(108,10%)
	-(NH_3+2HCN)(105,7%)
	-(C_2H_4+2HCN)or($CH_2N^{\cdot}$+2HCN)(94,3%)
$[M+29]^+$ (164)	-NH_3(147,11%)
	-C_2H_4 or CH_2N(136,100%)
	-(NH_3+C_2H_4)or(NH_3+$CH_2N^{\cdot}$)(119,15%)
$[M+H]^+$ (136)	-NH_3(119,100%)
	-HCN(109,4%)
	-CH_2N_2(94,14%)
	-CH_4N_2(92,9%)
$M^{+\cdot}$ (135)	-HCN(108,100%)
$[M+H-NH_3]^+$ (119)	-HCN(92,100%)
	-CH_2N_2(77,14%)
	-52(67,28%)
	-2HCN(65,22%)

表四、4-Aminopyrazolo pyrimidine(135.13)的 CAD 結果　(甲烷正離子)

$[M+41]^+$ (176)	-NH_3(159,47%)
	-HCN(149,100%)
	-C_2H_4or$CH_2N^{\cdot}$(148,43%)
	-C_3H_4(136,87%)
	-$C_3H_5^{\cdot}$(135,7%)
$[M+29]^+$ (164)	-NH_3(147,7%)
	-C_2H_4or$CH_2N^{\cdot}$(136,100%)
	-C_2H_7N(119,11%)
$[M+H]^+$ (136)	-NH_3(119,100%)
	-HCN(109,19%)
	-$CH_2N^{\cdot}$(108,6%)
	-CH_2N_2(94,18%)
	-(HCN+$CH_2N^{\cdot}$)(81,6%)
$M^{+\cdot}$ (135)	-HCN(108,100%)
	-$CH_2N^{\cdot}$(107,6%)

表五、2-Amino-6-purinethiol(167.19)的 CAD 結果　(甲烷正離子)

$[M+41]^+$ (208)	-NH_3(191,72%)
	-C_2H_4orCH_2N(180,11%)
	-SH(175,9%)
	-SH_2(174,9%)
	-C_3H_4(168,43%)
	-C_3H_5(167,100%)
	-C_3H_6(166,11%)
	-CH_3SH(160,9%)
	-(NH_3+C_3H_6)(149,27%)
	-C_3H_6S(134,16%)
$[M+29]^+$ (196)	-CH_3(181,26%)
	-NH_3(179,18%)
	-C_2H_4orCH_2N((168,61%)
	-SH(163,8%)
	-SH_2(162,9%)
	-73(123,5%)
$[M+15]^+$ (182)	-CH_3(167,16%)
	-NH_3(165,24%)
	-SH_2(148,11%)
	-(CH_3SH)(134,100%)
	-(NH_3+SH_2)(121,4%)
	-73(109,6%)
	-75(107,6%)
$[M+H]^+$ (168)	-NH_3(151,100%)
	-SH_2(134,13%)
	-CH_2N_2(126,9%)
	-(NH_3+CH_2N_2)(109,6%)
$M^{+\cdot}$ (167)	-NH_3(150,30%)
	-HCN(140,9%)
	-SH(134,29%)
	-CH_2N_2(125,100%)
	-(NH_2+CH_2N_2)(109,45%)
	-(NH_3+CH_2N_2)(108,36%)
	-(HCN+CH_2N_2)(98,10%)
$[M+H-NH_3]^+$ (151)	-HCN(124,40%)
	-CH_2N_2(109,100%)
	-2HCN(97,20%)
	-(HCN+CH_2N_2)(82,47%)
$[(M+2)-SH_2]^+$(135)	-NH_2(119,11%)
	-NH_3(118,4%)
	-26(109,24%)
	-HCN(108,100%)

	-CH_2NH(107,23%)
	-41(94,26%)
	-2HCN(81,11%)
	-(HCN+$CH_2N^{\cdot}$)(80,6%)
$[(M+H)-SH]^+$ or $[M-SH]^+$(134)	-HCN(107,100%)
	-CH_2N_2(92,12%)
	-2HCN(80,22%)

表六、2,6-dichoropurine(189.01)的 CAD 結果：(甲烷正離子)

$[M+H]^+$ (189)	-Cl+H_2O(172,6%)
	-HCl+H_2O(171,30%)
	-HCl+O(169,36%)
	-Cl or -Cl+H_2O-HCl+H_2O(154,9%)
	-HCl or -HCl+H_2O-HCl+H_2O(153,91%)
	-Cl+H_2O-HCl(136,7%)
	-HCl+H_2O-HCl(135,100%)
	-HCl+O-HCl (133,32%)
$M^{+\cdot}$ (188)	-Cl+H_2O(171,65%)
	-Cl+O(169,13%)
	-Cl or -Cl+H_2O-HCl+H_2O(153,100%)
	-Cl+H_2O-HCl(135,54%)
	-Cl+O-HCl(133,7%)
$[M-Cl+H_2O]^+$ (171)	-15(156,3%)
	-H_2O or -HCl+H_2O(153,13%)
	-HCl^{37}+H_2O(151,29%)
	-22(149,25%)
	-CO(143,2%)
	-HCl(135,24%)
	-HCl^{37}(133,100%)
	-(CO+HCl)(106,7%)
$[M-Cl+H_2O-HCl+H_2O]^+$ or $[M-Cl]^+$ (153)	-H_2O(135,9%)
	-HCN(126,16%)
	-Cl(118,80%)
	-52(101,4%)
	-61(92,100%)
	-70(83,4%)
	-(HCN+52)(74,6%)
	-(HCN+61)(65,9%)
$[M-Cl+H_2O-HCl]^+$(135)	-OH(118,18%)
	-HCN(108,59%)
	-CO(107,100%)
	-41(94,37%)
	-(HCN+CO)(80,53%)
	-(HCN+41)(67,10%)

表一、離子/分子反應結果：（DME 正離子）

Adenine(135)

$M^{+\cdot}$(135,27%)
$[M+H]^{+}$(136,100%)
$[M+13]^{+}$(148,5%)
$[M+15]^{+}$(150,9%)
$[M+45]^{+}$(180,46%)

6-mercaptopurine(152)

$M^{+\cdot}$(152,30%)
$[M+H]^{+}$(153,100%)
[M+13](165,26%)
[M+15](167,32%)
[M+45](197,21%)
$[M-H]^{+}$(151,3%)
$[M+H-NH_3]^{+}$ or $[M+13-NHCH_2]^{+}$ (136,6%)

4-aminopyrazolo pyrimdine(135)

$M^{+\cdot}$ (135,31%)
$[M+H]^{+}$ (136,100%)
$[M+13]^{+}$ (148,4%)
$[M+15]^{+}$(150,7%)
$[M+45]^{+}$(180,26%)

6-chloropurine(154)

$[M+H]^{+}$ (155,100%)
$[M+15]^{+}$(169,18%)
$[M+45]^{+}$(199,14%)

表二、Adenine 的 CAD 結果： (DME 正離子)

$M^{+\cdot}$ (135)	-HCN(108,100%)
$[M+H]^{+}$ (136)	$-NH_3$(119,50%)
	-HCN(109,100%)
	$-NCNH_2$ (94,13%)
	$-CH_2N^{\cdot}$(108,22%)
$[M+13]^{+}$ (148)	-12(136,23%)
	-HCN(121,100%)
	$-NHCH_2$(119,14%)
	-2HCN(94,5%)
$[M+15]^{+}$ (150)	$-NH_3$(133,100%)
	-HCN(123,18%)
	$-CH_2N^{\cdot}$(122,6%)
	$-CH_2CNH$ or -(HCN+$NHCH_2$)(109,10%)
$[M+45]^{+}$ (180)	-14(166,5%)
	$-CH_2O$(150,100%)
	$-CH_3OH$(148,94%)
	-44(136,3%)
	-59(121,3%)

表三、6-mercaptopurine (152)的 CAD 結果　(DME 正離子)

$[M-H]^+$(151)	-HCN(124,100%)
$M^{+\cdot}$ (152)	-SH+H_2O(137,4%) -HCN(125,100%) -SH(119,25%) -SH+H_2O-$NHCH_2$ (108,6%) -(HCN+NH_2CH_3)(94,5%)
$[M+H]^+$ (153)	-16(137,7%) -SH_2+H_2O(136,18%) -HCN(126,56%) -H_2S(119,100%) -35(118,44%) -59(94,14%)
$[M+13]^+$ (165)	-HCN(138,100%) +H_2O-$CH_2N^{\cdot}$(155,2%) -$CH_2N^{\cdot}$(137,10%) -$NHCH_2$(136,6%) +H_2O-$CH_2N^{\cdot}$-SH_2(121,34%) -SCH_2(119,49%) -2HCN(111,11%) +H_2O-$CH_2N^{\cdot}$-SH_2-HCN(94,4%) -40(125,25%) -59(106,10%)
$[M+15]^+$ (167)	-$CH_3^{\cdot}$ (152,9%) -HCN(140,40%) -SH_2(133,100%) -CH_2CNH)(126,20%) -CH_3SH (119,6%)
$[M+45]^+$ (197)	-CH_2O(165,17%) -CH_3OH(167,100%)
$[M-27]^+$ (125)	-HCN(98,100%) -2HCN(71,9%)

表四、4-Aminopyrazolo pyrimidine (135.13)的 CAD 結果　(DME 正離子)

$M^{\cdot}$ (135)	-HCN(108,100%)
$[M+H]^+$ (136)	$-NH_3+H_2O$(137,4%) $-NH_3$(119,19%) -HCN(109,100%) $-CH_2N^{\cdot}$(108,37%) $-NCNH_2$(94,10%) $-(HCN+CH_2N^{\cdot})$(81,8%)
$[M+13]^+$ (148)	-12(136,13%) -HCN(121,100%) -2HCN(94,3%)
$[M+15]^+$ (150)	$-NH_3$(133,57%) -HCN(123,35%) $-CH_2N^{\cdot}$(122,100%) $-CH_2CNH$(109,14%) $-(HCN+CH_2N^{\cdot})$(95,18%)
$[M+45]^+$ (180)	-14(166,1%) $-CH_2O$(150,47%) $-CH_2OH$(148,100%) -44(136,2%) -59(121,3%)

表五、6-chloropurine (154)的 CAD 結果　(DME 正離子)

$[M+H]^+$ (155)	$-HCl+H_2O$(137,13%) -HCl(119,100%) -62(93,21%)
$[M+15]^+$ (169)	$-HCl+H_2O$(151,14%) -HCl(133,100%)
$[M+45]^+$ (199)	$-CH_3OH$(169,100%) $-CH_2O$(167,6%) -66(133,2%)

表一、離子/分子反應結果（氧氣正離子）

2,6-dichloropurine(188)	
	M^+(188,100%)
	$[M-Cl+H_2O]^+$(171,8%)
	$[M-Cl]^+$(153,21%)
	$[M-Cl+H_2O-HCl]^+$(135,14%)
6-chloropurine(154)	
	M^+(154,100%)
	$[M-Cl+H_2O]^+$(137,16%)
	$[M-Cl]^+$(119,40%)
	$[M-Cl-HCN]^+$(92,3%)
6-mercaptopurine(152)	
	$[M+O]^+$(168,1%)
	M^+(152,100%)
	$[M-SH+H_2O]^+$(137,6%)
	$[M-HCN]^+$(125,14%)
	$[M-SH]^+$(119,5%)
Adenine(135)	
	$[M+H]^+$(136,100%)
	M^+(135,50%)
	$[M+H-NH_3]^+$(119,1%)
	$[M-HCN]^+$(108,11%)

表二、2,6-dichloropurine(188)的 CAD 結果（氧氣正離子）

M^+(188)	$-Cl+H_2O$(171,25%)
	-Cl(153,100%)
	$-Cl+H_2O-HCl$(135,41%)
	$-Cl_2$(118,5%)
$[M-Cl+H_2O]^+$(171)	$-H_2O$(153,11%)
	-HCl(135,100%)
$[M-Cl]^+$(153)	$+H_2O$(171,8%)
	$+H_2O-HCl$(135,20%)
	-HCN(126,22%)
	-Cl(118,100%)
	-HCl(117,4%)
	-2HCN(99,5%)
	-61(92,54%)
	-(Cl+HCN)(91,18%)
	$-Cl_2$(83,6%)
$[M-Cl+H_2O-HCl]^+$(135)	-HCN(108,100%)
	-CO(107,39%)
	-2HCN(81,8%)
	-(CO+HCN)(80,15%)

表三、6-chloropurine(154)的 CAD 結果（氧氣正離子）

M^+(154)	-Cl+H_2O(137,15%)
	-Cl(119,100%)
	-(Cl+HCN)(192,4%)
[M-Cl+H_2O]$^+$(137)	-H_2O(119,100%)
	-HCN(110,40%)
[M-Cl]$^+$(119)	+2H_2O(155,10%)
	+H_2O(137,1%)
	-HCN(92,78%)
	-CH_2N_2(77,6%)
	-52(67,15%)
	-2HCN(65,15%)

表四、6-mercaptopurine(152)的 CAD 結果（氧氣正離子）

[M+O]$^+$(168)	-9(159,9%)
	-O(152,4%)
	-HCN(141,12%)
	-CO(140,5%)
	-S(136,9%)
	-SH(135,14%)
	-(O+HCN)(125,38%)
	-48(120,100%)
	-(O+2HCN)(98,10%)
M^+(152)	-SH+H_2O(137,32%)
	-SH_2+H_2O(136,3%)
	-HCN(125,100%)
	-28(124,13%)
	-SH(119,67%)
	-SH+H_2O-$NHCH_2$(108,11%)
	-2HCN(98,22%)
	-(SH+HCN)(92,5%)
[M-SH+H_2O]$^+$(137)	-H_2O(119,100%)
	-HCN(110,56%)

表五、Adenine(135)的 CAD 結果（氧氣正離子）

[M+H]$^+$(136)	-NH_3(119,100%)
	-HCN(109,13%)
M^+(135)	-HCN(108,100%)
[M-HCN]$^+$(108)	-HCN(81,71%)
	-CH_2N_2(66,100%)

Ion-Molecule Reaction of Flavones and Flavanones with Dimethyl Ether in an External Source Ion Trap
(黃素母酮類藥物在離子阱質譜儀中之離子/分子反應)

Hui-Fen Wu*, Chao-Ching Wu and Chien-Hong Chen
Department of Chemistry
Tamkang University
Tamsui, Taipei Hsien, 25137, Taiwan, R. O. C.

摘要：

本研究使用 Finnigan 公司之 GCQ^{plus} 離子阱質譜儀，進行氣相離子/分子反應。由於藥物本身結構上的官能基對於藥性有很大的影響，換言之，官能基的位置、種類、數目及其大小對於藥物在生物體中的反應性有顯著的不同。因此，本實驗將藉由單純的氣相反應來瞭解藥物化合物的反應本質。本研究可以對藥物化合物的結構與反應性的關係作更深一層的了解。實驗使用四種黃素母酮(flavones)及一種二氧化黃色素母酮(flavanones)的藥物化合物，分別是 Baicalein、Chrysin、Morin、Fisetin 及 Naringenin。這類化合物具有抵抗癌症和抗氧活性的功效亦可作為抗 HIV 的活性抑制劑。

本實驗利用外部游離法之離子阱質譜儀並加上 CAD 技術，以二甲基醚(DME)作為化學游離試劑氣體。DME 在游離區中主要可生成 $CH3O=CH2^+$（m/z=45）及 $CH3OHCH3^+$（m/z=47）兩種離子，進而可與分析物形成許多的離子/分子產物，雖然黃素母酮類化合物產生微量之$[M+47]^+$ Adduct ion，由於 Finnigan GCQ^{plus} 具有超微量分析的特性，因此能成功地進行 CAD 的實驗。實驗結果顯示：五種黃素母酮類化合物可分別與 OH 官能基或雙鍵形成$[M+13]^+$以及在第 9 號位置的氧或第 4 號位置 C=O 的氧上形成$[M+15]^+$的離子/分子產物。此外，第 2 號及第 3 號碳之間雙鍵和第 3 號碳上 OH 基的存在與否，對於生成子離子的碎片形式有很大的影響，除了常見的掉 H2O 和 CO 以外，亦可見到母離子有中央斷裂的模式存在。壓力效應方面，分別控制不同壓力之 DME 試劑氣體，進行離子/分子反應，實驗結果可以觀察到，較高壓力下，較有利於生成$[M+H]^+$離子。本研究除了可以了解這些藥物其結構與反應性的關係外，產物離子的解離途徑與反應機構，亦可由串聯質譜的分析中詳細被研究。此外，將藉由理論計算方法輔助反應機構的推導。

導論：

一般化合物結構上的官能基其反應活性一直都扮演重要的角色，尤其在藥物化合物的藥性有很大的影響。因此藥物化合物的結構中取代基的位置、種類、數目及大小對於藥物在生物體中的表現有顯著的不同。在本研究中，藉由單純的氣相反應來瞭解藥物化合物的反應途徑及官能基活性。對於以往藥物在溶劑效應下會影響官能基的反應性，本研究可以對藥物化合物的本質作更深一層的探討及推論。而串聯質譜儀是目前唯一對藥物化合物能作確切結構分析的儀器，過去在傳統的內部游離的離子阱質譜儀，DME 是具有選擇性的最有效之正離子化學游離試劑，而外部游離的離子阱質譜儀(Finnigan 之 GCQ^{plus})為最新的設計，在文獻上僅有甲烷的正離子研究報告。本實驗室將 DME 之選擇性，於外部游離之離子阱質譜儀中進行反應。因此，其重要性在此尤其顯著。

本研究使用四種黃素母酮（flavones）及一種二氧化黃色素母酮(flavanones)的藥物化合物，分別是 Baicalein、Chrysin、Morin、Fisetin 及 Naringenin (見圖一)。這類化合物通常用作研究人體或實驗用老鼠的肝臟微粒體（Microsome）[1 - 2]。更有人利用 HPLC - UV 及 LC - MS 調查發現丹參人民日常生活飲食中含有較多的黃素母酮類化合物，對於癌症的關連作過討論和研究[3]。此外，也用作抗氧活性的研究[4 - 5]。另外，亦被研究作為抗 HIV 的活性抑制劑[6 - 7]。因此在生化及藥物的研究領域上被廣泛地應用[8 - 10]。He 等人利用 HPLC - ES - MS 的技術分離出酸柑橘中含有八種黃素母酮類化合物[11]進一步說明此類化合物與人體健康的關係。對於結構鑑定方面，過去曾使用數種不同的游離方式，研究黃素母酮類化合物的碎片型態，並且推導反應機構。Lin 等人提供 Thermospray LC/MS/MS 與 CID 的方法來鑑識茶樹植物中的黃素母酮類化合物[12]，藉由 CID 的圖譜歸納出三種在 pyran ring 上的斷裂型式，作為分辨 flavanone，flavone 及 flavonol 的依據，並且比較 EI、CI 及 FAB 等游離法的優劣。甚至，Barbara 等人使用 TSQ45 之三段四極式質譜儀分別以 EI、PCI 及 NCI 加上 CAD 技術，將橘子及葡萄汁中對於微量的 Naringenin 及 Hesperitin 進行定性分析[13]。先前，Kingstone 針對黃素母酮類藥物化合物有不同位置、數目的 OH 官能基或 OMe 官能基，以 EI 的方式推導出一連串的解離反應途徑[14]，說明碎片離子的形式與相對強度，會因官能基在碳上的位置而有所不同，本研究中離子/分子反應結果所產生$[M+15]^+$以及$[M+13]^+$的 Adduct ion，其造成結構的甲基化以及亞甲基化，能夠經由碰撞活化解離結果，觀察其碎片的改變。Borttger 利用 AEI MS9 及 DuPont 21-490B 型高解析度質譜儀以 methane 及 isobutane 作為化學游離試劑氣體，將某些黃素母酮類藥物化合物，其中包括 Morin 及 Chrysin，在各種不同游離源壓力下，進行離子/分子反應[15]，其中提到當壓力增加時，

在環上具有愈多 OH 官能基愈有利於生成$[M+H]^+$，換言之，OMe 官能基取代 OH 官能基則$[M+H]^+$產物減少，因此壓力的控制在化學游離法中是一個很大的影響因素，通常與化合物的結構有相當的關聯，本研究亦針對不同壓力，說明$M^{+\cdot}$以及$[M+H]^+$相對強度的改變。另外，isobutane 對於只有 OH 官能基的化合物形成$[M+15]^+$離子，因此具有選擇性。Towers 使用氘的同位素取代黃素母酮類化合物中 OH 官能基的氫[16]，詳細說明各種的解離途徑，也瞭解到 OH 官能基在裂解時所扮演的角色，另外，亦針對不同取代 flavanones 及 dihydroflavonols 利用質譜進行結構分析[17]，分別產生不同相對強度之$[M-43]^+$ 以及$[M-57]^+$離子，再度說明取代基扮演了極重要的角色。Kavka 等人曾經陸續研究一系列之$[M-H]^+$黃素母酮化合物[18~20]，由所有的反應機構可以了解，一個$H^\cdot$的掉落能夠引發一連串 CO 的碎片產生，此結果與本研究中連續 CO 的掉落，有若干類似的地方。Cerrati 等人[21]更是主要研究不同位置及數目的 OMe 官能基，得到不同的 EI 圖譜，有利於進一步觀察本研究中$[M+13]^+$及$[M+15]^+$的裂解途徑。然而，早在 60 年代，黃素母酮類化合物的裂解過程便開始詳細討論[22，23]，如今建立了明確的基本解離途徑[24]。另外，Popov 使用 amines 作為試劑氣體研究黃素母酮類化合物[25]，其中也包括 Morin 及 Naringenin，同樣產生具有特異性及選擇性的結果。

質譜儀發展至今，化學游離法一直佔有相當的地位，尤其在試劑氣體方面。由於二甲基醚（DME）試劑氣體在傳統離子阱質譜儀中進行氣相離子/分子反應中對於分析化合物結構上的官能基具有特殊的選擇性，也因此本研究使用二甲基醚作為試劑氣體。從以往的文獻中記載 DME 在游離區中形成 $CH3O=CH2^+$（m/z=45）及 $CH3OHCH3^+$（m/z=47）的兩種形式[27－47]，更進而與分析物形成離子/分子產物，就以本研究中五種黃素母酮類化合物而言，分別與 OH 及 CO 官能基形成$[M+13]^+$及$[M+15]^+$的離子/分子產物，接著控制離子阱質譜儀中環狀及端蓋電極的電壓，將所要分析的母離子分離出來，再施加一特定 AC 電壓，使得母離子斷裂成子離子碎片形式，這就是所謂的碰撞活化解離（Collisional Activated Dissociation）技術，藉由其碎片離子，可以推論出其解離途逕，進一步地推測其反應機構。本研究使用外部化學游離法在離子阱質譜儀針對黃素母酮類藥物化合物進行氣相離子/分子反應，來瞭解其結構之反應性，並以理論計算作為輔助的方法，以與實驗的結果比較。

實驗：

本實驗使用 Finnigan 公司之（Finnigan－MAT，San Jose，CA）GCQ^{plus}離子阱質譜儀的 mass-selective instability mode 進行離子的偵測及操作。選擇二甲基醚（DME）作為化學游離試劑，當二甲基醚以 8×10^{-5} torr 壓力在游離源保持 200℃下形成 m/z=45 及 m/z=47 的兩種型式離子，離子阱中的氦氣壓力為 1 m torr。利用 70 ev 的電壓撞擊游離二甲基醚，形成帶電荷離子，再與分析物在游離源區完成反應形成離子/分子產物，AGC(Auto Gain Control) Prescan 的時間為 1 ms，控制 Lens 1 開啟在 0.3~25 ms 之間，導引離子進入離子阱中。將分析物以 DIP 探針導入游離源區，以 70~100℃/min 的速度加熱到 250℃~390℃之間，使之氣化游離。分離出欲觀察的離子，然後進行時間為 15 ms 的碰撞活化解離，反應所施加的電壓範圍在 0.9~1.5V 之間。另外，也控制試劑氣體壓力至 6×10^{-4} torr 下進行離子/分子反應。理論計算部份，使用 Hyper Chem 5.1 版(Hypercube,Inc.，Gainesville，Florida)的 AM1 計算方法。本研究中五種黃素母酮類化合物，Chrysin、Baicalein、Morin、Fisetin 及 Naringenin。其中 Baicalein 和 DME 購自 Aldrich（Milwaukee，WI），Chrysin、Morin 和 Naringenin 購自 Sigma（Louis，MO），Fisetin 購自 Acros (Pittsburgh，PA)。

結果與討論：

本研究中 GCQ 離子阱質譜儀以 PCI 為外部游離法，化學游離試劑可與進行分析的化合物形成$M^{+\cdot}$、$[M+H]^+$、及選擇性地形成$[M+13]^+$、$[M+15]^+$、$[M+45]^+$或$[M+47]^+$的離子/分子產物（見表一），並且在不同之 DME 試劑氣體壓力下，探討$M^{+\cdot}$與$[M+H]^+$之間相對強度的改變。加上 GCQ 儀器靈敏度極佳，更可以針對反應性的強度及碰撞活化解離的結果，瞭解分析物結構上官能基的位置、大小、數目及種類與解離途逕的關聯，並利用理論計算的方式補充說明中央斷裂的結果，估計離子/分子反應之生成熱以及反應熱，作為最有利反應位置的參考依據。以下將探討五種黃素母酮類藥物化合物(見圖一)應用在離子阱之外部化學游離法，並說明它們結構上反應的差異性。

(1) 黃素母酮與 DME 的離子/分子反應之理論計算：

本研究中利用 AM1 半經驗法考慮分子內氫鍵，計算出離子/分子反應中$[M+H]^+$、$[M+13]^+$及$[M+15]^+$的反應熱(見表二之一)及五種黃素母酮形成$[M+H]^+$、$[M+13]^+$及$[M+15]^+$之生成熱(見表二之二~表二之六)，其中反應熱的值，是由所有產物之生成熱的值減去所有反應物之生成熱的值($\Delta Hrxn = \Sigma\Delta Hf \text{ of products} - \Sigma\Delta Hf \text{ of reactants}$)，例如：表二之一中 Chrysin 於第 5 號位置的 OH 基與 DME 的 $CH3OCH2^+$(m/z=45)

離子形成[M+13]$^+$離子，其反應熱為-31 Kcal/mole，乃是由表二之二、Chrysin 之生成熱理論計算結果中，[M+13]$^+$離子與 CH3OH 的生成熱之和(-48 Kcal/mole+89.3596 Kcal/mole)，減去 M 與 $CH3OCH2^+$(m/z=45)離子的生成熱之和(-85.3161 Kcal/mole+158 Kcal/mole)。但實驗中[M+15]$^+$的來源可能為[M+45]$^+$及[M+47]$^+$，所以將兩種生成途徑均予以計算。由於 DME 對於結構中的官能基具有選擇性，往往在結構中可能參與反應的位置不止一種，因此必須利用理論計算的方法以計算出最有利生成離子/分子反應的官能基位置或反應途徑，進而了解其反應機構的推導。然而黃素母酮類化合物所表現的中央斷裂結果能夠提供部份反應位置的訊息，計算最有利的反應位置，作為反應機構推導的依據。

(2) 黃素母酮類藥物化合物與 DME 的離子/分子反應：

表一為離子/分子反應的結果，可以觀察到有形成 Adduct ion：[M+47]$^+$、[M+45]$^+$、[M+15]$^+$、[M+13]$^+$、[M+H]$^+$、$M^{\cdot+}$以及中央斷裂碎片離子。其中 Adduct ion 為二甲基醚離子與黃素母酮類化合物反應後因特定官能基所造生成，[M+H]$^+$為 m/z=47 之二甲基醚離子所進行的 proton transfer。過去文獻曾經觀察到黃素母酮類化合物進行化學游離法時，可以得到 $M^{\cdot+}$的離子[15，25]，並且解釋為 charge exchange 所造成，因此本實驗針對不同的試劑氣體壓力，清楚說明壓力對於 $M^{\cdot+}$及[M+H]$^+$的影響：圖六、為 Baicalein 在 8×10^{-5} torr 時的離子/分子反應圖譜，m/z = 270 為 $M^{\cdot+}$離子，m/z = 271 為[M+H]$^+$離子，其中 $M^{\cdot+}$為明顯的 base peak，[M+H]$^+$的相對強度只有 21%，然而，圖七、為 Baicalein 在 6×10^{-4} torr 時的離子/分子反應圖譜，m/z = 271 的[M+H]$^+$離子反而成為了 base peak，$M^{\cdot+}$離子的相對強度幾乎為零，Naringenin 亦發生類似的情形(見圖八、圖九)。觀察以上現象可以瞭解，較高的試劑氣體壓力有利於[M+H]$^+$離子的生成，主要為 proton transfer 的反應途徑。探討 $M^{\cdot+}$離子的產生，可能為化合物濃度低於試劑氣體的 10^3~10^4 倍時，電子束較有機會撞擊游離化合物(M+e1→$M^{\cdot+}$+e1+e2) 形成 $M^{\cdot+}$離子。本研究中所觀察到之中央斷裂模式，在先前所提到的文獻所述[13~17，20，21~24]的 Retro-Diels-Alder(RDA) cleavage 相符，通常發生在不飽和的環上[26]。黃素母酮類化合物所產生之中央斷裂碎片，可能經由 Adduct ion，[M+H]$^+$及 $M^{\cdot+}$而來，所以經由分離出特定離子進行碰撞活化解離，能夠幫助其結構上的鑑定。

由於離子/分子反應的進行是在於游離源區，而並非為傳統在離子阱中所生成之離子/分子產物，因此產物離子經由加速電板導入離子阱的同時，系統便給予母離子足夠的動能以及較高的內能，以造成中央斷裂的情形，另一方面也得到大量掉 CO 及 H2O 的碎片離子。在 Naringenin 的結構中，第 2、3 號位置的碳間不具有雙鍵，其中央斷裂之 RDA 分裂步驟較其它含有雙鍵的化合物更為顯著，並且無法和其它類型的化合物一般，形成掉 CO 及 H2O 之產物離子。由表三及表四之碰撞活化解離結果可知，Naringenin 的 m/z=179 碎片離子，其來源可能是[M+H]$^+$掉 C6H6O 或 $M^{+\cdot}$掉 C6H5O 或[M+45]$^+$掉 C8H10O2 所造成；m/z=166 的碎片離子，其來源可能是 $M^{+\cdot}$掉 C7H6O 或[M+H]$^+$掉 C7H7O 所造成；m/z=153 的碎片離子來源則可能為以下的情形：$M^{+\cdot}$掉 C8H7O、[M+H]$^+$掉 C8H8O、[M+13]$^+$掉 C9H8O、[M+15]$^+$掉 C8H7O 及 $CH3^\cdot$、[M+45]$^+$掉 C8H4O4。另外 m/z=120 的碎片離子則為 charge migration 形成掉 C7H4O4 的碎片。Chrysin 與 Baicalein(圖十與圖十一為離子/分子反應質譜圖)則為 charge retention 分別掉 C8H6 以形成 m/z=152 以及 m/z=168 的碎片離子，而更進一步掉一個 CO 形成 m/z=124 及 m/z=140 之碎片離子。Morin 與 Fisetin(圖十二與圖十三為離子/分子反應質譜圖)在第 3 號位置上的 OH 基不利於結構進行 RDA 的 α-cleavage，造成複雜的裂解。參考文獻[27]提到：愈多的官能基取代之不飽和環將愈減少 RDA 的裂解。另外 Morin 及 Fisetin 均有[M-OH]$^+$的碎片離子產生，推測其為第 3 號位置上 OH 基的掉落，所以 RDA 的裂解過程中，OH 基的掉落是為重要的關鍵，使得 Morin 產生 m/z=153 的碎片離子，其來源可能是 $M^{+\cdot}$掉 C8H5O3、[M+H]$^+$掉 C8H6O3、[M+13]$^+$掉 C9H6O3、[M+15]$^+$掉 C8H4O4；m/z=137 的碎片離子，其來源為[M+H]$^+$掉 C8H6O4。同樣地 Fisetin 亦有 m/z=137 的碎片離子，其來源為 $M^{+\cdot}$掉 C8H5O3 或[M+H]$^+$掉 C8H6O3。

過去文獻中[15]，Borttger 以 methane 作為化學游離試劑氣體所得到的結論：OH 官能基的存在將導致[M+H]$^+$離子的生成，此結果與本實驗的結果相符合。[M+H]$^+$離子是由 $CH3OHCH3^+$(m/z = 47)離子 proton transfer 而來，根據實驗結果：Fisetin 中第 3'和 4'位置的碳上有相鄰的 OH 基，由於 ortho effect 形成穩定較大的相對強度 5% 的[M+47]$^+$產物。Fisetin 並沒有如同其它化合物有 CO 的掉落，因此第 5 號位置上的 OH 官能基的存在與否是影響第 4 號位置 carbonyl group 的主要因素。除了 Naringenin 外，其餘四種化合物之 $M^{+\cdot}$及[M+H]$^+$結果相似，以 $M^{+\cdot}$為 base peak。結構中的官能基位置會比數量來得重要許多，Naringenin 在第 4'位置上的 OH 基、Morin 在第 2'、4'位置上的 OH 基及 Fisetin 在 3'、4'上的 OH 基，導致有明顯較多的 Adduct ion 形成，對於 DME 的 m/z=45 及 m/z=47 的競爭反應可以知道，ortho 位置有利於形成[M+47]$^+$。至於[M+13]$^+$及[M+15]$^+$的發生反應的可能位置，無法直接由離子/分子反應得知，必須進一步進行碰撞活化解離，並且運用理論計算的方法，估計其中最有利於發生反應的位置。

(3) 比較 $M^{+\cdot}$及[M+H]$^+$離子碰撞活化解離的結果：

表三為 $M^{+\cdot}$及[M+H]$^+$離子碰撞活化解離的結果，由於離子阱質譜儀所提供 Tandem in time MS 的功能，針對分離出的離子施加 AC 電壓使之碰撞緩衝氣體的機率增加，導致自身的內能上升，裂解成為碎片離子。本實驗中二甲基醚的 m/z=47 離子提供質子化條件，形成[M+H]$^+$離子，針對黃素母酮類化合物進行[M+H]$^+$及 $M^{+\cdot}$之碰撞活化解離比較，其中最重要的部份為 RDA 裂解之中央斷裂模式，藉由此中央斷裂的結果可以推論出 protonation site，表六及表七即對不同的裂解方式，更進一步作探討，並利用理論計算的方法，計算出最有利反應的位向(見表二)，以助於瞭解反應機構的進行。

Chrysin 和 Baicalein 的 $M^{+\cdot}$離子碰撞活化解離結果(見圖十四及十五)可得到掉乙炔基-苯(C8H6)的 neutral loss，是為第 2 號和第 9 號間碳氧鍵的斷裂以及第 3 號和第 4 號間碳鍵的斷裂(Path a)。對於[M+H]$^+$而言，Baicalein 及 Chrysin (圖十六為 Chrysin 之[M+H]$^+$ CAD 圖譜)，同樣有乙炔基-苯的 neutral loss，進而分別形成 m/z=169 及 m/z=153 的子代離子，同樣的斷裂方式(path a)，可以清楚地看出，藉由理論計算的方法，判斷兩種化合物的 protonation site 為第 4 號位置的 CO 基以及第 5 號位置的 OH 基之間(Chrysin：ΔH = -26 kcal/mole，Baicalein：-24 kcal/mole)，單一質子與氧原子的孤對電子形成氫鍵。這與 Lin 等人所研究一系列黃素母酮化合物所得到的裂解途徑結果相當吻合[12]。

Naringenin 的 $M^{+\cdot}$離子碰撞活化解離結果可知(見圖十七與表六：path d)，碎片離子 m/z=179 為 phenyl ring(C6H5O)的 radical 掉落，而[M+H]$^+$(圖十八為 Naringenin 形成[M+H]$^+$之 CAD 圖譜)卻為 C6H6O 的 radical 掉落(表七：path d)，藉由表五的理論計算結果，因此判斷 protonation site 為環上第 3'位置的雙鍵(ΔH = -19 kcal/mole)。另外由表七的結果，可以觀察到當進行裂解途徑 a 或 c 時，理論計算推論其最有可能的 protonation site 為第 3'位置的雙鍵或第 4 號位置的 C=O 官能基(ΔH = -41 kcal/mole)。$M^{+\cdot}$與[M+H]$^+$的解離差異在於 b 的裂解途徑，當 Naringen 在第 4 號位置的 C=O 官能基被質子化後，便會有不同的裂解結果，分別為 m/z=137 及 m/z=147 的碎片離子。由此可知，質子化反應可能改變整體結構的裂解反應。

Morin 的 protonation site 與 Naringenin 相似，依據實驗結果(見表三、圖十九、二十)與表二的理論計算結果顯示，質子化的最有可能位置為第 3'位置的雙鍵(ΔH = -1 kcal/mole)及第 4 或第 5 位置的氧(ΔH = -20 kcal/mole)上，比較圖二及圖三的裂解型式可知：當質子化後，便增加了 b 途徑的裂解。結果中可以見到有大量的 OH radical 掉落，比較 Naringenin 和 Fisetin 結構以及結果得知，掉落的 OH radical 為第 2'號位置上的 OH 基，因為第 3 號位置的 OH 基可以與鄰近的 C=O 基形成分子內氫鍵，穩定存在，而同樣在 Naringenin 的第 4'號位置的 OH 基，並沒有造成大量 OH radical 掉落。

Fisetin 的 protonation site 根據理論計算結果與碰撞活化解離(見圖二十一及圖二十二)的中央斷裂碎片(表六)，判斷最有可能在於第 6'位置的雙鍵(ΔH = -6 kcal/mole)抑或第 4 號位置的 C=O 官能基(ΔH = -21 kcal/mole)上，同樣地，比較圖二與圖三的裂解方式能夠瞭解：Fisetin 質子化過程也增加了對 b 途徑的裂解。另一方面，透過表六中 Morin 及 Fisetin 的 $M^{+\cdot}$中央斷裂模式可以証實，path a 所造成 m/z=153 及 m/z=137 的碎片離子，其原因為：當第 3 號及第 4 號間的碳鍵斷裂時，第 3 號位置的 OH 基的氫原子(第　號位置的 OH 與第 4 號位置的氧形成分子內氫鍵)會被相鄰的 CO 所抓取，鍵結在氧上形成碎片離子。

觀察本研究中黃素母酮類化合物之 $M^{+\cdot}$碰撞活化解離結果(見表三)可知，Chrysin 及 Baicalein 在第 5 號位置有一個 OH 官能基，並沒有與第 4 號位置的 CO 形成有力的分子內氫鍵，造成 Chrysin 上的第 4 號位置的 CO 容易掉落，造成[M-CO]$^+$(m/z=226)有 100% 的相對強度，同理，Baicalein 的[M-CO]$^+$(m/z=242)亦有 34% 的相對強度。然而，對於 Naringenin 而言，則以中央斷裂的情形為主要裂解途徑，無法由中央斷裂結果，作為判斷是否容易掉 CO 的依據。另一方面 Fisetin 則在第 3 號位置有一個 OH 官能基，它與 CO 形成的分子內氫鍵仍然微弱，使得[M-CO]$^+$(m/z=258)亦有 23% 的相對強度。因此歸納以上的推論，對於 Morin 而言，同時具備第 3 號位置及第 5 號位置的 OH 官能基，使得分子內氫鍵變成顯著，由 Morin 的[M-CO]$^+$(m/z=274)相對強度只有 2% ，可以再次清楚地了解，官能基的位置不同對於分子結構的反應性有很大的影響。

(4) [M+13]$^+$、[M+15]$^+$、[M+45]$^+$、[M+47]$^+$離子/分子產物碰撞活化離的結果：

本系列黃素母酮類化合物的[M+13]$^+$、[M+15]$^+$、[M+45]$^+$、[M+47]$^+$ Adduct ion 之 CAD 結果詳列於表四。而表八及表九分別為[M+13]$^+$及[M+15]$^+$之中央斷裂結果列表，由圖四及圖五便可以了解其斷裂的方式。實驗結果類似 $M^{+\cdot}$和[M+H]$^+$的結果，有 1 個 H2O 以及數個 m/z = 28 的 loss，也有中央斷裂的模式。原本結構中最具有反應性的位置被 DME 反應形成 adduct ion 之後，結構的穩定性必將隨之改變，CAD 的結果也就不盡相同。至於所形成 adduct ion 的反應位置，與前一段落所描述的方法相同，利用理論計算來探討每個可能發生加成反應的位置，根據計算出的反應熱，提供作為碰撞活化解離之反應機構的參考(見表二)。

(5) $[M+13]^+$的離子碰撞活化解離的結果：

$[M+13]^+$的來源為$[M+45]^+$之 CH3OH neutral loss。Chrysin、Baicalein 比較$[M+13]^+$(見圖二十三、圖二十四)與$[M+H]^+$、$M^{+\cdot}$的碰撞活化解離之中央斷裂結果(表六、七、八：path a)，同樣有乙炔基-苯的 neutral loss，可以得知 Chrysin、Baicalein 的甲烯基化的位置相似於質子化的位置，經由表五得知，甲烯基化的反應在第 5 號位置的 OH 基(ΔH = -31 kcal/mole)。Scheme 1A 為描述 Chrysin 形成 m/z=221 的碰撞活化解離反應機構，因為第 5 及第 7 位置的 OH 基參與的 H2O 的掉落，所以推測甲烯基化發生在第 4'位置的雙鍵上(ΔH = -3 kcal/mole)；Scheme 2B 則描述第 5 號位置 OH 基的甲烯基化與中央斷裂反應機構。

分析碰撞活化解離碎片(見表四及圖二十五)以及理論計算結果(見表二)可以研判，Naringenin 的亞甲基化位置有兩種可能：一、為第 8 號位置的雙鍵(見 cheme 2) (ΔH = -47 kcal/mole)，以表八之 path a 中央斷裂模式掉落 C8H8O 的碎片，形成 m/z=165 的子代離子，或是經由表八之 path b 掉落 C6H6O 碎片，形成 m/z=191 的子代離子。二、為第 3'位置的雙鍵(ΔH = -30 kcal/mole)，經由表八之 a 途徑斷裂形成 m/z=153 的子代離子。

由表二理論計算結果得知，並觀察中央斷裂碎片(見表四及圖二十六)，推測 Morin 的甲烯基化可能發生在第 5 位置的 OH 基(ΔH = -20 kcal/mole)或第 5'位置的雙鍵上(ΔH = -26 kcal/mole) (見表八)。因此反應在第 5 位置的 OH 基，經由表八之 b 途徑所斷裂的過程，第 3 位置的 OH 基會與同時斷裂的間位雙 OH 基取代之苯環形成 1、2、4-trihydroxyl benzene 的 neutral loss，於是產生 m/z=189 的子代離子。另外甲烯基化發生在第 5'位置的雙鍵，經由 path b 的裂解則產生 m/z=139 的子代離子。甲烯基化發生在第 5'位置的雙鍵，經由 path a 則產生 m/z=153 的子代離子。

Fisetin 的甲烯基化離子，碰撞活化解離的結果(見表四及圖二十七)，並沒有見到中央斷裂模式，表示 Fisetin 的$[M+13]^+$離子，抑制了 RDA 裂解之中央斷裂模式的反應進行，但由理論計算的觀點可以知道其最有利之反應位置在第 2'位置的雙鍵上(ΔH = -36 kcal/mole)。

(6) $[M+15]^+$的離子碰撞活化解離的結果：

本研究中$[M+15]^+$甲基化離子之來源，除了從$[M+45]^+$掉 CH2O 外，由$[M+47]^+$亦可掉 CH3OH 以形成$[M+15]^+$離子。表九為$[M+15]^+$之中央斷裂結果，圖五為$[M+15]^+$之中央斷裂途徑。所有$[M+15]^+$的 adduct ion 均有掉 CH3• 的現象，說明甲基對於分子結構的鍵結力普遍不強，所以最初離子/分子反應時，其$[M+15]^+$的強度均低於 10% ，另外，化合物本身容易掉 CO，亦會造成$[M+15]^+$形成的機會降低。

根據碰撞活化解離的結果推斷(見圖二十八及圖二十九)，Chrysin 與 Baicalein 之中央斷裂為表九的 path a 所造成，表二之理論計算結果指出第 4 號位置的 C=O 官能基有利於形成甲基化離子(ΔH = -23 kcal/mole，-19 kcal/mole)，分別產生 m/z=167 及 m/z=183 的碎片離子(Scheme 3)。

Naringenin 的$[M+15]^+$離子之形成以及中央斷裂反應機構，詳述於 Scheme 4 中，圖三十為 Naringenin 形成$[M+15]^+$離子之 CAD 圖譜，理論計算顯示反應位置在第 9 號位置的氧上(ΔH = -13 kcal/mole)，經由表九之 path a 產生 m/z=167 的碎片離子，path b 則產生 m/z=137 的碎片離子。反應位置在第 4 號位置的 C=O 官能基上(ΔH = -39 kcal/mole)，則經由 path c 產生 m/z=161 的碎片離子。

Morin 的理論計算結果可知(見表二)，甲基化反應位置在第 9 號位置的氧上(ΔH = -8 kcal/mole)，圖三十一為 Morin 形成$[M+15]^+$離子之 CAD 圖譜，經由表九之 path b 產生 m/z=139 之碎片離子，經由 path c 則產生 m/z=165 之碎片離子，另外，反應在第 4 號位置的氧(ΔH = -18 kcal/mole)，經由表九之 path a 產生 m/z=167 之碎片離子。

Fisetin 的$[M+15]^+$離子碰撞活化解離結果(見表四及圖三十二)，並沒有中央斷裂的情形，此結果與$[M+13]^+$相似，甲基化的過程抑制了 RDA 的裂解，然而，從其它 neutral loss 所得到的碎片離子，無法得知其甲基化的位置，因此利用理論計算的方法，推論第 4 號位置的氧為最有可能的反應位置(ΔH = -22 kcal/mole)。

(7) $[M+45]^+$的離子碰撞活化解離的結果：

根據以往文獻記載$[M+45]^+$會生成$[M+13]^+$及$[M+15]^+$，其結果是依化合物本身結構而定，事實上，形成$[M+13]^+$或$[M+15]^+$是為競爭反應，因此藉由碰撞活化解離的結果，能夠進一步了解其中反應性的優勢。本研究中$[M+45]^+$掉 CH3OH 形成$[M+13]^+$之相對強度皆為 100%，原因為化合物結構中的 OH 基或雙鍵所提供的反應途徑形成$[M+13]^+$均比由第 4 號或第 9 號反應位置的氧形成$[M+15]^+$的來得容易。

由於 Chrysin 的 OH 基最少，$[M+15]^+$的相對強度也高達 59% (圖三十三為 Chrysin 形成$[M+45]^+$之 CAD 圖譜)，但 Baicalein 在第 6 號的位置多了 1 個 OH 基，$[M+15]^+$的相對強度下降到只有 3%，說明官能基的

位置是決定化合物結構反應性的重要關鍵。Morin 形成$[M+45]^+$後碰撞活化解離有掉 H2O 的現象，並且形成$[M+13]^+$、$[M+15]^+$的離子後也掉 H2O，可見發生掉 H2O 的官能基與形成 adduct ion 的官能基並不相同。Fisetin 卻在形成$[M+45]^+$ adduct ion 後可掉 CO，因此，主要使$[M+45]^+$結構穩定而不會有掉 CO 的現象，取決於第 5 號位置的 OH 基存在與否。Naningenin 之$[M+45]^+$碰撞活化解離結果產生一系列類似中央斷裂的碎片離子，然而判斷其碎片的來源，只能由$[M+13]^+$及$[M+15]^+$的碰撞活化解離結果作為依據，m/z=165 的碎片離子，其來源為$[M+13]^+$掉 C8H8O 所造成，m/z=153 的碎片離子，其來源為$[M+13]^+$掉 C9H8O 或$[M+15]^+$掉 C8H7O 及
$CH3\bullet$所造成。

(8) $[M+47]^+$的離子碰撞活化解離的結果：

本研究中所有的$[M+47]^+$離子經過碰撞活化解離均產生$[M+15]^+$的離子，此點非常特殊，因為文獻上$CH3OHCH3^+$（m/z=47）為 protonation agent，$[M+47]^+$離子進行碰撞活化解離後，一般產生$[M+H]^+$離子而非$[M+15]^+$離子。其中 Chrysin 有掉 CH2O(見圖三十四)，表示具有較強拉 $CH3^+$自由基及質子的能力，Morin 形成$[M+47]^+$離子仍然有掉 H2O，情形與$[M+45]^+$離子碰撞活化解離結果相同，同樣地，Fisetin 也有掉 1 個 CO 及 1 個質子的情形，此現象與前述之$[M+45]^+$碰撞活化解離結果相似，亦取決於第 5 號位置的 OH 基存在與否。

(9) 離子/分子反應產生的碎片離子進行碰撞活化解離結果：

表五為反應形成碎片產物離子 CAD 的結果，其中以碎片中相對強度較強的$[M+H-CO]^+$及$[M-CO]^+$為主。從表中所顯示的碎片型態可知，幾乎為掉 1 個 H2O 和掉數個 m/z= 28 (可能為 CO 或 C2H4)的結果，原本推論的中央斷裂模式，無法觀察到有顯著規則性的斷裂，原因是 RDA 的裂解牽涉到六員環上π電子所造成的α-cleavage，然而本實驗中 Chrysin、Baicalein、Naringenin 的$[M+H-CO]^+$及$[M-CO]^+$離子推測是為第 4 號位置的 C=O 掉下所形成的離子，因此不利於 RDA 的裂解。Fisetin 及 Morin 的$[M+H-OH]^+$和$[M-OH]^+$碰撞活化解離也是沒有明顯中央斷裂的現象，所以第 3 號位置的 OH 基掉落同樣不利 RDA 裂解，所以對於最初離子/分子反應時，所形成的中央斷裂碎片並未被以上的碎片產物離子所貢獻，而是接下來的逐步斷裂。由先前所述的結果可知，母離子斷裂成碎片的途徑為 1 個 H2O 及數個 CO 的逐漸斷裂模式，但是另一方面 Naringenin 即使掉 CO，仍然有掉 phenyl ring 的現象，以其他化合物而言，第 2 號及第 3 號碳間雙鍵的存在，同樣也能夠共振加強第 1 號及第 2 號間的碳鍵，因此，除了官能基的效應以外，此雙鍵對於化合物斷裂生成碎片離子的反應機構，亦扮演極重要的角色。

結論：

本研究利用理論計算的方法，以及黃素母酮類化合物具有中央斷裂的特徵，加上串聯質譜儀的優點，作為判斷化合物進行離子/分子反應時，其最有可能的反應位向。因此本實驗所使用之離子阱質譜儀，以及結合碰撞活化解離技術，對於氣相分子之間反應性的探討，本研究方法能夠提供更進一步的瞭解。與傳統質譜技術相比，不僅離子阱質譜儀具有高靈敏度外，對於定性分析方面，亦具有相當之可信度。

參考資料:

[1]M.C.CanivencLavier,M.F.V_roevaut,M.Totis,*Toxicology*,**1996**,114,19-27.
[2]M.H.Siess,J.Leclerc,M.C.CanivencLavier,*Z.Pflanzenk Pflanzen*,**1994**,101,662-665.
[3]U.Justesen,P.Knuthsen,T.Leth,*Cancer Lett*.,**1997**,114,165-167.
[4]T.Yokozawa,E.Dong,Z.W.Liu,M.Shimizu,*Phytother Res*.,**1997**,11,446-449.
[5]A.Mori,H.Hamada,H.Ohyama,M.Hiramatsu,S.Shinohara,*Proc.Int.Symp.Nat.Antioxid.:Mol.Mech.Health Eff*.,**1995**,45-53.
[6]J.W.Critchfield,S.T.Butera,T.M.Folks,*AIDS Res.Hum.Retroviruses*,**1996**,12,39-46.
[7]J.K.Buolamwini,K.John,K.Raghavan,M.R.Fesen,Y.Pommier,K.W.Kohn,J.N.Weinstein,*Pharm.Res*.,**1996**,13,1892-1895.
[8]A.M.S.Silva,M.Weidenborner,J.A.S.Cavaleiro,*Mycol.Res*.,**1998**,102,638-640.
[9]M.Weidenborner,H.C.Jha,*Mycol.Res*.,**1997**,101,733-736.
[10]M.Weidenborner,H.C.Jha,*Z.Pflanzenk Pflanzen*,**1994**,101,662.
[11]X.G.He,L.Z.Lian,L.Z.Lin,M.W.Bernart,*J.Chromatogr.A*,**1997**,791,127-134.
[12]Y.Y.Lin,K.J.Ng,Shenjiang Yang,*J.Chromatogr*.,**1993**,629,389-393.
[13]A.W.Randy,A.Barbara,V.J.Jodie,A.Y.Richard,*J.Agric.Food Chem*.,**1995**,43,1966-1968.
[14]D.G.I.Kingston ,*Tetrahedron*,**1971**,27,2691-2700.

[15]J.Yinon,D.Issachar and H.G.Boettger,*Organic Mass Spectrometry*,**1978**,13,167-171.
[16]F.Balza and G.H.N.Towers,*Phytochemistry*,**1984**,23,2333.-2337.
[17]F.Balza,W.J.Crins,B.A.Bohm and G.H.N.Towers,*Phytochemistry*,**1988**,27,2715-2717.
[18]F.H.Guidugli,M.J.Pestchanker,J.Kavka and P.J.Nathan,*Org. Mass Spectrom.*,**1984**,19,502-505.
[19]F.H.Guidugli,C.E.Ardanaz,J.Kavka,M.E.Garibay and P.J.Nathan,*Org. Mass Spectrom.*,**1986**,21,117-124.
[20]F.H.Guidugli,J.Kavka, M.E.Garibay,R.L.Santilan and P.J.Nathan,*Org. Mass Spectrom.*,**1987**,22,479-485.
[21]T.Berahia,E.M.Gaydou,C.Cerati and J.C.Wallet,*J.Agri.Food Chem.*,**1994**,42,1697-1700.
[22]Y.Itagaki,T.Kurokawa,S.Sasaki,C.T.Chang and F.C.Chen,*Bull. Chem. Soc. Japan*,**1966**,39,538-543.
[23]A.Pelter and P.Stainton,*J.Chem.Soc.(c)*,**1967**,1933-1937.
[24]N.Chaves,J.J.Rios,C.Gutierrez,J.C.Escudero and J.M.Olias,*J.Chromatogr.*,**1998**,799,111-115.
[25]V.S.Bankova,N.N.Mollova and S.S.Popov,Org. *Mass Spectrom.*,**1986**,21,109-116.
[26]F.W.McLafferty, *Interpretation of Mass Spectra*,**1993**,4th ed.,University Science Books Press,Mill Valley,CA.
[27]T. Donovan and J. Brodbelt, *J. Am. Soc. Mass Spectrom.*, **1992**, 3, 47-59.
[28]J. J. Isbell and J. S. Brodbelt, *J. Am. Soc. Mass spectrom.*, **1996**, 7, 565-572.
[29]T. D. McCarley and J. Brodbelt, *Anal. Chem.*, **1993**, 65, 2380-2388.
[30]E. J. Alvarez and J. S. Brodbelt, *J. Mass Spectrom.*, **1996**, 31, 901-907.
[31]J. X. Shen and J. Brodbelt, *J. Mass Spectrom.*, **1996**, 31, 1389-1398.
[32]C.-C. Liou, E. S. Eichmann and J. S. Brodbelt, *Org. Mass Spectrom.*, **1992**, 27, 1098-1104.
[33]J. S. Brodbelt, J. N. Louris and R. G. Cooks, *Anal. Chem.*, **1987**, 59, 1278-1285.
[34]T. Keough, *Anal. Chem.*, **1982**, 54, 2540-2547.
[35]J. S. Brodbelt, *Mass Spectrom. Rev.*, **1997**, 16, 91-110.
[36]T. Donovan, C.-C. Liou and J. Brodbelt, *J. Am. Soc. Mass Spectrom.*, **1992**, 3, 39-46.
[37]A. Colorado and J. Brodbelt, *Anal. Chem.*, **1994**, 66, 2330-2335.
[38]T. Donovan and J. Brodbelt, *Biol. Mass Specrtom.*, **1992**, 21, 254-258.
[39]E. S. Eichmann and J. S. Brodbelt, *Org. Mass Spectrom.*, **1993**, 28, 665-671.
[40]J. Brodbelt, C.-C. Liou and T. Danovan, *Anal. Chem.*, **1991**, 63, 1205-1209.
[41]E. S. Eichmann and J. S. Brodbelt, *Org. Mass Spectrom.*, **1993**, 28, 737-744.
[42]C.-C. Liou, J. Isbell, H.-F. Wu, J. S. Brodbelt, R. A. Bartsch, J. C. Lee and J. L. Hallman, *J. Mass Spectrom.*, **1995**, 30, 572-580.
[43]G. F. Bauerle, Jr, B. J. Hall, N. V. Tran and J. S. Brodbelt, *J. Am. Soc. Mass Spectrom.*, **1995**, 7, 250-260.
[44]T. Donovan and J. Brodbelt, *Org. Mass Spectrom.*, **1992**, 27, 9-16.
[45]G. F. Bauerle, Jr and J. S. Brodbelt, *J. Am. Soc. Mass Spectrom.*, **1995**, 6, 627-633.
[46]E. J. Alvarez and J. S. Brodbelt, *J. Mass Spectrom.*, **1995**, 30, 625-631.
[47]M. Tang, J. Isbell, B. Hodges and J. Brodbelt, *J. Mass Spectrom.*, **1995**, 30, 977-984.

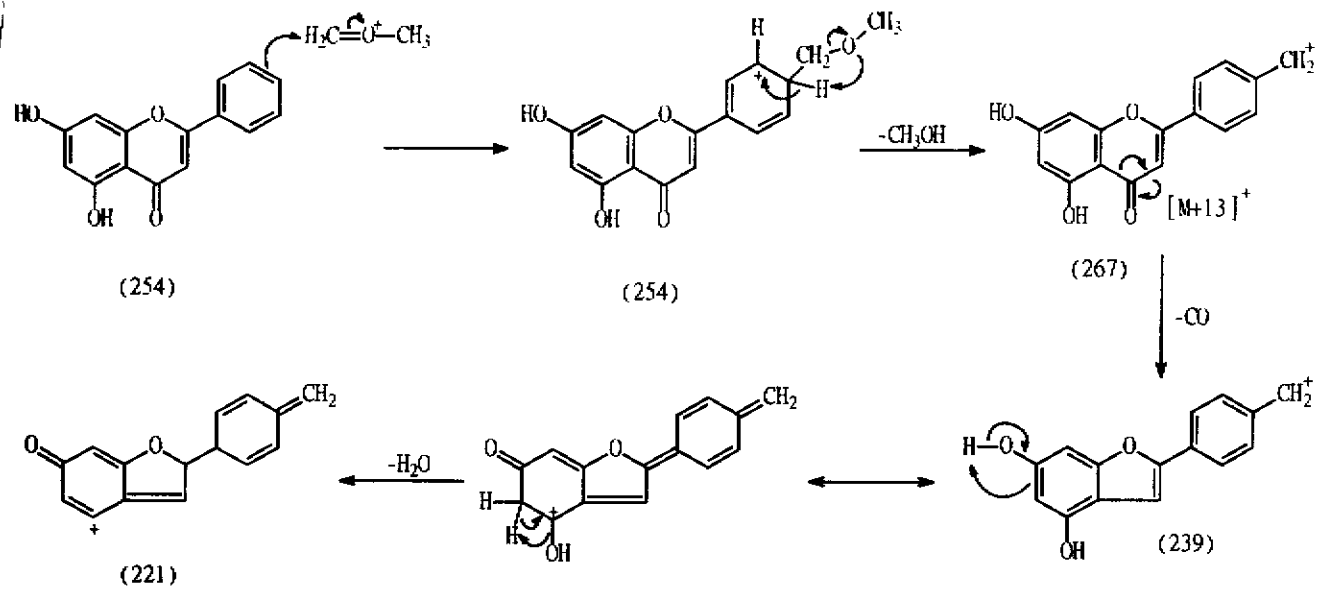

Scheme. 1A

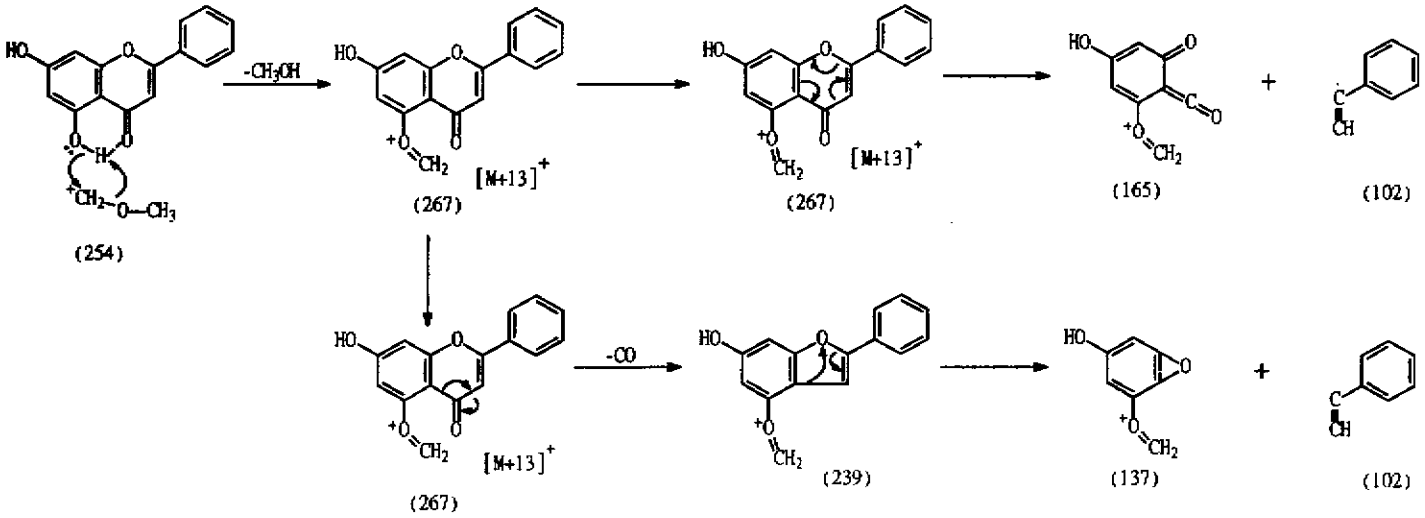

Scheme. 1B

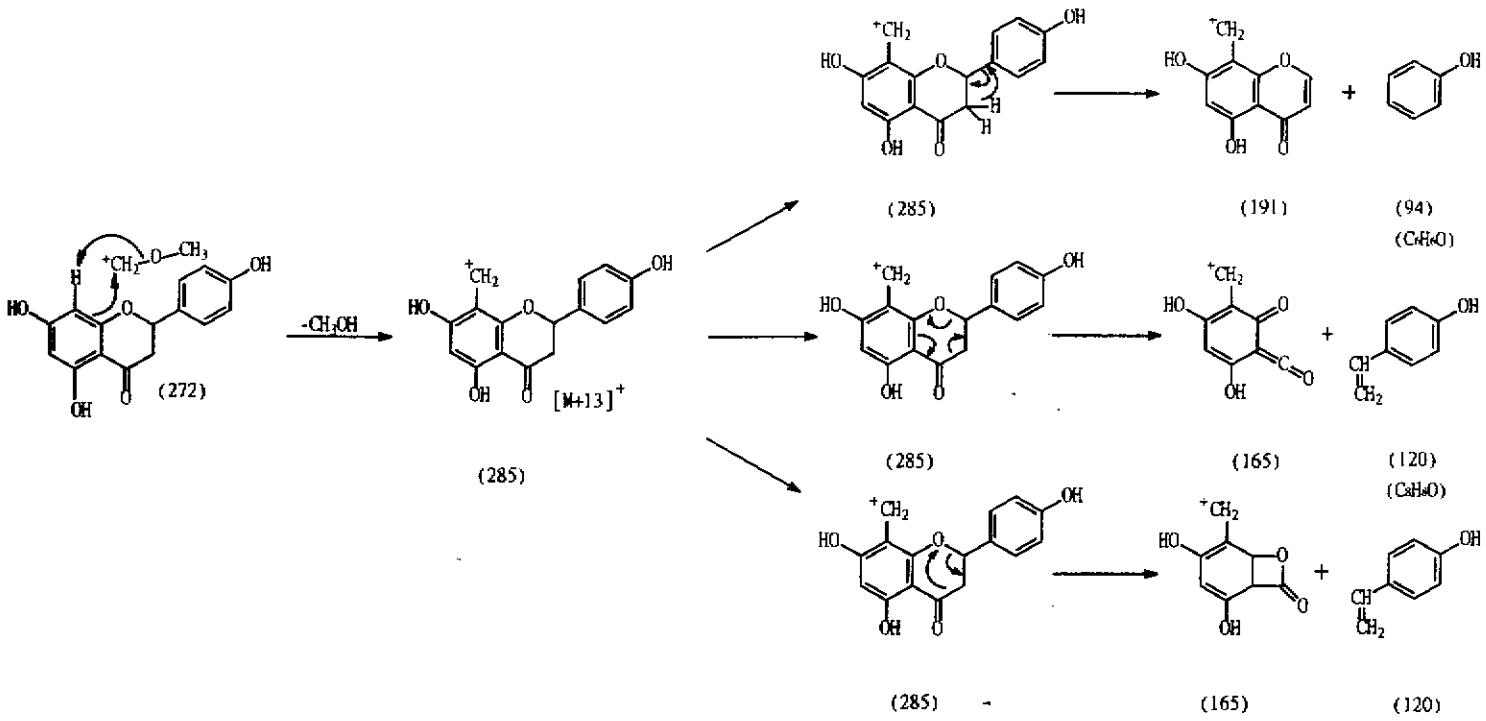

Scheme. 2

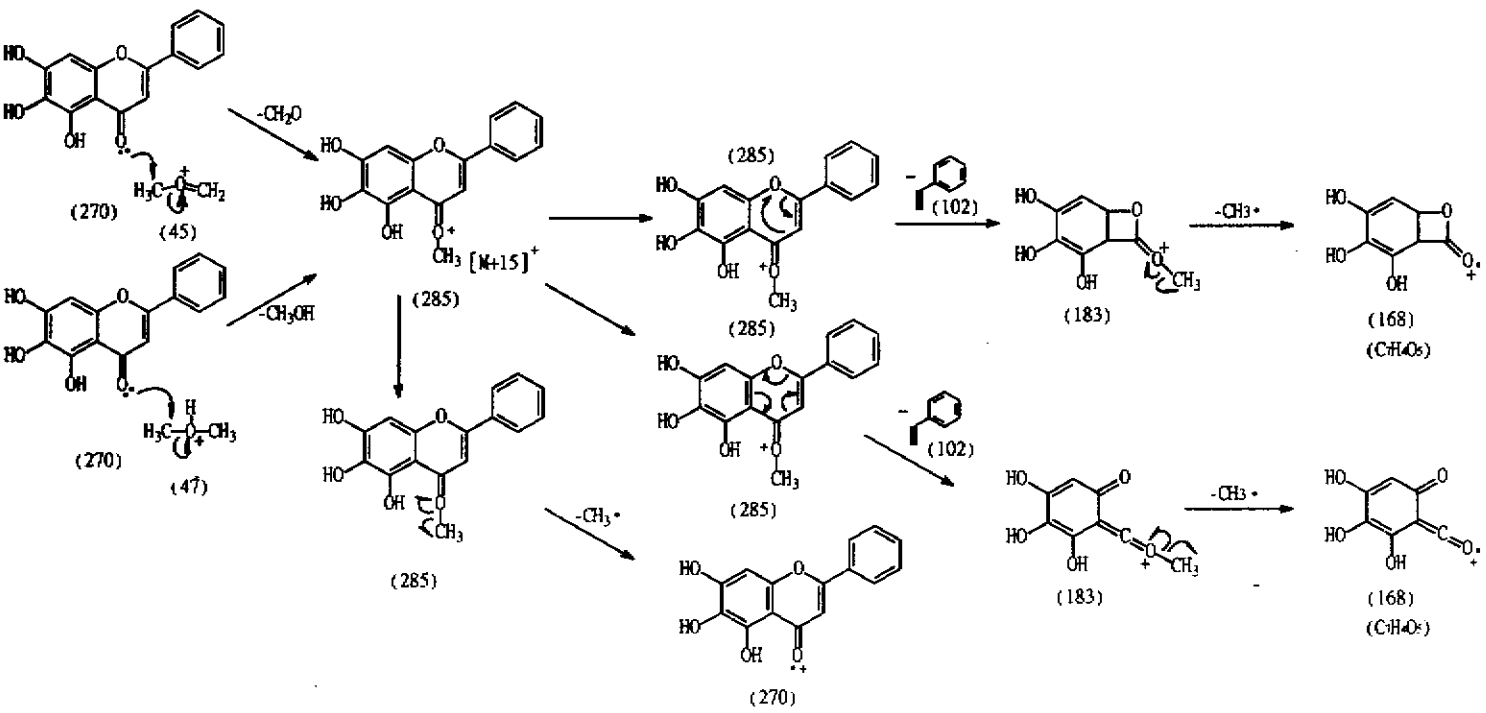

Scheme. 3

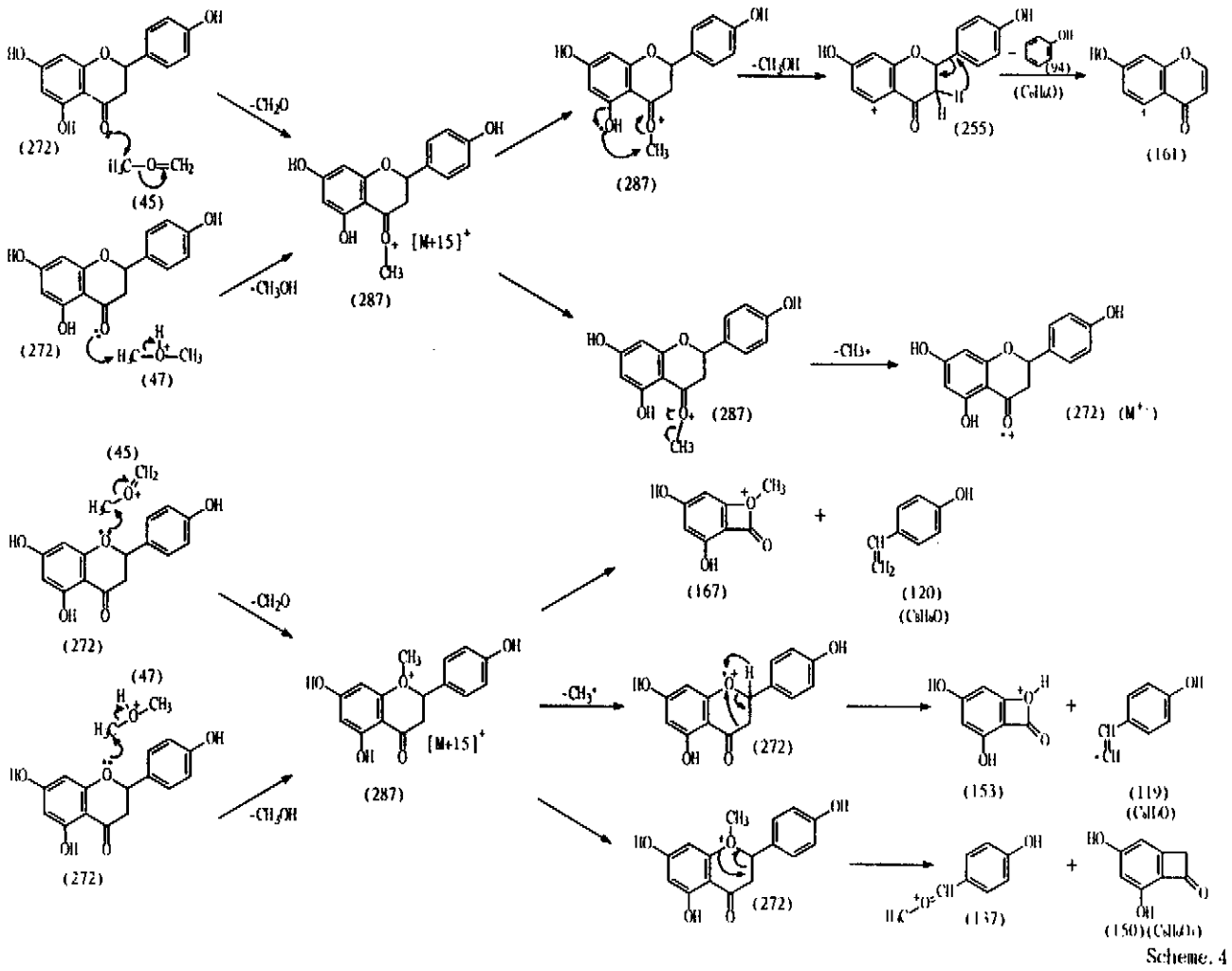
(272)
(45)
-CH2O
(287)
[M+15]+
-CH3OH
(47)
(272)
(287)
-CH3OH
(255)
-(94)
(C6H6O)
(161)
(287)
-CH3•
(272) (M+•)
(45)
(272)
-CH2O
(167)
(120)
(C8H8O)
(47)
(272)
-CH3OH
(287)
[M+15]+
-CH3•
(272)
(153)
(119)
(C7H8O)
(272)
(137)
(150)(C8H6O2)

Scheme. 4

表一、黃素母酮類藥物與二甲基醚離子之離子/分子反應的結果

Chrysin(254)	$[M+47]^+$(301,<1%) $[M+45]^+$(299,2%) $[M+15]^+$(269,3%) $[M+13]^+$(267,3%) $[M+H]^+$(255,22%) $M^{+\bullet}$(254,100%) $[M-CO]^{+\bullet}$(226,15%) $[M-H-2CO]^{+\bullet}$(197,1%) $[M-CO-2\times28]^{+\bullet}$(170,2%) $[M-C_8H_6]^{+\bullet}$(152,8%) $[M-C_8H_6-CO]^{+\bullet}$(124,6%)
Baicalein(270)	$[M+47]^+$(317,<1%) $[M+45]^+$(315,1%) $[M+15]^+$(285,1%) $[M+13]^+$(283,6%) $[M+H]^+$(271,21%) $M^{+\bullet}$(270,100%) $[M-CO]^{+\bullet}$(242,4%) $[M-CO-2\times28]^{+\bullet}$(186,2%) $[M-C_8H_6]^{+\bullet}$(168,9%) $[M-C_8H_6-CO]^{+\bullet}$(140,4%)
Naringenin(272)	$[M+47]^+$(319,<1%) $[M+45]^+$(317,25%) $[M+15]^+$(287,6%) $[M+13]^+$(285,25%) $[M+H]^+$(273,100%) $M^{+\bullet}$(272,96%) $[M-H_2O]^+$(254,12%) $[M-C_6H_5O]^+$(179,14%) or $[M+H-C_6H_6O]^+$ $[M-C_7H_6O]^+$(166,31%) or $[M+H-C_7H_7O]^+$ $[M-C_8H_7O]^+$(153,30%) or $[M+H-C_8H_8O]^+$
	$[M-C_7H_4O_4]^+$(120,24%)
Morin(302)	$[M+47]^+$(349,<1%) $[M+45]^+$(347,4%) $[M+15]^+$(317,4%) $[M+13]^+$(315,17%) $[M+H]^+$(303,38%) $M^{+\bullet}$(302,100%) $[M+H-OH]^+$(286,38%) $[M-OH]^+$(285,57%) $[M-H-CO]^+$(273,11%) $[M-C_8H_5O_3]^+$(153,27%) or $[M+H-C_8H_6O_3]^+$ $[M+H-C_8H_6O_4]^+$(137,29%) 121 14% 108 9%
Fisetin(286)	$[M+47]^+$(333,5%) $[M+45]^+$(331,6%) $[M+15]^+$(301,8%) $[M+13]^+$(299,20%) $[M+H]^+$(287,33%) $M^{+\bullet}$(286,100%) $[M+H-OH]^+$(270,45%) $[M-OH]^+$(269,19%) 167 39% 152 51% $[M-C_8H_5O_3]^+$(137,29%) or $[M+H-C_8H_6O_3]^+$ 123 21%

表二之一、黃素母酮類藥物離子/分子反應理論計算結果

$[M+H]^+$	Reaction site												
	2	3	4	5	6	7	8	9	2'	3'	4'	5'	6'
Chrysin	40[a]	-9	-26	-26	-7	26	-10	25	11	15	12	—	—
Baicalein	43	-9	-24	19	19	20	-7	25	12	16	13	—	—
Naringenin	—	—	-41	-9	-34	1	-37	-26	-11	-19	-1	—	—
Morin	5	60	-20	-20	-4	29	-7	65	11	-1	20	4	19
Fisetin	8	10	-21	-18	3	26	-3	23	-4	12	12	6	-6

$[M+13]^+$	Reaction site												
	2	3	4	5	6	7	8	9	2'	3'	4'	5'	6'
Chrysin	—	-17	—	-31	-16	15	-20	—	-1	-1	-3	—	—
Baicalein	—	-17	—	-31	8	10	-18	—	1	-0.7	-2	—	—
Naringenin	—	—	—	-45	-43	-10	-47	—	-22	-30	-12	—	—
Morin	—	4	—	-26	-12	18	-18	—	9	-14	10	-20	0.6
Fisetin	—	-18	—	-22	-8	-4	-12	—	-36	-17	-17	-5	-14

$[M+15]^+$ from $[M+47]^+$	Reaction site	
	4	9
Chrysin	-17	28
Baicalein	-23	28
Naringenin	-33	-7
Morin	-12	-1
Fisetin	-16	25

$[M+15]^+$ from $[M+45]^+$	Reaction site	
	4	9
Chrysin	-23	22
Baicalein	-29	22
Naringenin	-39	-13
Morin	-18	-8
Fisetin	-22	19

a. heat of reaction (kcal/mole)

表二之二、Chrysin 之生成熱理論計算結果

位置	反應物		生成物		
	M	47 of DME	$[M+H]^+$	CH_3OCH_3	ΔH
2	-85.3161842	130	129.1342798	-44	40.450464
3	-85.3161842	130	79.652095	-44	-9.0317208
4	-85.3161842	130	62.6412827	-44	-26.042533
5	-85.3161842	130	62.639132	-44	-26.044684
6	-85.3161842	130	82.0209685	-44	-6.6628473
7	-85.3161842	130	114.243577	-44	25.5597612
8	-85.3161842	130	78.5175836	-44	-10.166232
9	-85.3161842	130	113.9672745	-44	25.2834587
2'	-85.3161842	130	99.8345316	-44	11.1507158
3'	-85.3161842	130	103.9036435	-44	15.2198277
4'	-85.3161842	130	100.669929	-44	11.9861132

	M	47 of DME	$[M+15]^+$	CH_3OH	ΔH
4	-85.3161842	130	75.6371119	-48	-17.046704
9	-85.3161842	130	120.7424905	-48	28.0586747

	M	45 of DME	$[M+15]^+$	CH_2O	ΔH
4	-85.3161842	158	75.6371119	-26	-23.046704
9	-85.3161842	158	120.7424905	-26	22.0586747

	M	45 of DME	$[M+13]^+$	CH_3OH	ΔH
3	-85.3161842	158	103.2823191	-48	-17.401497
5	-85.3161842	158	89.3596957	-48	-31.32412
6	-85.3161842	158	104.9820138	-48	-15.701802
7	-85.3161842	158	135.1341845	-48	14.4503687
8	-85.3161842	158	100.4117668	-48	-20.272049
2'	-85.3161842	158	119.5294773	-48	-1.1543385
3'	-85.3161842	158	119.6652276	-48	-1.0185882
4'	-85.3161842	158	117.6407258	-48	-3.04309

表二之三、Baicalein 之生成熱理論計算結果

位置	反應物		生成物		
	M	47 of DME	$[M+H]^+$	CH_3OCH_3	ΔH
2	-128.5567626	130	88.2573937	-44	42.8141563
3	-128.5567626	130	36.7960502	-44	-8.6471872
4	-128.5567626	130	21.2015804	-44	-24.241657
5	-128.5567626	130	64.1744137	-44	18.7311763
6	-128.5567626	130	64.1618776	-44	18.7186402
7	-128.5567626	130	65.8888913	-44	20.4456539
8	-128.5567626	130	38.6659526	-44	-6.7772848
9	-128.5567626	130	70.8314547	-44	25.3882173
2'	-128.5567626	130	57.2072097	-44	11.7639723
3'	-128.5567626	130	61.0827463	-44	15.6395089
4'	-128.5567626	130	58.0513137	-44	12.6080763

	M	47 of DME	$[M+15]^+$	CH_3OH	ΔH
4	-128.5567626	130	25.9820767	-48	-23.4611607
9	-128.5567626	130	77.5625026	-48	28.1192652

	M	45 of DME	$[M+15]^+$	CH_3OH	ΔH
4	-128.5567626	158	25.9820767	-26	-29.4611607
9	-128.5567626	158	77.5625026	-26	22.1192652

	M	45 of DME	$[M+13]^+$	CH_3OH	ΔH
3	-128.5567626	158	60.4215218	-48	-17.0217156
5	-128.5567626	158	46.9404948	-48	-30.5027426
6	-128.5567626	158	85.0452463	-48	7.6020089
7	-128.5567626	158	87.4801795	-48	10.0369421
8	-128.5567626	158	59.8939096	-48	-17.5493278
2'	-128.5567626	158	78.7663305	-48	1.3230931
3'	-128.5567626	158	76.7258621	-48	-0.7173753
4'	-128.5567626	158	74.9461373	-48	-2.4971001

表二之四、Naringenin 之生成熱理論計算結果

位置	反應物		生成物		
	M	47 of DME	$[M+H]^+$	CH_3OCH_3	ΔH
4	-129.9575264	130	3.4053104	-44	-40.6371632
5	-129.9575264	130	35.0971642	-44	-8.9453094
6	-129.9575264	130	9.9187836	-44	-34.12369
7	-129.9575264	130	44.8976743	-44	0.8552007
8	-129.9575264	130	6.8909144	-44	-37.1515592
9	-129.9575264	130	18.3412051	-44	-25.7012685
2'	-129.9575264	130	33.0645789	-44	-10.9778947
3'	-129.9575264	130	25.5389485	-44	-18.5035251
4'	-129.9575264	130	42.7743624	-44	-1.2681112

	M	47 of DME	$[M+15]^+$	CH_3OH	ΔH
4	-129.9575264	130	15.1867373	-48	-32.8557363
9	-129.9575264	130	40.918345	-48	-7.1241286

	M	45 of DME	$[M+15]^+$	CH_2O	ΔH
4	-129.9575264	158	15.1867373	-26	-38.8557363
9	-129.9575264	158	40.918345	-26	-13.1241286

	M	45 of DME	$[M+13]^+$	CH_3OH	ΔH
5	-129.9575264	158	30.7822986	-48	-45.260175
6	-129.9575264	158	33.3086552	-48	-42.7338184
7	-129.9575264	158	66.2268445	-48	-9.8156291
8	-129.9575264	158	28.691522	-48	-47.3509516
2'	-129.9575264	158	53.9199973	-48	-22.1224763
3'	-129.9575264	158	45.8938147	-48	-30.1486589
4'	-129.9575264	158	63.7548153	-48	-12.2876583

表二之五、Morin 之生成熱理論計算結果

位置	反應物		生成物		
	M	47 of DME	$[M+H]^+$	CH_3OCH_3	ΔH
2	-215.510292	130	-36.9999628	-44	4.5103292
3	-215.510292	130	18.0890614	-44	59.5993534
4	-215.510292	130	-61.5984727	-44	-20.0881807
5	-215.510292	130	-61.2790071	-44	-19.7687151
6	-215.510292	130	-45.0911571	-44	-3.5808651
7	-215.510292	130	-12.9268176	-44	28.5834744
8	-215.510292	130	-48.9013716	-44	-7.3910796
9	-215.510292	130	23.592059	-44	65.102351
2'	-215.510292	130	-30.4043902	-44	11.1059018
3'	-215.510292	130	-42.8008836	-44	-1.2905916
4'	-215.510292	130	-21.4483303	-44	20.0619617
5'	-215.510292	130	-37.4997902	-44	4.0105018
6'	-215.510292	130	-22.5717186	-44	18.9385734

	M	47 of DME	$[M+15]^+$	CH_3OH	ΔH
4	-215.510292	130	-48.9910299	-48	-11.4807379
9	-215.510292	130	-38.612643	-48	-1.102351

	M	45 of DME	$[M+15]^+$	CH_2O	ΔH
4	-215.510292	158	-48.9910299	-26	-17.4807379
9	-215.510292	158	-38.612643	-26	-7.612643

	M	45 of DME	$[M+13]^+$	CH_3OH	ΔH
3	-215.510292	158	-5.906798	-48	3.603494
5	-215.510292	158	-35.1077594	-48	-25.5974674
6	-215.510292	158	-21.1594875	-48	-11.6491955
7	-215.510292	158	8.2248158	-48	17.7351078
8	-215.510292	158	-27.5476785	-48	-18.0373865
2'	-215.510292	158	-0.8005618	-48	8.7097302
3'	-215.510292	158	-23.2807008	-48	-13.7704088
4'	-215.510292	158	0.5391402	-48	10.0494322
5'	-215.510292	158	-29.9577433	-48	-20.4474513
6'	-215.510292	158	-8.9284532	-48	0.5818388

表二之六、Fisetin 之生成熱理論計算結果

位置	反應物		生成物		
	M	47 of DME	$[M+H]^+$	CH_3OCH_3	ΔH
2	-167.541795	130	14.3046878	-44	7.8464828
3	-167.541795	130	16.7178175	-44	10.2596125
4	-167.541795	130	-14.4199319	-44	-20.8781369
5	-167.541795	130	25.9398766	-44	19.4816716
6	-167.541795	130	9.2669427	-44	2.8087377
7	-167.541795	130	32.3496998	-44	25.8914948
8	-167.541795	130	3.8492212	-44	-2.6089838
9	-167.541795	130	28.975399	-44	22.517194
2'	-167.541795	130	2.6696285	-44	-3.7885765
3'	-167.541795	130	18.754005	-44	12.2958
4'	-167.541795	130	18.7106042	-44	12.2523992
5'	-167.541795	130	12.7146245	-44	6.2564195
6'	-167.541795	130	0.8950402	-44	-5.5631648

	M	47 of DME	$[M+15]^+$	CH_3OH	ΔH
4	-167.541795	130	-5.8097128	-48	-16.2679178
9	-167.541795	130	35.396401	-48	24.938196

	M	45 of DME	$[M+15]^+$	CH_2O	ΔH
4	-167.541795	158	-5.8097128	-26	-22.2679178
9	-167.541795	158	35.396401	-26	18.938196

	M	45 of DME	$[M+13]^+$	CH_3OH	ΔH
3	-167.541795	158	19.9683635	-48	-18.4898415
5	-167.541795	158	16.2733387	-48	-22.1848663
6	-167.541795	158	30.6399887	-48	-7.8182163
7	-167.541795	158	34.3187774	-48	-4.1394276
8	-167.541795	158	26.0914227	-48	-12.3667823
2'	-167.541795	158	2.7621455	-48	-35.6960595
3'	-167.541795	158	21.0359154	-48	-17.4222896
4'	-167.541795	158	21.0595255	-48	-17.3986795
5'	-167.541795	158	33.1558775	-48	-5.3023275
6'	-167.541795	158	24.5818972	-48	-13.8763078

表三、$M^{+\bullet}$及$[M+H]^+$離子的 CAD 結果

Chrysin(254)	$[M+H]^+$	-H(254,29%)
		-(H+H_2O)(236,<1%)
		-CO(227,100%)
		-43(212,5%)
		-(H_2O+CO)(209,5%)
		-(H+2CO)(198,1%)
		-71(184,2%)
		-C_8H_6(153,12%)
	$M^{+\bullet}$	-H(253,14%)
		-(H+H_2O)(235,1%)
		-CO(226,100%)
		-43(211,7%)
		-(H+2CO)(197,2%)
		-71(183,4%)
		-C_8H_6(152,2%)
Baicalein(270)	$[M+H]^+$	-H_2O(253,93%)
		-CO(243,42%)
		-(H_2O+CO)(225,72%)
		-(H_2O+CO+28)(197,24%)
		-C_8H_6(169,100%)
		-(C_8H_6+CO)(141,15%)
	$M^{+\bullet}$	-H_2O(252,5%)
		-CO(242,34%)
		-(H_2O+CO)(224,10%)
		-(H_2O+CO+28)(196,9%)
		-C_8H_6(168,100%)
		-(C_8H_6+CO)(140,10%)
Naringenin(272)	$[M+H]^+$	-H(272,20%)
		-H_2O(255,11%)
		-(H_2O+CO+28)(199,3%)
		-(CO+2×28)(189,5%)
		-C_6H_6O(179,10%)
		-(H_2O+CO+2×28)(171,5%)
		-C_7H_6O(167,3%)
		-C_7H_7O(166,4%)
		-(CO+3×28)(161,3%)
		-C_8H_8O(153,100%)
		-$C_6H_6O_3$(147,73%)
		-$C_7H_6O_4$(119,9%)
	$M^{+\bullet}$	-H(271,100%)
		-H_2O(254,48%)
		-(H_2O+CO)(226,1%)
		-C_8H_8O(179,12%)
		-C_7H_6O(166,42%)
		-C_8H_7O(153,6%)
		-$C_8H_7O_2$(137,3%)
		-$C_8H_8O_4$(107,4%)
Morin(302)	$[M+H]^+$	-OH(286,100%)
		-H_2O(285,26%)
		-CO(275,4%)
		-(H+CO)(274,9%)
		-(H_2O+CO)(257,35%)
		-(CO+28)(247,3%)
		-(H_2O+CO+28)(229,21%)
		-(CO+2×28)(219,2%)
		-$C_7H_6O_3$(165,4%)
		-$C_8H_6O_3$(153,9%)
		-$C_7H_6O_4$(149,8%)
		-$C_8H_6O_4$(137,3%)
	$M^{+\bullet}$	-OH(285,100%)
		-CO(274,2%)
		-(OH+CO)(257,<1%)
		-(OH+CO+28)(229,<1%)
		-$C_8H_5O_3$(153,3%)
Fisetin(286)	$[M+H]^+$	-H(286,100%)
		-H_2O(269,16%)

	-CO(259,27%)
	-(H_2O+CO)(241,34%)
	-(CO+28)(231,15%)
	-(H_2O+CO+28)(213,30%)
	-(H_2O+CO+2×28)(185,10%)
	-$C_7H_6O_3$(149,9%)
	-$C_8H_6O_3$(137,8%)
	-$C_8H_6O_4$(121,3%)
$M^{+\bullet}$	-H(285,100%)
	-H_2O(268,2%)
	-CO(258,23%)
	-(H_2O+CO)(240,3%)
	-(CO+28)(230,4%)
	-(H_2O+CO+28)(212,6%)
	-(H_2O+CO+2×28)(184,2%)
	-$C_8H_5O_3$(137,2%)

表四、$[M+13]^+$、$[M+15]^+$、$[M+45]^+$及$[M+47]^+$離子的 CAD 結果

Chrysin(254)	$[M+13]^+$	-CO(239,11%) -(CO+H_2O)(221,3%) -(CO+28)(211,10%) -58(209,16%) -(CO+2×28)(183,28%) -C_8H_6(165,100%) -114(153,5%) -(C_8H_6+CO)(137,5%)
	$[M+15]^+$	-$CH_3^•$(254,100%) -($CH_3^•$+CO)(226,11%) -C_8H_6(167,1%) -116(153,1%)
	$[M+45]^+$	-CH_2O(269,59%) -CH_3OH(267,100%)
	$[M+47]^+$	-CH_2O(271,19%) -CH_3OH(269,100%)
Baicalein(270)	$[M+13]^+$	-H_2O(265,11%) -CO(255,100%) -(CO+H_2O)(237,8%) -(CO+28)(227,26%) -(CO+H_2O+28)(209,8%) -(CO+2×28)(199,6%) -C_8H_6(181,21%) -114(169,1%) -(C_8H_6+CO)(153,10%)
	$[M+15]^+$	-$CH_3^•$(270,100%) -CO(257,46%) -(CO+H_2O)(239,5%) -(CO+H_2O+28)(211,1%) -(CO+2×28)(201,6%) -C_8H_6(183,10%)
		-(C_8H_6+$CH_3^•$)(168,2%)
	$[M+45]^+$	-CH_2O(285,3%) -CH_3OH(283,100%)
	$[M+47]^+$	-CH_3OH(285,100%)
Naringenin(272)	$[M+13]^+$	-$CH_3^•$(270,100%) -($CH_3^•$+CO)(242,58%) -(CO+H_2O+28)(211,2%) -(CO+H_2O+2×28)(183,19%) -C_8H_6O(191,9%) -C_8H_8O(165,70%) -C_9H_8O(153,5%)
	$[M+15]^+$	-$CH_3^•$(272,17%) -CH_3OH(255,17%) -C_8H_8O(167,100%) -$C_6H_6O_3$(161,38%) -(C_8H_7O+$CH_3^•$)(153,46%) -$C_8H_6O_3$(137,64%)
	$[M+45]^+$	-CH_3OH(285,100%) -120(197,18%) -138(179,9%) -(CH_3OH+C_8H_8O)(165,11%) -(CH_3OH+C_9H_8O)(153,11%) or -(CH_2O+C_8H_7O+$CH_3^•$) -170(147,26%) -178(139,11%) -198(119,3%)
	$[M+47]^+$	-CH_3OH(287,100%)
Morin(302)	$[M+13]^+$	-H_2O(297,15%) -CO(287,31%) -(CO+H_2O)(269,23%) -(CO+28)(259,35%)

		-(CO+H_2O+28)(241,16%)
		-(CO+2×28)(231,27%)
		-(CO+H_2O+2×28)(213,13%)
		-(CO+3×28)(203,100%)
		-($C_6H_6O_3$)(189,14%)
		-140(175,16%)
		-$C_7H_6O_4$(161,20%)
		-$C_9H_6O_3$(153,17%)
		-168(147,10%)
		-$C_9H_4O_4$(139,6%)
	[M+15]$^+$	-CH_3^*(302,90%)
		-H_2O(299,28%)
		-CH_3OH(285,100%)
		-(CO+H_2O)(271,41%)
		-(CO+28)(261,16%)
		-(CO+H_2O+28)(243,34%)
		-(CO+2×28)(233,8%)
		-(CO+H_2O+2*28)(215,6%)
		-(CO+3×28)(205,7%)
		-$C_7H_8O_3$(177,5%)
		-$C_8H_6O_3$(167,7%)
		-$C_8H_8O_3$(165,4%)
		-154(163,5%)
		-$C_8H_4O_4$(153,9%)
		-$C_8H_7O_4$(150,<1%)
		-$C_9H_6O_4$(139,12%)
	[M+45]	-H_2O(329,4%)
		-CH_3OH(315,100%)
		-(CH_2O+H_2O)(299,5%)
		-(CH_3OH+H_2O)(297,3%)
	[M+47]	-H_2O(331,11%)
		-CH_3OH(317,100%)
		-(CH_3OH+H_2O)(299,43%)
Fisetin(286)	[M+13]$^+$	-CH_3^* (284,41%)
		-H_2O(281,73%)
		-CO(271,40%)
		-(CO+H_2O)(253,100%)
		-(CO+28)(243,12%)
		-(CO+H_2O+28)(225,21%)
	[M+15]$^+$	-CH_3^*(286,100%)
		-CO(273,7%)
		-(CO+H_2O)(255,11%)
		-(CO+28)(245,10%)
		-(CO+H_2O+28)(227,8%)
		-(CO+2×28)(217,8%)
	[M+45]$^+$	-CH_3OH(299,100%)
		-CH_2O(301,8%)
		-(CH_3OH+CO)(271,9%)
	[M+47]$^+$	-(CO+H)(304,25%)
		-CH_3OH(301,100%)

表五、黃素母酮類藥物與二甲基鹼離子反應形成碎片產物離子的 CAD 結果

Chrysin(254)	$[M+H-CO]^+$(227)	-(H+28)(198,100%) -45(182,21%) -2×28(171,50%) -70(157,10%) -(H+3×28)(142,24%)
	$[M-CO]^+$(226)	-(H+28)(197,100%) -45(181,22%) -2×28(170,<1%) -69(157,24%) -(H+3×28)(141,29%)
Baicalein(270)	$[M+H-CO]^+$(243)	-H_2O(225,94%) -29(214,71%) -(H_2O+28)(197,98%) -(29+28)(186,81%) -(H_2O+2×28)(169,100%) -(29+2×28)(158,15%) -(H_2O+3×28)(141,20%)
	$[M-CO]^+$(242)	-H_2O(224,75%) -29(213,80%) -(H_2O+28)(196,81%) -(29+28)(185,81%) -(H_2O+2×28)(168,100%) -(29+2×28)(157,19%) -(H_2O+3×28)(141,3%)
Naringenin(272)	$[M+H-CO]^+$	-OH(228,100%) -29(216,28%) -94(151,28%)
	$[M-CO]^+$	-OH(227,100%) -29(215,40%) -94(150,55%)
Morin(302)	$[M+H-OH]^+$(286)	-H(285,100%) -CO(258,29%) -(H_2O+CO)(240,16%) -(CO+28)(230,10%) -(H_2O+CO+28)(212,8%)
	$[M-OH]^+$(285)	-H_2O(267,13%) -24(261,87%) -CO(257,80%) -(24+H_2O)(243,78%) -(CO+H_2O)(239,100%) -(CO+28)(229,99%) -(H_2O+2×28)(211,34%) -(CO+2×28)(201,65%) -98(187,63%) -108(177,64%)
Fisetin(286)	$[M+H-OH]^+$(270)	-H(269,90%) -OH(253,100%) -CO(242,65%) -(H+CO)(241,23%) -(H+CO+28)(213,16%) -73(197,14%) -84(186,12%)
	$[M-OH]^+$(269)	-CO(241,100%) -(CO+H_2O)(223,10%) -(CO+C_2H_4)(213,41%) -72(197,6%) -84(185,3%)

(27)

P-1b-AN-084

Dopamine 及 Nortriptyline 與二甲基醚離子的氣相離子/分子反應的溫度效應之研究

吳慧芬*、林雅萍、鍾森鈞
淡江大學化學研究所

當離子阱質譜儀的 source 區域溫度升高或是降低時，在 source 區域中的離子是否會由於溫度升高時，離子內能增加而造成了熱解離是本研究要探討的主題。本實驗將變化離子阱質譜儀中之 source 區域的溫度，針對 Dopamine 及 Nortriptyline 與二甲基醚離子的反應做溫度效應的探討。實驗所使用的離子阱質譜儀為 Finnigan GCQ，並以化學游離法(chemical ionization)作為離子阱質譜儀的游離源，使用對於此二種藥物的官能基有選擇性的 DME(dimethyl ether)作為化學游離試劑氣體，source 區域的溫度變化由 80℃～225℃。實驗結果顯示 Nortriptyline 的離子-分子產物$[M+H]^+$、$[M+13]^+$、$[M+15]^+$、$[M+45]^+$及$[M+47]^+$的離子與 Dopamine 的$[M-H]^+$及M^+離子的相對強度隨溫度升高而降低，但是 Dopamine 的$[M+H]^+$及$[M+13]^+$離子的相對強度則明顯的隨溫度升高而增加。有些碎片離子因溫度升高而增加，其原因可能由於溫度高時，離子內能增加，造成了熱解離，而有些碎片離子卻不因為溫度變化而其相對強度有所影響，乃是因為本身就很容易解離。

Characterization of Uracil Derivatives by Electron Capture Detection in an Ion Trap Tandem Mass Spectrometer with an External Ionization Source

Hui-Fen Wu*, Chien-Hong Chen, Ming-Yi Ho and Miao-Chun Chung

Department of Chemistry

Tamkang University

Tamsui, Taipei Hsien, 25137, Taiwan, R. O. C.

Abstract

This is a study of the influence of different substituents on Electron Capture Detection (ECD), utilizing an external source benchtop ion trap mass spectrometer, to perform collisionally activated dissociation experiments for an array of uracil derivatives.

In addition to observation of the formation of M^-, $[M-H]^-$, $2M^-$ and $[2M-H]^-$, along with their fragment ions, we find from the CAD results, that these compounds can eliminate neutral loss of HNCO, CO and HCN related to the breaking of the structure of the pyrimidine ring or halogen atoms, and this depends on the different substituents on the pyrimidine ring. The relationship between the structural difference with their ECD reactivity is also discussed.

Introduction

Electron Capture Detection (ECD) Mass Spectrometry is an extremely sensitive and selective technique for use in the analysis of compounds containing electrophilic functional groups [1-28]. The process has been used extensively in the analysis of many classes of compounds in the traditional mass spectrometers such as sector and quadrupole [1-28]. However, in performing negative ion analysis [29-34] difficulties have been encountered with the ion trap mass spectrometer (ITMS). GCQ represents the first commercial benchtop ion trap mass spectrometer with the capability of performing effective negative ion analysis.

The process of negative ion formation by ECD is typically the result of the interaction of electron and molecules by the following three mechanisms [1,6]:

I. Resonance electron capture:

$$MX + e^-(\sim 0ev) \rightarrow MX^-$$

II. Dissociative resonance capture:

$$MX + e^-(0\sim 15ev) \rightarrow M + X^-$$

III. Ion-Pair Formation:

$$MX + e^-(>15ev) \rightarrow M+ \quad X^- + e^-$$

In this study, an array of uracil halogenated compounds, the structures of which are shown in Figure 1, were examined by ECD in the ion trap tandem mass spectrometer with an external source (the Finnigan GCQ^{plus}). Since these halogenated uracil derivatives possess higher electron affinities, there is the potential for formation of negative ions during the resonance electron capture process.

As the constituent of nucleic acid bases, the important role played by uracil in biochemistry cannot be overstated. Uracil derivatives are classified as important pharmaceutical compounds [35-42], with pharmacological properties that are related to the different substituents of the halogen atoms on the pyrimidine ring [35]. Various mass spectrometric techniques, such as GC/MS, EI and FAB [43-51], have been used to examine these compounds, however, the knowledge gained from these experiments was limited to positive ion analysis, and no negative ion analysis has ever been undertaken for these important biochemistry and biochemical compounds. Therefore, in order to provide structural information for these compounds, in conjunction with CAD techniques, we utilize the ECD method in GCQ, using methane as the reagent gas, to probe the dissociation pathways for a number of negative product ions produced by ECD reactions to uracil derivatives; methane is the most common ECD reagent gas in general use for ECD applications in the traditional mass analyzers [14, 15, 21, 23, 25, 27, 28,]. These novel experiments can provide valuable information on negative ions that were previously undetected by the traditional internal ionization ion trap mass spectrometer [29-34].

Experimental

All mass spectrometric experiments were carried out in an external source ion trap mass spectrometer (Finnigan MAT GCQ) [52-55] in which ECD was used with methane as the reagent gases. GCQ was operated in the mass selective instability mode. The pressures of He buffer gas and ECD reagent gas were 1 mtorr and 4 x 10^{-4} torr, respectively. The pressure in the ion source region was 100 mtorr measured by a convectron gauge. Ion source temperature was 200^{0}C. Ionization times were set using automatic gain control (AGC). The ion injection time (from source to mass analyzer) was 0.3-25 msec. Collisional experiments were performed by applying a supplementary tickle

voltage to the endcaps of the ion trap at q_z = 0.225. The collisional activation time was 15 msec. Signal width for selection of the parent ions was from 0.5-1 amu; the collision energy for fragmentation of the parent ions was from 0.5-1.7 V. Samples were introduced to the ion source region via a temperature controlled direct insertion probe (DIP) to assist the desorption of the sample. The probe tip was heated to a temperature of 150℃ to 370℃ at a speed of 80-100℃/min. Spectra were acquired from 50 to 650 amu at a rate of 0.5 s/scan. The identification of all isotope peaks was achieved using "isoform 1.02" software. All compounds were purchased from Aldrich Chemical Company (Milwaukee, WI) except 5-bromouracil and uracil that were obtained from Alfa Chemical Company (Ward Hill, MA).

Results and Discussion

Electron Capture Detection spectra using methane as reagent gases

Negative ion spectra typically produce much lower signals than positive ion spectra within the traditional mass analyzer. However, in GCQ, we find that ECD can also produce signals just as intense as the positive ion spectra signals [52-54]. Table 1 lists the ECD spectra of all compounds using methane as the reagent gas at an ion source temperature of 200°C. For the isotopic peaks of Cl, only the intensity of Cl^{35} ions were recorded, whilst for the isotopic peaks of Br, either Br^{79} or Br^{81} ions were recorded.

The formation of ECD products in GCQ includes the molecular anion, dimeric ions and their fragment ions. Uracil is the only compound that cannot form anion from ECD in GCQ, and this may be due to its low electron affinity (0.086 eV) [56], since it is the only compound that does not possess any halogenated substituents on the pyrimidine ring. Other halogenated uracil substituents possess higher electron affinities, thus negative ions can be formed through the resonance electron capture process [1-28].

With the exceptions of 5-bromouracil, 5-bromo-1,3-dimethyluracil, 5-bromo-6- methyluracil and 5-iodouracil, for all compounds the base peaks of ECD results were $[M-H]^-$. 5-bromouracil, 5-bromo-1,3-dimethyluracil, 5-bromo-6- methyluracil and 5-iodouracil mainly produced 100% Br^- and

I^- ions and a very low abundance of M^- ions (0-5%). This reflects the fact that Br and I atoms are more easily eliminated than F and Cl atoms, a fact which is rationalized by the order of the bond dissociation energies for C-F and C-Cl, which are typically higher than that of C-Br and C-I bonds. For example, the homolytic bond dissociation energies observed for C_6H_5X of F, Cl, Br and I are 565, 397, 335 and 268 KJ mol^{-1} at 298 K, respectively [47]. In addition, for fluoro-substituent compounds, there were no observations of any F^- ions, although elimination of HF and F radicals could be observed for all fluoro-substituent compounds.

The intensities of dimeric ions and their fragment ions are typically in the range of 0% to 43% depending on the compounds, apart from the Br or I substituents which cannot produce any dimeric ions or its fragments ions; again, this is because the bond strength for Br or I substituents is too weak. Furthermore, the formation of type and relative abundance of the dimeric ions was mainly determined by position 5 of the halogenated substituent atoms on the pyrimidine ring. The F or Cl substituents can typically produce substantial amounts of dimeric ions or its fragment ions. As to the relative intensity of M^- ions, this ranged from 0%-35% depending on the compounds.

Formation of the adduct ions of $[M+X]^-$ was only observed for 5-chlorouracil ($[M+Cl]^-$, 30%), 5-bromouracil ($[M+Br]^-$, 12%), and 5-bromo-6-methyluracil ($[M+Br]^-$, 2%). In a comparison of the ECD spectra of 5-fluoro-1,3-dimethyluracil with that of 5-bromo-1,3-dimethyluracil, although both compounds possess two methyl groups at the 1 and 3 nitrogen atom of the the pyrimidine ring, the former produced many ECD products whilst the latter produced mainly Br^- ions and only a very limited amount of M^-.

CAD results for ECD spectra using methane as reagent gases.

The CAD technique was applied to the adduct ions, molecular anion M^-, $[M-H]^-$, dimeric ions $2M^-$, $[2M-H]^-$ and their fragment ions, in order to investigate the structural information of ECD products. Table 2 lists the CAD results produced from ECD MS using methane as the reagent gas. The CAD results demonstrate that these compounds can eliminate some typical neutral losses of HNCO, CO, HCN, CH_3NCO (or the formation of the NCO^- ions) depending on the breaking of the

structure of the pyrimidine ring. They can also eliminate HF, HCl, HBr, CH_3, NH_2 and halogen atoms (F, Cl, Br and I) depending on the different substituents on the pyrimidine ring.

From the CAD spectra of the ECD product ions, typical fragmentation processes could be elucidated. HNCO is the most common neutral loss for most compounds, however, if the structure of the compounds possess two methyl groups at the 1 and 3 nitrogen atom of the the pyrimidine ring (for example, 5-fluoro-1,3-dimethyluracil and 5-bromo-1,3-dimethyluracil), then the elimination of CH_3NCO and CH_3 could be observed instead. Although the relative intensity of some ECD product ions is very small (from 0%-5% only), GCQ possesses as excellent MS/MS capability for negative ions as in the case of the PCI of dimethyl ether [52, 53], and CAD experiments can still be successfully performed for all of these low abundance ECD product ions. In a comparison of the CAD results for M^- with $[M-H]^-$, only 5-trifluoromethyluracil, 5-fluorouracil and 5-fluorocytosine showed similar neutral loss patterns.

The bonding strength of the dimeric ions can also be probed by CAD, for example, comparing the CAD results of the dimeric ions $2M^-$ and $[2M-H]^-$ of 5-trifluoromethyluracil with those of 5-fluorouracil, 5-trifluoromethyluracil eliminated only one molecule of M, indicating that the bonding strength of the $2M^-$ and $[2M-H]^-$ of 5-trifluoromethyluracil is very weak. However, in the CAD results of the $2M^-$ and $[2M-H]^-$ of 5-fluorouracil, in addition to the elimination of one molecule of M, it also produced many fragment ions, indicating that the bonding strength of the $2M^-$ and $[2M-H]^-$ of 5-fluorouracil is much stronger than that of the 5-trifluoromethyluracil. The reason for this is that position 5 of the three F atoms on the pyrimidine ring of 5-trifluoromethyluracil is in the alkyl group.

A comparison of the CAD results of M^- and $[M-H]^-$ of 5-trifluoromethyluracil with those of 5-fluorouracil, also shows dramatically different patterns. The CAD of M^- and $[M-H]^-$ of 5-trifluoromethyluracil eliminated one molecule of HF, whilst the CAD of M^- and $[M-H]^-$ of 5-fluorouracil produced mainly NCO^- ions. In a comparison of the CAD results of M^- and $[M-H]^-$ of 5-fluorouracil with those of 5-fluorocytosine, the CAD of the M^- and $[M-H]^-$ of the latter eliminated mainly one molecule of HNCO although NCO^- ions were also observed. The CAD results of M^- of

5-fluorouracil, 5-chlorouracil, 5-bromouracil and 5-iodouracil showed that they mainly produced NCO^- ions, eliminated one molecule of HCl, and produced Br^- and I^- ions, respectively. This again was attributed to the order of bonding strength of the halogenated sustituents as discussed earlier. Finally, the position of the methyl group also seems to be a very important factor in bonding strength. For example, in a comparison of the CAD results of M^- of 5-bromouracil, 5-bromo-6-methyluracil, and 5-bromo-1,3-dimethyluracil, the CAD of M^- of 5-bromouracil and 5-bromo-6-methyluracil produced mainly Br^-, whilst the CAD of M^- of 5-bromo-1,3-dimethyluracil eliminated mainly CH_3NCO and CH_3.

Conclusion

This work has demonstrated that the GCQ ion trap mass spectrometer possesses excellent ECD capabilities. Additionally, the use of methane as the ECD reagent gas in GCQ provides good sensitivity. These novel experiments have provided valuable information with regard to past NCI studies that the traditional internal ionization ITMS was incapable of performing. We find that a combination of ECD with CAD in GCQ is a very unique analytical technique. Moreover, because of its excellent sensitivity in ECD, and its MS/MS capability, GCQ is ideal for negative ion analysis of these pharmaceutical compounds in many future applications.

Acknowledgments

The support from the National Science Council of the Republic of China (Grant No. NSC 89-2113-M-032-005) and Tamkang University is gratefully acknowledged.

References

[1]J. G. Dillard, *Chem. Rev.*, 1973,73,589.

[2] D. F. Hunt and F. W. Crow, *Anal. Chem*. 1978 1781.

[3]D. F. Hunt and F. W. Crow, *Anal. Chem.*, 1978, 50, 1781.

[4] G. T. Tomy and G. A. Stern, *Anal. Chem*. 1999,71, 4860.

[5] N. L. Kelleher, R. A. Zubarev, K. Bush, B. Furie, B. C. Furie, F. W. McLafferty, and C.T. Walsh,

Anal. Chem. 1999, 71, 4250.

[6]V. S.Ong and R. A. Hites, *Mass Spectrom., Rev*. 1994, 13, 259.

[7]K. Ueda, S. L. Morgan, A. Fox, J. Gilbart, A. Sonesson, L. Larsson and G. Odham, *Anal. Chem.*, 1989, 61, 265.

[8]K. Mizuishi, M. Takeuchi and T. Hobo, *J. Chromator. A*, 1998, 800, 267.

[9]S.-A. Fredriksson, L.-G. Hammarstrom, L. Henriksson and H.-A.Lakso, *J. Mass Spectrom*., 1995, 30, 1133.

[10]S. A. Tittlemier, M. Simom, W. M. Jarman, J. E. Elliott and R. J. Norstrom, *Environ. Sci. Technol.*, 1999, 33, 26.

[11]Z. Zdrahal, *J. Chromator. A,* 1998, 793, 214.

[12]J. R. Moyer and J. L. Elder, *J. Agric. Food Chem.*, 1984, 32, 866.

[13]D. W. Kuehl, M. J. Whitaker and R. C. Dougherty, *Anal. Chem.*, 1980, 52, 935.

[14]M. Oehem, D. Stockl and H. Knoppel, *Anal. Chem.*, 1986, 58, 554.

[15]E. A. Stemmler, R. A. Hites, B. Arbogast, W. L. Budde, M. L. Deinzer, R. C. Dougherty, J. W. Eichelberger, R. L. Foltz, C. Grimm E. P. Grimsrud, C. Sakashita and L. J. Sears, *Anal. Chem.*, 1988, 60, 781.

[16]W. Vetter and B. Luckas, *Rapid Communi. Mass Spectrom*., 12, 312, 1998.

[17]B. Arbogast, W. L. Budde, Mdeinzer, R. C. Dougherty, J. Eichelberger, R. D. Foltz, C. C. Grimm, R. A. Hites, C. Sakashita and Estenmler ,*Org. Mass Spectrom*, 1990, 25, 191.

[18]W. Vetter and B. Luckas, *Rapid Communi. Mass Spectrom*.,1998,12,312.

[19]I. Hahndorf, E. Illenberger, *Int. J. Mass Spectrom and Ion Proc.*, 1997, 167/168, 87.

[20] A. G. Harrison, Chemical Ionization Mass Spectrometry; CRC Press: Boco Ratan 1983.

[21]L. R. Hilpert, G. D. Brd and V. R. Vogt, *Anal.Chem.*, 1984, 56, 1842.

[22]J. Alaramee', B. C. Arbogast and M. L. Deinzer, *Anal.Chem*, 1986, 58, 2907.

[23]J. M. Trainor and P. Voures, *Anal.Chem* , 1987, 59, 601.

[24]M. Oehme, *Anal. Chem.*,1983,55,2290.

[25]J. R. Hass, M. D. Frlesen, D. J. Haren and C. E. Parker, *Anal.Chem* ,1978, 50, 1474.

[26]T. Ramdahl and K. Urdal, *Anal.Chem*, 1982, 54, 2256.

[27]M. V. Buchanan and G. Olerich, *Org. Mass Spectrom*,1984, 19, 486.

[28]S. Daishima, Y. Iida, A. Shibate and F. kanda *Org. Mass Spectrom,* 1992, 27, 571.

[29]S. A. McLuckey, G. L. Glish and P. E. Kelley, *Anal. Chem.* ,1987, 59, 1670.

[30]S. Catinella, P. Traldi, X. Jiang, F. A. Londry, R. J. S. Morrison, R. E. March, S. Gregoire, J. – C. Mathurin and J. – C. Tabet, *Rapid Commun. Mass Spectrom*.,1995,9,1302.

[31]B. L. Williamson and C. S. Creaser, *Rapid Commun. Mass Spectrom*.,1997, 11, 1235.

[32]D. W. Berberich and R. A. Yost, *J. Am. Soc. Mass Spectrom*, 1994, 5,757.

[33]E. R. Lovejoy and R. R. Wilson, *J. Phys. A* 1998, 102, 2309.

[34]M. L. Langford and J. F. J. Todd, *Org. Mass Spectrom*. 28, 773,1993.

[35] J. C. Martin, *Nucleotide Analogs as Antiviral Agents*. ACS Symposium Series. No. 401, American Chemical Society, Washington, DC, 1989.

[36] P. Calabresi and R. E. Parks Jnr, in *Goodman and Gilman's the Pharmacological Basis of Therapeutics*, 7th edn, chapt. 55. Macmillan, New York, 1985.

[37] L.J.Marx, *Science*, 1989, 346.

[38]L.S.Kelley and A. B. Teicher, *Science*, 1988,1813.

[39]N.Benford and D. Gage, *Health*, 1988, 20,28.

[40]L.C.Norris, L.P.Meisenheimer and H.T.Koch, *J. Am. Chem. Soc.,* 1996, 118, 5776.

[41]O.Modesto, H. Begona and L.F.Javier, *J. Phys. Chem. B,* 1998, 102, 5228.

[42]E.Matsushima, K. Yoshida, R. Kitamura and Y. K. Ichiro, *J.Chromatogr. B*, 1997, 691, 95.

[43]D.A.Anderson, D.J. Kerr, C.Blesing, and L.W.Seymour , *J.Chromatogr. B,* 1997, 87.

[44]R.W.Reiser, *Org. Mass Spectrom,* 1969, 2, 467.

[45]J.Ulrich, R.Teoule, R.Massot and A.Cormu, *Org. Mass Spectrom.* 1969, 2, 1183.

[46]D. D. Des Marteau, G.Resnati, D.Favretto and P.Traldi, *Org. Mass Spec-trom.,* 1992, 27, 204.

[47]F. Favetto, P. Traldi, E. Celon and G. Resnati, *Org. Mass.Spectrom.*, 1993, 28, 1179.

[48]J. M. Rice; G . O. Dudek and M. Barber, *J. Am. Chem. Soc.*, 1965, 87, 4569.

[49] J. Ulrich; R. Teoule, R. Massot and A. Cornu, *Org. Mass Spectrom.*, 1969, 2, 1183.

[50]S. K. Sethi; C. C. Nelson and J. A. McCloskey, *Anal . Chem.*, 1984, 56, 1977.

[51]D. Favretto; P. Traldi; P. Bravo and F. Viani, *Rapid Commun. Mass Spectrom.*, 1991, 5, 72.

[52]H.-F. Wu and Y.-P. Lin, *J. Mass Spectrom.*, 1999, 34,1283.

[53]H.-F. Wu and Y.-P. Lin, *Eur. Mass Spectrom.*, 2000, in press.

[54]H.-F. Wu, *J. Mass Spectrom.*, 2000, in press.

[55]S.-A. Barshick and W. H. Griest, *Anal. Chem.*, 1998,70, 3015.

[56]N. A. Oyler and L. Adamowicz, *J. Phys. Chem.*, 1993, 97, 11122.

Captions

Figure 1. structures of uracil and related compounds.

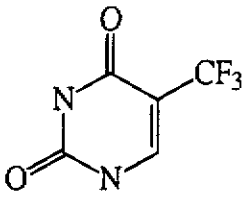

5-(trifluoromethyl)uracil(180)

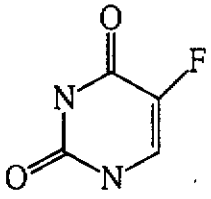

5-fluorouracil(130)

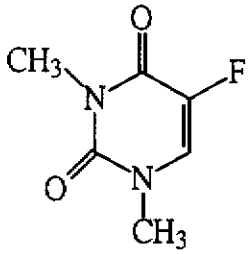

5-fluoro-1,3-dimethyluracil(158)

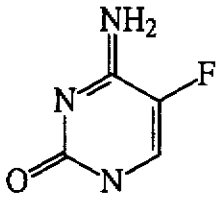

5-fluorocytosine(129)

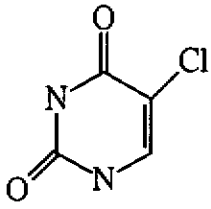

5-chlorouracil(146)

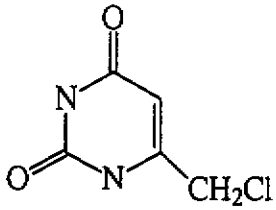

(6-chloromethyl)uracil(160)

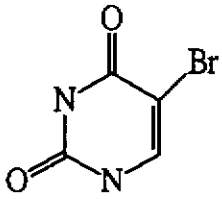

5-bromouracil (190)

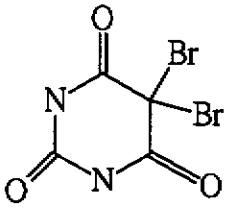

5,5-dibromobarbitaric acid(286)

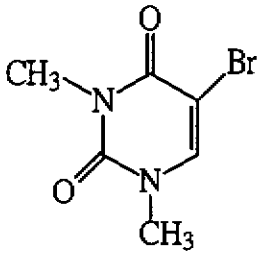

(5-bromo-1,3-dimethyl)uracil(219)

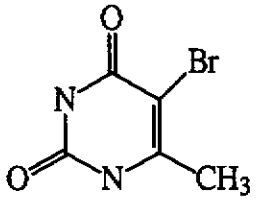

5-bromo-6-methyluracil (205)

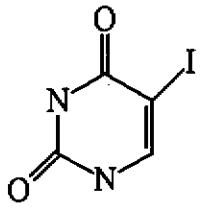

5-iodouracil(238)

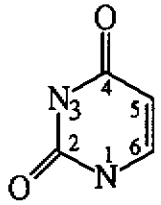

uracil(112)

Figure 1

Table 1. ECD results of uracil derivatives by using methane as reagent gas

Compound	m/z	Product	%
5-trifluoromethy luracil(180)	180	$M^{-\cdot}$	5
	179	$[M-H]^-$	100
	360	$2M^{-\cdot}$	1
	359	$[2M-H]^-$	10
5-fluorouracil(130)	130	$M^{-\cdot}$	5
	129	$[M-H]^-$	100
	260	$2M^{-\cdot}$	2
	259	$[2M-H]^-$	26
	240	$[2M-HF]^-$	3
	239	$[(2M-H)-HF)]^-$	4
	220	$[(2M-H)-(HF+F)]^-$	5
	192	$[(2M-H)-(HF+F+CO)]^-$	2
	165	$[(2M-H)-(HF+F+CO+HCN)]^-$	4
	144		3
	111	$[M-F]^-$	<1
	42	NCO^-	3
5-fluoro-1,3 dimethyluracil(158)	158	$M^{-\cdot}$	28
	157	$[M-H]^-$	100
	277	$[2M-(HF+F)]^-$	8
	262	$[2M-(HF+F+CH_3\cdot)]^-$	12
	261	$[(2M-H)-(HF+F+CH_3\cdot)]^-$	40
	259	$[2M-CH_3NCO]^-$	20
	246	$[(2M-H)-(HF+F+2CH_3\bullet)]^-$	43
	218	$[(2M-H)-(HF+F+2CH_3\bullet+CO)]^-$	11
	204	$[(2M-H)-(HF+F+2CH_3\bullet+NCO)]^-$	50
	177	$[(2M-H)-(HF+F+2CH_3\bullet+NCO+HCN)]^-$	73
	42	NCO^-	10
5-florocytosine(129)	129	$M^{-\cdot}$	15
	128	$[M-H]^-$	100
	242	$[2M-NH_2]^-$	4
	218	$[(2M-H)-(F+HF)]^-$	18
	173		48
	144		18
	85	$[M-HNCO]^-$	5
	64		20
	42	NCO^-	2
5-Chlorouracil(146)	146	$M^{-\cdot}$	11
	145	$[M-H]^-$	100
	292	$2M^{-\cdot}$	7
	291	$[2M-H]^-$	7
	256	$[2M-HCl]^-$	2
	220	$[(2M-H)-(Cl+HCl)]^-$	31

	181	$[M+Cl]^-$	30
	110	$[M-HCl]^-$	20
	42	NCO^-	3
6-chloromethyl uracil(160)	160	$M^{\bullet-}$	35
	159	$[M-H]^-$	100
	320	$2M^{\bullet-}$	15
	319	$[2M-H]^-$	21
	124	$[M-HCl]^-$	1
	42	NCO^-	3
	35	Cl^-	1
5-bromouracil(190)	190	$M^{\bullet-}$	5
	271	$[M+Br]^-$	12
	221		5
	111	$[M-Br]^-$	6
	81	Br^-	100
5,5-Dibromo barbituric acid (286)	286	$M^{\bullet-}$	6
	285	$[M-H]^-$	100
	207	$[M-Br]^-$	80
	206	$[M-HBr]^-$	74
	203	$[(M-H)-HBr]^-$	29
	81	Br^-	3
5-bromo-1,3-dimethyluracil(219)	219	$M^{\bullet-}$	<1
	81	Br^-	100
5-bromo-6-methyluracil (205)	205	$M^{\bullet-}$	2
	285	$[M+Br]^-$	2
	125	$[M-HBr]^-$	1
	81	Br^-	100
5-Iodouracil(238)	238	$M^{\bullet-}$	1
	127	I^-	100

Table 2. CAD results of ECD spectra of uracil derivatives using methane as reagent gas

Compound	Isolation	Fragment ion (m/z,intensity%)
5-trifluromethyl uracil(180)	$M^{-\cdot}$(180)	-HF(160,100%) -(2HF+CO)(112,1%)
	$[M-H]^-$(179)	-HF(159,100%) -(2HF+CO)(111,9%)
	$2M^{-\cdot}$(360)	-M(180,100%)
	$[2M-H]^-$(359)	-M(179,100%) -(M+HF)(159,1%)
5-fluorouracil(130)	$M^{-\cdot}$(130)	NCO^-(42,100%)
	$[M-H]^-$(129)	$-C_2HF$(85,3%) NCO^-(42,100%)
	$2M^{-\cdot}$(260)	245,29% -CO(232,36%) -M(130,29%)
	$[2M-H]^-$(259)	-HF(239,19%) 244,28% -CO(231,15%) -HNCO(216,100%) -(HF+HNCO)(196,14%) -M(129,13%)
	$[2M-HF]^-$(240)	-HF(220,100%) -HNCO(197,35%) -(HF+CO)(192,31%)
	$[(2M-H)-HF)]^-$(239)	-HNCO(196,100%) -(HNCO+HCN)(169,12%) -(HNCO+HCN+NH_3)(152, 10%)
	$[(2M-H)-HF+F)]^-$ (220)	-CO(192,38%) -HNCO(177,100%) -(CO+HCN)(165,5%) -2CO(164,5%) -(HNCO+HCN)(150,19%) -(2CO+CH_3NH_2)(133,8%)
	$[(2M-H)-(HF+F+CO)]^-$(192)	-HCN(165,8%) -CO(164,8%) -HNCO(149,100%)
	$[(2M-H)-(HF+F+CO+HCN)]^-$(165)	-HCN(138,11%) $[M-H]^-$(129,100%)

		-HNCO(122,26%) -(HCN+CO)(110,5%) 93,7% 66,13%
	144	$[M-H]^-$129,62% $-C_2HF$(100,100%) 69,16%
	$[M-F]^-$(111)	NCO^-(42,100%)
5-fluro-1,3-dimethyluracil(158)	$M^{\bullet-}$ (158)	$-CH_3\bullet$(143,37%) -CO(130,25%) 108,100%
	$[M-H]^-$(157)	$-CH_3\bullet$(142,26%) $-CH_3NH_2$(126,6%) $-(HF+CH_2NH)$(108,100%)
	$[2M-(HF+F)]^-$(277)	$-CH_3\bullet$(262,100%) -CO(249,30%) $-C_2HF$(233,30%) $-CH_3NCO$(220,58%) $-(CH_3NCO+CO)$(192,25%) (185,90%)
	$[2M-(HF+F+CH_3\bullet)]^-$ (262)	$-CH_3\bullet$(247,100%) -CO(234,9%) $-(CO+CH_3\bullet)$ (219,11%) $-CH_3NCO$(205,67%) $-(CH_3NCO+CO)$(177,15%)
	$[(2M-H)-(HF+F+CH_3\bullet)]^-$(261)	$-CH_3\bullet$(246,12%) (220,5%) $-CH_3NCO$(204,76%) $-(CH_3NCO+CO)$(176,100%)
	$[(2M-H)-(HF+F+2CH_3\bullet)]^-$(246)	$-CH_3\bullet$(231,11%) $-CH_2NH$(217,74%) -2HF(206,100%) $-CH_3NCO$(189,9%) $-(CH_3NCO+2HF)$(149,12%)
	$[(2M-H)-(HF+F+2CH_3\bullet+CO)]^-$(218)	$-CH_3\bullet$(203,84%) -HF(198,100%) $-CH_3NCO$(161,13%) $-(CH_3NCO+HF)$(141,80%)
	$[2M-(HF+F+CH_3\bullet+CH_3NCO+CO]^-$ (177)	$-CH_3\bullet$(162,22%) (153,39%) -CO(149,15%) (153-CO)(125,100%)

		-CH_3NCO(120,20%)
5-fluorocytosine (129)	$M^{\bullet-}$	-HNCO(86,100%) NCO^-(42,70%)
	$[M-H]^-$(128)	-HNCO(85,100%) NCO^-(42,14%)
	$[2M-NH_2]^-$(242)	-HCN(215,74%) 141,100%
	$[(2M-H)-(F+HF)]^-$ (218)	-NH_2(202,21%) -(NH_2+HCN)(175,100%) -(NH_2+CO)(174,94%)
	173	-HNCO(130,100%)
	144	-16(128,13%) -C_2HF, (100,100%) 69,18% NCO^-(42,5%)
	$[(M-H)+HNCO]^-$ (85)	-HCN(58,100%)
5-Chlorouracil (146)	$M^{\bullet-}$	-HCl (110,100%)
	$[M-H]^-$(145)	-HNCO(102,100%) -119,16% -(HNCO+HCN)(75,66%)
	$[(2M-H)-(Cl+HCl)]^-$ (220)	-CH_3•(205,30%) -CO(192,28%) -HNCO(177,100%) -(HNCO+CO)(149,72%) -(HNCO+CO+CH_3)(134,8%)
	$[M+Cl]^-$ (181)	-HCl (145,100%) (109,3%)
	$[M-HCl]^-$(110)	-CO(82,100%) -(CO+CH_3•)(67,89%)
6-chloromethyl uracil(160)	$M^{\bullet-}$	-CO(132,29%) 116,50% 80,24% NCO^-(42,100%)
	$[M-H]^-$(159)	-HNCO(116,91%) 129,100%
5-bromouracil(190)	$M^{\bullet-}$	Br^-(81,100%) -HBr(110,3%)

	221	-HNCO (78,98%) -(HNCO+HCN)(151,100%)
5,5-Dibromobarbituric acid(285)	$M^{-\cdot}$	250,100%
	$[M-H]^-$(285)	249,100%
	$[M-Br]^-$(207)	-HNCO(164,100%) 120,75%
	$[M-HBr]^-$(206)	-CO(178,47%) -HNCO(163,67%) 124,100% 118,53%
	$[M-Br]^-$(205)	-HNCO(162,90%) 118,100%
5-bromo-6-methyluracil(205)	$M^{-\cdot}$ (205)	Br^-(81,100%)
5-bromo-1,3-dimethyluracil(219)	$M^{-\cdot}$ (219)	$-CH_3NCO$(162,41%) $-CH_3$(205,100%) 190,18% Br^-(81,5%)
5-Iodouracil(238)	$M^{-\cdot}$ (238)	I^-(127,100%)

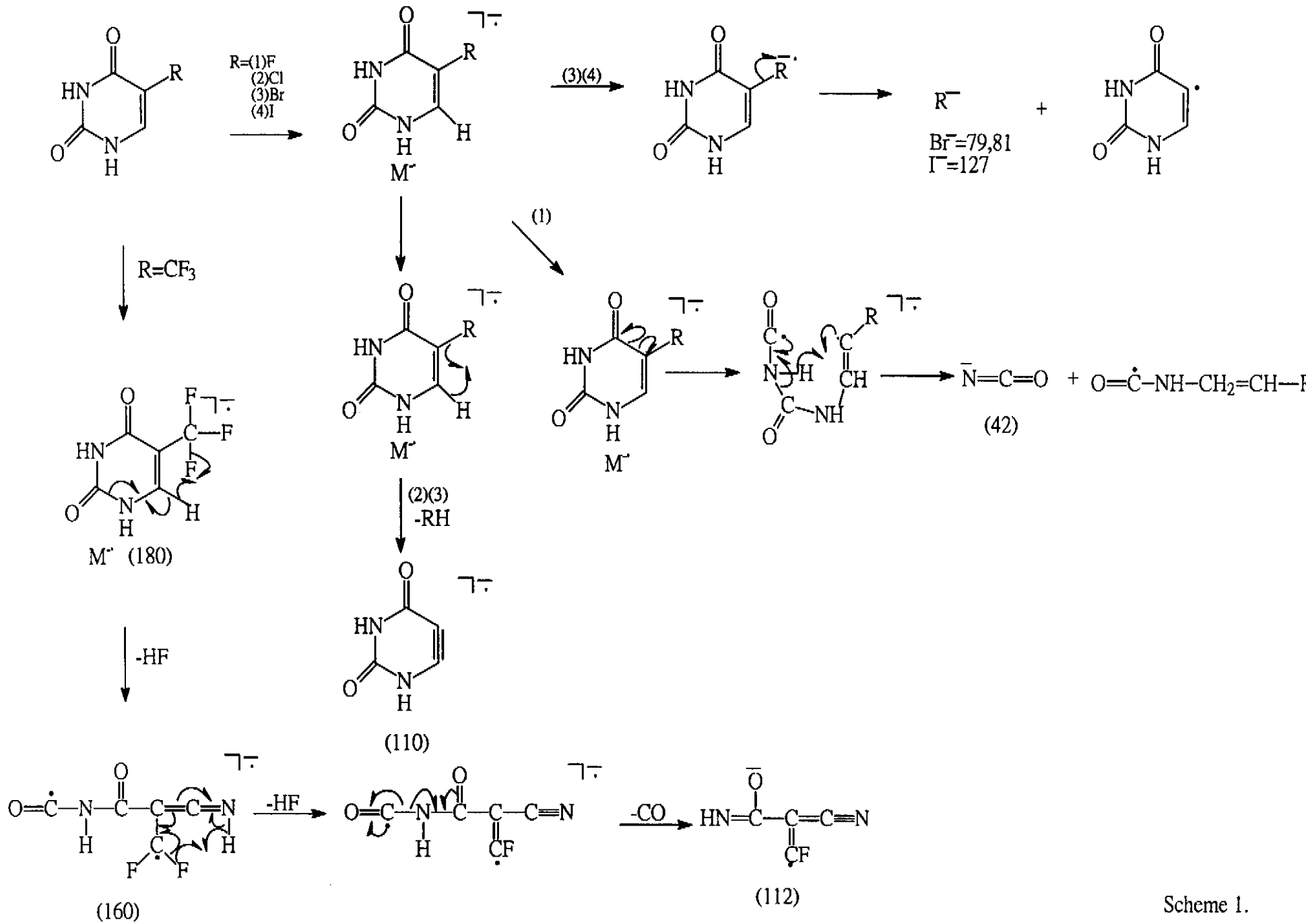
R=(1)F
(2)Cl
(3)Br
(4)I
(3)(4)
R⁻
Br⁻=79,81
I⁻=127
M⁻
(1)
R=CF3
(2)(3)
-RH
(110)
M⁻ (180)
-HF
(160)
-HF
-CO
(112)
(42)

Scheme 1.

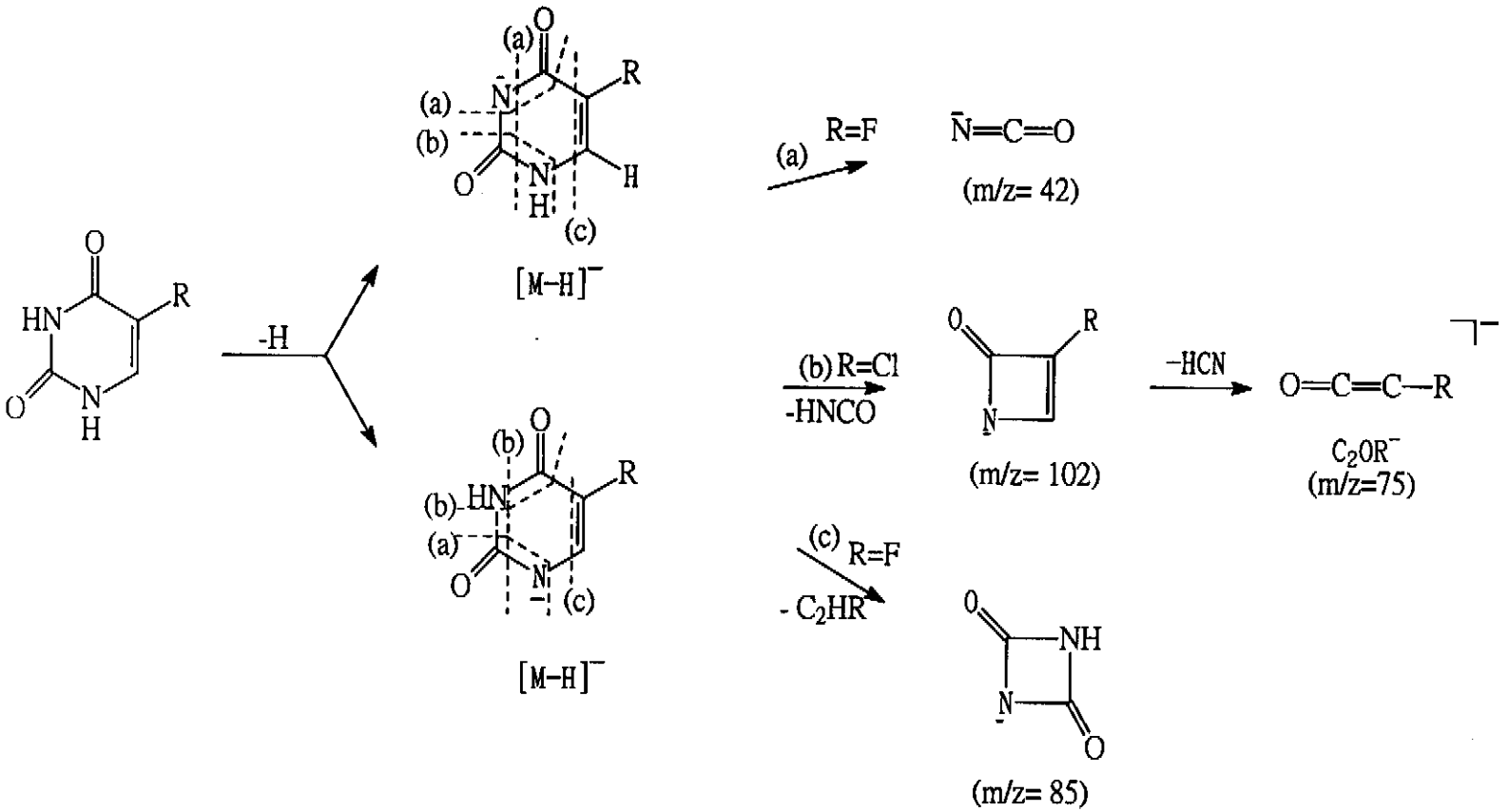
-H
[M-H]⁻
[M-H]⁻
(a) R=F
N̄=C=O
(m/z= 42)
(b) R=Cl
-HNCO
(m/z= 102)
-HCN
O=C=C—R
C2OR⁻
(m/z=75)
(c) R=F
- C2HR
(m/z= 85)

Scheme 2.